Experimental Investigatn on Physio-Mechanical and Micro-Structural Properties of Bio-Based Self-Healing Concrete

Zerihun Mamo Asamenew

A Thesis Submitted to Department of Civil Engineering School of Civil Engineering and Architecture

Presented in Partial Fulfillment of the Requirements of Masters of Science in Civil Engineering (Specialization in Construction Engineering and Management)

Office of Graduate Studies

Adama Science and Technology University

June, 2022

Adama, Ethiopia

Experimental Investigation on Physio-Mechanical and Micro-Structural Properties of Bio-Based Self-Healing Concrete

Zerihun Mamo Asamenew

Advisor: Fikreyesus Demeke (Ph.D.)

A Thesis Submitted to Department of Civil Engineering School of Civil Engineering and Architecture

Presented in Partial Fulfillment of the Requirements of Masters of Science in Civil Engineering (Specialization in Construction Engineering and Management)

Office of Graduate Studies

Adama Science and Technology University

June, 2022

Adama, Ethiopia

DECLARATION

This thesis entitled **"Experimental Investigation on Physio-Mechanical and Micro-Structural Properties of Bio-Based Self-Healing Concrete"** is my own work and has not been submitted to any university for similar purposes. Proper citations duly acknowledge the references used in this thesis.

Zerihun Mamo ______________________ ________________

Signature Date

RECOMMENDATION OF ADVISOR

I, the principal advisor of this thesis, hereby certify that I have closely advised and supervised the student while developing this thesis and have read the draft thesis entitled **"Experimental Investigation on Physio-Mechanical and Micro-Structural Properties of Bio-Based Self-Healing Concrete"** prepared under my guidance by Zerihun Mamo.

Therefore, I recommend submitting the thesis to the department for further review and evaluation.

Fikreyesus Demeke (Ph.D.)	______________________	_______________
Major Advisor	Signature	Date

APPROVAL PAGE

I, the principal advisor of this thesis, hereby certify that the recommendations and suggestios given by the thesis review Committee are appropriately incorporated into the final thesis entitled **"Experimental Investigation on Physio-Mechanical and Micro-Structural Properties of Bio-Based Self-Healing Concrete"** by Zerihun Mamo.

____________________________ _________________________ _________________

Major Advisor Signature Date

APPROVAL OF BOARD REVIEWERS

We, the undersigned members of the Board of Reviewers of the research open defense by Zerihun Mamo, have read and evaluated the thesis entitled **"Experimental Investigation on Physio-Mechanical and Micro-Structural Properties of Bio-Based Self-Healing Concrete"** and have assessed the understanding of the candidate about the research. This is, therefore, to certify that the thesis is accepted and we recommend its implementation.

____________________	____________________	____________________
Chairperson	Signature	Date
____________________	____________________	____________________
Reviewer 1	Signature	Date
____________________	____________________	____________________
Reviewer 2	Signature	Date
____________________	____________________	____________________
Department Head	Signature	Date
____________________	____________________	____________________
School Dean	Signature	Date
____________________	____________________	____________________
Office of Postgraduate Studies, Dean	Signature	Date

ACKNOWLEDGMENT

I would like to acknowledge Adama Science and Technology University (ASTU) for giving me the MSc opportunity and research fund to accomplish this thesis. Furthermore, I would like to acknowledge the Biology department of ASTU, the Material Science and Engineering department of ASTU, and the Civil Engineering Department of ASTU for allowing me to use laboratory facilities. I would like to express my deepest gratitude to my advisor, Fikreyesus Demeke (Ph.D.), for his continual support and guidance throughout the preparation of this thesis. I am greatly indebted to my friend, Mr. Biruk Alebachew, for his multifaceted support and for motivating me to work on self-healing concrete. My thanks also extend to Ms. Senayet, Mr. Mesele Yoma, Mr. Urgessa, Mr. Adem Bedaso, Mr. Yosef Fanta, and some staff members of the Civil Engineering Department who helped me to accomplish this thesis. I would like to express my special thanks to my family. Your help throughout my life was immeasurable. I am blessed to have a family like you. I am also greatly indebted to the different researchers and authors whose work I have quoted or referred to in my work. Finally, I am grateful to all the people who contributed to the successful completion of this work.

ABSTRACT

Concrete is the most versatile construction material, yet it is prone to cracking owing to environmental stress. As a result, cracks in concrete weaken its strength and durability. Cracks also require maintenance and repair, necessitating the use of additional materials and incurring repair costs. Self-healing concrete, which can automatically heal cracks as they occur, can help to avoid cracks. Unfortunately, the initial cost of self-healing concrete is higher than normal concrete due to the higher cost of nutrient and bacterial growth medium. In the current study, the workability, compressive strength, water absorption, self-healing efficiency, microstructure, and environmental and economic aspects of conventional and self-healing concrete were investigated. To make self-healing concrete samples, ordinary portland cement, fine aggregate, coarse aggregate, water, calcium lactate, and Bacillus subtilis bacteria (9.84 x 10^6 and 4.56 x 10^8 cells/mL) were immediately mixed together. The results of the slump cone test showed that bacterial concrete is more workable than regular concrete. Moreover, all bacterial concrete samples outperformed conventional concrete samples in terms of strength and water absorption. At 28 days of curing, 9.84 x 10^6 cells/mL of bacterial concentration at a dosage of 20 mL showed the greatest improvement in strength and water absorption by 14.37% and 23.05%, respectively than conventional concrete. This could be because Bacillus subtilis bacteria precipitate calcite to fill voids and microcracks inside the concrete matrix. When a crack occurs, moisture and oxygen enter the concrete through the cracks, causing bacteria to awaken from dormancy and begin feeding on calcium lactate, precipitating calcite as a healing product. Based on the test results, crack width of less than 0.5 mm was healed completely after 14 days of curing. Furthermore, to lower the initial cost, calcium lactate was synthesized from waste eggshells and lactic acid. This can bring the price of bacterial concrete down to 1.742 times that of traditional concrete. In general, the current study emphasizes the use of bacterial self-healing concrete, which is eco-friendly, cost-effective, and makes concrete workable, strong, durable, and crack-healing without external human intervention.

Keywords/terms: *Self-Healing Concrete; Bacteria; Crack; Calcium Lactate; Calcium Carbonate*

TABLE OF CONTENTS

CONTENTS PAGE

LIST OF TABLES

TABLES PAGE NO.

LIST OF FIGURES

LIST OF ACRONYMS

Acronyms	Full name
pH	Potential of Hydrogen
LWA	Light Weight Aggregate
FA	Fly Ash
RHA	Rice Husk Ash
SMA	Shape Memory Alloy
MP	Mega Pascal
ACI	American Concrete Institute
SEM	Scanning Electron Microscope
IS	International Standard
CA	Coarse Aggregate
XRD	X-Ray Diffraction
OPC	Ordinary Portland Cement
CA	Coarse Aggregate
ASTM	American Society for Testing Materials
FA	Fine Aggregate
BFS	Blast Furnace Slag
FM	Fineness Modulus
SEM	Scanning Electron Microscope
OD	Optical Density
UWFA	Unit Weight of Fine Aggregate
UWCA	Unit Weight of Coarse Aggregate
SSD	Saturated Surface Dry
Bsg	Bulk specific gravity
Asg	Apparent specific gravity
EE	Embodied Energy
EEC	Embodied Energy Coefficient
CO_2EC	Carbon dioxide Emission Coefficient
TGA	Thermo-Gravimetric Analysis
RPM	Revolution Per Minute
MJ	Megajule
SHC	Self-Healing Concrete

LIST OF CHEMICAL FORMULAS

Formulas	Name of Chemical Compound	Formulas	Name of Chemical compound
H_3O^+	Hydromium ion	$2CaO.SiO_2$	Dicalcium silicate
HCO_3^-	Bicarbonate ion	$3CaO.SiO_2$	Tricalcium silicate
H_2CO_3	Carbonic Acid	$3CaO.Al_2O_3$	Tricalcium Aluminate
C-S-H	Calcium Silicate Hydrate	$4CaO.Al_2O_3.Fe_2O_3$	Tetracalcium aluminoferrite
CO_2	Carbon Dioxide	$CaSO_4.2H_2O$	Calcium Sulphate Dhydrate
NH_2COOH	Carbamic Acid	CaO	Calcium Oxide
CO_3^{2-}	Carbonate ion	MgO	Magnesium Oxide
$CO(NH_2)_2$	Urea	Na_2O	Sodium Oxide
OH^-	Hydroxide ion	K_2O	Potassium Oxide
H^+	Hydrogen ion	Fe	Iron
$CaC_6H_6O_{10}$	Calcium Lactate	NH_4^+	Ammonium ion
$CaCO_3$	Calcium Carbonate	O_2	Oxygen
$Ca(OH)_2$	Calcium Hydroxide	Cr	Chromium
NH_3	Ammonia	$C_3H_6O_3$	Lactic acid
Ca^{2+}	Calcium ion	Co	Cobalt
H_2O	Water	Ca^{2+}	Calcium ion
W	Tungsten	CH	Calcium Hydroxide
Mo	Molybdenum	Cu	Copper

1. INTRODUCTION

1.1 Background of the Study

Concrete is one of the world's most versatile and widely used construction materials, which plays an important role in constructing dams, buildings, roads, storage tanks, tunnels, seaports, bridges, subways, and other infrastructures (Seifan et al., 2016). Concrete is mainly a combination of cement paste and aggregates. The paste, composed of cement and water, binds and fills the voids between the aggregates into a rock-like mass as the paste hardens due to the hydration reaction of water and cement (Goshu, 2018). The unique properties of concrete, including high compressive strength, versatility, availability, affordability, simple preparation, fire resistance, excellent thermal resistance, compatibility with steel reinforcement bar, and the possibility of casting in desired shapes, make concrete the most used construction material in the world, next to water (Seifan, 2018).

Concrete is vulnerable to a wide range of damages, all of which result in cracks. These cracks can be structural cracks or non-structural cracks. Structural cracks can be produced by construction and design deficiencies, while non-structural cracks are caused by environmental issues such as humidity, material quality, freeze and thaw cycles, temperature differences, chemical attacks, overloading, and other environmental issues (Alazhari, 2017; Amiri et al., 2018). The formation of concrete cracks results in a decrease in the durability and strength of the concrete structures.

The major factors that affect the durability of concrete are alkali-aggregate reaction, sulfate attack, chloride attack, reinforcement corrosion, and harsh environmental conditions. Among those major factors, corrosion of reinforcement within concrete has a significant impact on its durability. This usually occurs as a result of one of the aggressive agents attacking the concrete due to decreased permeability when carbonates, chlorides, sulfate, and water penetrate the concrete through its "cracks" (Jakhrani et al., 2019). The consequences of corrosion include the loss of the link between the steel and concrete and an increase in the size of steel within the concrete, which reduces the concrete's serviceability and strength (Hussein et al., 2019; Meharie et al., 2017). The damaged concrete structures need maintenance and repair, which requires a huge amount of resources and capital. Every year, several countries throughout the world spend billions of dollars on repairing their infrastructure. In Europe, 50% of the annual construction budget has been set aside for the rehabilitation and repair of existing structures (Cailleux et al., 2009). It is estimated that about half of the United Kingdom's construction budget is spent on the repair and maintenance of existing structures (Tabbaa et al., 2019). Furthermore, the average cost of bridge maintenance and repair in the United States is more than 5 billion dollars (Sangadji et al., 2012). Hence, it is important to prevent the expansion of cracks and heal them as quickly as possible. However, most concrete treatment methods, such as sealing, injecting chemicals, and grouting, are traditional because they rely on key components such as acrylics, epoxies, and polymers. These materials are incompatible with concrete rehabilitation because of the coefficient of thermal expansion and their production pollutes the environment (Khaliq et al., 2016). In addition, those methods require higher maintenance and repair costs. Therefore, better and new methods to repair and maintain the damaged concrete structure were investigated, and self-healing concrete was one of them (Jonkers et al., 2010).

Self-healing concrete is a relatively new addition to the construction industry, with many areas still being researched with the goal of constructing concrete structures that are both crack-free and durable (Tang et al., 2021). Self-healing concrete works on the idea of using calcium carbonate to precipitate microorganisms to heal cracks. The introduction of bacteria into concrete can create calcium carbonate, which fills the pores in the concrete. The bacteria chosen are determined by their capacity to survive in an alkaline environment and high pH, because in an environment with a pH greater than ten, the majority of microorganisms die (Luhar et al., 2015; Mahmoodi et al., 2019). Bacillus strains have been discovered to survive in an alkaline environment. The bacteria defend themselves against the alkaline environment by generating spores that are extremely thick to survive while waiting to germinate in a better environment to heal cracks (Mahmoodi et al., 2019).

Micro-fractures up to 0.2 mm in width can be healed autogenously (Joy et al., 2018) due to the hydration reaction of unhydrated cement in the concrete with water, it is not enough to seal larger cracks. Furthermore, the calcium carbonate ($CaCO_3$) formed in the control concrete as a result of the interaction between CO_2 in the environment and calcium hydro-oxide ($Ca(OH)_2$) in the concrete is disrupted in this scenario due to the low concentration of carbon dioxide (CO_2). The general reaction is given by (Jonkers et al., 2008):

$$CO_2 + Ca(OH)_2 \rightarrow CaCO_3 + H_2O \text{ ....Equation 1.1}$$

Because of the low CO_2 concentration, a soluble $Ca(OH)_2$ mineral dissolves in water and leaches out of the crack (Joy et al., 2018). Therefore, the autonomous self-healing mechanism is much more efficient. This process happens due to the continual metabolic process of calcium nutrients by the bacteria contained in bacterial blended concrete, and calcium lactate is converted into carbonate (Tziviloglou et al., 2016)

$$C_6H_{10}CaO_6 + 6O_2 \rightarrow CaCO_3 + 5CO_2 + 5H_2O \text{ ……..Equation 1.2}$$

$CaCO_3$ is generated in equation (1.2) as a result of microbiological reactions and the automatic healing of concrete. This results in a bacteria-based crack sealing technique that is effective (Lucas et al., 2018). Because the bacteria remain dormant for long periods of time, the bacteria-based self-healing technique has been shown to effectively fill cracks as large as 0.5 mm (Joy et al., 2018) and 0.5 mm (Wang et al., 2014a). When a concrete building deteriorates and water seeps into the cracks, bacteria feed on the calcium lactate, devouring oxygen and converting the soluble calcium lactate to insoluble limestone (Alves et al., 2019). As a result, the fissures in the concrete are sealed. The use of oxygen in the bacterial conversion process offers an additional benefit in preventing steel corrosion, and its durability is enhanced (Magaji et al., 2019). The presence of calcium lactate increased the compressive strength 10% more than that of normal mortar (Sakna et al., 2021). The addition of Bacillus subtilis bacteria enhances compressive strength by 15.8% and tensile strength by 30.94% at 28 days of curing (Arulsivanantham et al., 2015). The inclusion of Bacillus megaterium with a concentration of 3 x 10^6 cells/ml also enhanced the strength by 24% at 28 days of curing (Huang et al., 2016). The incorporation of bacteria into concrete improves workability (Vijay et al., 2020), reduces water permeability (Hussein et al., 2019; Meera et al., 2016), and increases chloride and sulfate ion penetration (Meera et al., 2016)

Biological concrete is more expensive than conventional concrete due to the high cost of calcium lactate, bacterial culture medium, and the method of concrete casting. In the bacterial encapsulation method, the calcium lactate and the bacteria are enclosed in a capsule to protect the bacteria from a harsh environment. But, the casting methods of concrete consisting of capsules are expensive and laborious. The direct mixing of bacteria and calcium lactate with the concrete ingredients for the preparation of concrete samples is easy and inexpensive. Thus, the researcher employed the direct mix approach for concrete sample preparation. Besides this, cracks affect the structure's strength and durability and increase the chance of repair and maintenance. The need for maintenance and repair also causes the overuse of resources, which results in CO_2 emissions and embodied energy consumption.

In the current study, the properties of bio-based self-healing concrete such as workability, compressive strength, water absorption, and self-healing efficiency were investigated experimentally. In addition, micro-structural tests were performed. The calcium lactate ($C_6H_{10}CaO_6$) nutrient, which the bacteria feed on, was prepared from discarded eggshell ($CaCO_3$) and lactic acid to lower the cost of self-healing concrete, and its production was checked by X-ray diffraction (XRD) and scanning electron microscope (SEM) images. Moreover, the environmental and economic feasibility of biological concrete was evaluated.

1.2 Statement of the Problem

Concrete is generally weak in resisting tensile stress, which leads to cancer of hardened concrete, so-called cracking. The major causes of concrete cracks are variations in temperature, structural concerns, freeze-thaw cycles, low tensile strength, dry shrinkage, early-age shrinkage, and a combination of these elements (Mahmoodi et al., 2019). This crack in concrete allows harmful substances like water, oxygen, chlorides, moisture, sulfate, and aggressive environmental agents to penetrate the concrete structure. The entrance of harmful agents through cracks results in structural deterioration, reduced strength, shortens the lifespan of structures, and increases the chance of corrosion (Rodrigues et al., 2021). As a result, it increases repair and maintenance costs and concrete usage, which causes increased CO_2 emissions and environmental pollution. Therefore, it is critical to keep fractures from spreading and repair them as quickly as possible.

The use of Bacillus species bacteria as a self-healing agent in self-healing concrete based on calcium carbonate precipitation is a better solution for crack repair (Hussein et al., 2019; Sakna et al., 2021). This relies on the metabolic activity of bacteria and calcium lactate minerals in the concrete to produce inorganic $CaCO_3$. The production of calcium carbonate fills cracks, prevents the entry of impurities and moisture, restores strength and durability, and reduces permeability and maintenance costs.

The initial cost of self-healing concrete is high due to the high cost of calcium lactate and bacterial culture medium (Lee et al., 2018; Stanaszek, 2020). Besides this, cracks in concrete structures are still a bottleneck for strength and durability problems. Therefore, the current study focused on synthesizing calcium lactate that the bacteria feed on from discarded eggshells and commercial lactic acid to lower the initial cost of bacterial concrete. Besides this, to lower the cost of the bacterial growth medium, molasses and yeast extract were used. In the current study, the workability, compressive strength, microstructural analysis, self-healing efficiency, and water absorption of biological and conventional concrete were investigated.

1.3 Objectives

1.3.1 General Objective

The main objective of this study was to investigate the physio-mechanical and microstructural properties of bio-based self-healing concrete.

1.3.2 Specific Objectives

- To investigate the workability of bacterial and conventional concrete,
- To investigate the compressive strength, water absorption, and microstructure of self-healing and conventional concrete,
- To determine the self-healing efficiency of bacterial self-healing concrete,
- To evaluate the economic and environmental feasibility of bacterial concrete

1.5 Significance of the Study

This study proposes that extracting calcium carbonate from waste eggshells can help reduce waste. Furthermore, by lowering concrete usage and regulating cracks without the use of external human intervention, it reduces carbon dioxide emissions and produces a sustainable environment. Additionally, producing calcium lactate from discarded eggshells lowers the cost of self-healing concrete and reduces maintenance and repair expenditures. In addition, concrete strength and durability can be enhanced.

1.6 Scope of the Study

The study's goal was to look into the physio-mechanical and microstructural features of bio-based self-healing C-30 concrete. The research focused on determining fine and coarse aggregate properties, as well as the extraction and characterization of calcium carbonate from the waste eggshells. It also looked at the synthesis and characterization of calcium lactate from $CaCO_3$ and lactic acid, as well as the influence of Bacillus subtilis bacteria on crack healing without the need for human intervention. Workability, compressive strength, self-healing efficiency, and water absorption were also investigated, as well as the characterization of crack healing products and bacterial and conventional concrete. Finally, the study considered the environmental and economic implications of bacterial concrete.

1.7 Organization of the Study

The study was organized mainly into five chapters. The first chapter introduces the background, the statement of the problem, the objectives, and the scope of the study. The second chapter was mainly a literature review that stated the study's matter. This section covers reviews on concrete ingredients; the meaning of self-healing concrete; mechanisms of self-healing concrete; factors affecting the efficiency of self-healing concrete; mechanical and microstructural properties of self-healing concrete; environmental and economic feasibility; and research gaps were covered. Chapter three presented materials, methods, and experimental procedures to characterize the properties of materials like cement, sand, coarse aggregate, water, bacteria, lactic acid, calcium carbonate, and calcium lactate physically and chemically. The procedures to assess properties of material like gradation, workability, silt content, densities, extraction of calcium carbonate from eggshells, and production of calcium lactate were covered. Then, proportioning of the mix for compressive strength was done. The fourth chapter relied on the presentation, analysis, and interpretation of results. This chapter covered all the findings of the experimental investigation, like gradation curve, silt content, workability status, characterization result of calcium carbonate, and calcium lactate. The compressive strength and water absorption were analyzed based on the result, and finally, the self-healing efficiency was determined, including concrete characterization to determine the morphology and calcite formation. The fifth chapter was concerned with the conclusion and recommendations.

2. LITERATURE REVIEW

2.1 Introduction

This chapter contains a brief discussion of a different approach that researchers have taken to address self-healing mechanisms in concrete. The approach can be autogenous or autonomous self-healing mechanisms. The general purpose of this chapter is to provide an extensive review of recent papers on concrete problems and their treatment mechanisms. Besides this, factors affecting self-healing efficiency and different micro and macro-level tests are extensively covered.

2.1.1 General concepts about Concrete and its Ingredients

Concrete is one of the most frequently used construction building materials and plays an essential role in many areas (Seifan, 2018). Concrete is the most commonly used construction material and is mainly composed of cement, fine aggregates, coarse aggregates, and water.

2.1.1.1 Cement

Cement is the most significant component of infrastructure construction and the most crucial input for the construction industry, particularly in infrastructure and housing projects. It produces cement paste when mixed with water in the hydration reaction, and the paste is a temporary plastic that can be shaped or deformed. The paste ensures that the concrete elements are properly bonded. Calcium, silica, aluminum, iron, and other materials are combined in a well-controlled chemical reaction to create cement (Goshu, 2018).

Table 2.1 shows the general composition of cement, which includes additional minor compounds. The properties of its constituents determine cement's properties. Different types of cement are manufactured depending on the intended use, such as Ordinary Portland Cement (OPC), Modified, Rapid-Hardening, Low-Heat, Sulfate Resisting, High Slag Blast-Furnace, and Pozzolana Portland.

Ordinary Portland cement is a controlled blend of aluminates, ferrates, and calcium silicates that are ground to a fine powder with gypsum and other materials. OPC is divided into 3 types based on the strength obtained at 28 days.

1. OPC 33 grade: strength at 28 days of not less than 33 N/mm^2.
2. OPC 43 grade:-strength not less than 43 N/mm^2 at 28 days
3. OPC 53 grade:-strength not less than 53 N/mm^2 at 28 days

Alite (C_3S), belite (C_2S), aluminate (C_3A), and alumino ferrite (C_4AF) are the main constituents of cement. Despite their tiny percentages, minor compounds can have a significant impact on the characteristics of fresh and cured cement paste. The major oxide composition of OPC is given in Table 2.1 (Goshu, 2018).

Table 2.1 Composition of Ordinary Portland Cement

Abbreviations	Oxide compositions	Chemical compound
	Major compounds	
C_2S	$2CaO.SiO_2$	Dicalcium silicate
C_3S	$3CaO.SiO_2$	Tricalcium silicate
C_3A	$3CaO.Al_2O_3$	Tricalcium Aluminate
C_4AF	$4CaO.Al_2O_3.Fe_2O_3$	Tetracalcium aluminoferrite
	Minor compounds	
CSH_2	$CaSO_4.2H_2O$	Gypsum
M	MgO	Magnesium
N,K	Na_2O and K_2O	Alkali Oxides

C_3S and C_2S are the essential compounds that contribute to the strength of cement paste. The inclusion of C_3A in cement aids early strength. C_4AF is also found in small concentrations in cement, and it has little effect on behavior when compared to the other three compounds. High C_3S (low C_2S) percentages produce a lot of early strength, but they also produce a lot of heat while the concrete cures. Low C_3S and high C_2S, on the other hand, develop strength more slowly and produce less heat. C_3A creates undesirable heat and has a rapid reaction rate, which can be mitigated by adding $CaSO_4$ to the final product.

Consistency Test of Cement

The quantity of water to make cement paste is regarded as normal consistency (ASTM, C187). The amount of water necessary to achieve a normal consistency as indicated by Vicat plunger penetration of 10±1 mm (ASTM, C187) is represented as a percentage of the weight of the dry cement, with the typical range being around 22% to 30%.

2.1.1.2 Fine and Coarse Aggregates

Aggregates are the most fundamental components of concrete, accounting for around 75% of the entire volume. The enormous number of aggregates in concrete emphasizes their importance. Fine aggregates (less than 4.75 mm) and coarse aggregates (more than 4.75 mm) must be graded in the production of concrete (Ukala, 2019).

A) Fineness Modulus of Fine and Coarse Aggregates

The particle size distribution of an aggregate is referred to as aggregate grading. Smaller particles fill in the gaps created by larger particles, which is how grading works. The right amounts of various sized aggregates can be used to form a composite aggregate mix that is properly graded. Dense concrete requires less fine aggregate and cement since it is constructed with suitably graded aggregate. The fraction of weight retained on a set of standard sieves is used to grade aggregate. Sieves with mesh sizes of (20 mm, 19 mm, 12.5 mm, 9.5 mm, 4.75 mm, and pan) (Table 2.2) are used to grade coarse material (Haque et al., 2012).

Table 2.2 Coarse Aggregate Grading Limit

Sieve size	Percentage passing by mass ASTM C136
20 mm	100
19 mm	95 to 100
12.5 mm	40 to 80
9.5 mm	20 to 55
4.75 mm	0 to 10
Pan	--

In addition, IS sieves with (4.75 mm, 2.36 mm, 1.18 mm, 0.60 mm, 0.30 mm, 0.15 mm, and pan) are used for grading fine aggregate (Table 2.3).

Table 2.3 Fine Aggregate Grading Limit

Sieve size	Percentage passing by mass ASTM C136
4.75 mm (No. 4)	98 to 100
2.36 mm (No. 8)	80 to 100
1.18 mm(No.16)	50 to 85
0.6 mm (No.30)	25 to 60
0.3 mm (No.50)	5 to 30
0.15 mm (No.100)	0 to 10
pan	---

B) Specific Gravity and Water Absorption of Fine and Coarse Aggregates

Specific gravity is defined as the mass of a unit volume of aggregate divided by the mass of the same volume of water at a certain temperature. It's a non-dimensional value that's used to assess material strength and quality. To distinguish between unwanted particles that are lighter than other particles and excellent aggregates, specific gravity is used. It's used to calculate the amount of solid aggregate in a concrete mix (Bikya, 2012).

Table 2.4 Specific Gravity and Water Absorption Formulas

Items	Formula (Bikya, 2012)	Descriptions
Apparent specific gravity (Gsa)	$\mathrm{Asg} = \frac{\mathrm{A}}{\mathrm{A}-\mathrm{C}}$	A = oven dry mass of aggregate C = mass of aggregate in water
Bulk Specific Gravity (Bsg)	$\mathrm{Bsg} = \frac{\mathrm{B}}{\mathrm{A}-\mathrm{C}}$	A = oven dry mass of aggregate B = SSD mass of aggregate C = mass of aggregate in water
Water absorption	$\%\ \mathrm{Absorption} = \frac{\mathrm{B}-\mathrm{A}}{\mathrm{A}}$	A = oven dry mass of aggregate B = SSD mass of aggregate

C) Silt Content of Fine Aggregate

Sand typically contains clay, silt, loam, and dust. Materials with a thickness of 0.06 mm to 0.002 mm are classified as silt (Ayodele et al., 2015). Sand with such particles affects the compressive strength and long-term durability of concrete. Silt is less long-lasting than other fine aggregates. They have the ability to absorb water and change its properties. Silt will prevent aggregates from bonding to cement in concrete. When silt in hardened concrete's air spaces comes into contact with water, it might shrink or swell, increasing internal pressure or leaving larger voids, weakening the concrete (Ayodele et al., 2015). However, depending on the quantity of silt/clay, which should not exceed 4%, it still remains in concrete, generating undesirable hairlines or massive fractures (Ngugi et al., 2014). The presence of silt or clay in fine aggregates beyond a specific proportion necessitates the use of extra cement to coat other concrete ingredients.

2.1.1.3 Water

The amount of water added to the concrete mix affects workability, compressive strengths, permeability, water tightness, durability, weathering, drying shrinkage, and cracking potential in both fresh and hardened concrete. Concrete mixing and curing were traditionally thought to require only potable water. The water's pH value must not be acidic, and it must meet the concrete and curing standards (Babu et al., 2018). The water in concrete mixes serves two purposes: first, it reacts chemically with the cement, causing it to set and harden; and second, it lubricates all other materials and makes the concrete workable. The proportion of water to cement determines the quality of cement paste (water-to-cement ratio). An excessive amount of water prevents proper setting. Insufficient water prevents hydration, a complete chemical reaction in which water and cement interact chemically to form a new compound.

2.1.2 Concrete Batching

Concrete batching is the process of weighing or volumetrically proportioning the various components of concrete (cement, sand, coarse aggregate, and water) prior to mixing (Joshua et al., 2018). In a study on concrete, Hedidor et al. (2017) conclude that using the volumetric batching method in concrete production is bad building practice.

2.1.3 Concrete Mix Design

Concrete mix design establishes the right proportions of cement, fine aggregate, and coarse aggregate in concrete to achieve the desired strength. Concrete mix design is the cost-effective proportioning of concrete components for increased strength and durability based on the construction site. Nominal concrete mix and designed concrete mix are the two types of concrete mix design. The nominal concrete mix may contain more cement, while the amount of cement required for the same grade of concrete for a specific site may be less in a designed mix (Chabi et al., 2018). A concrete mix design is created utilizing locally accessible ingredients to make the concrete. Strength, durability, and workability are the three most important properties to specify before designing a concrete mix. The two most essential criteria that impact the qualities of concrete are the water-to-cement ratio and the aggregate-to-cement ratio. As a result, mix design is the process of calculating the proper concrete proportions of cement, fine aggregate, and coarse aggregate.

2.1.4 Fresh Concrete Test

2.1.4.1 Slump Test

The concrete slump test is used to determine the consistency of fresh concrete before it hardens. It is used to determine the workability of freshly mixed concrete, as well as the concrete's ability to be placed, transported, and flow readily.

2.1.5 Concrete Casting and Curing

Curing concrete entails providing adequate moisture, temperature, and time for the cement to continue to hydrate until the concrete reaches the desired properties. Curing improves the durability, strength, watertightness, abrasion resistance, volume stability, and freezing and thawing resistance of hardened concrete (Dnyanoba et al., 2020). Curing methods include immersion, spraying, and moist coating (James et al., 2011). This study uses the immersion curing procedure in water to evaluate the features of hardened concrete.

2.1.6 Hardened Concrete

Hardened concrete is one of the most durable and robust building materials available, capable of supporting structural and service loads. Hardened concrete qualities include compressive strength and durability.

2.1.6.1 Compressive Strength of Concrete

The ability of hardened concrete to sustain axial stresses without cracking or deflection is known as compressive strength. The failure load divided by the cross-sectional area resisting the load yields the compressive strength of concrete. The compressive strength of cubic concrete was calculated according to Equation 2.1.

$$S = P/A \quad \text{……………. ………………………..Equation 2.1}$$

S denotes the compressive strength of concrete (MPa), P the compressive force at failure (N), and A the concrete cross-sectional area (mm^2) (Syarif et al., 2021).

2.1.6.2 Durability of Concrete

The ability of concrete to endure weathering, chemical attacks, abrasions, and other degrading processes is referred to as its durability. The ability of concrete to move fluids through it as a result of a pressure head differential is referred to as permeability. This property of concrete contributes to the concrete's longevity by preventing the entry of moisture, which may contain harsh chemicals, as well as the flow of water during heating and freezing (Goshu, 2018).

2.1.7 Challenges on Concrete Structures

Strength and durability are two important properties that directly affect the life of the concrete. Concrete has high compressive strength, but its tensile strength is low, and cracks are likely to occur. Cracks are a major cause of concrete deterioration and decrease bonding, durability, and suitability for purpose (Khan, 2010; Mehndi et al., 2014). Cracks in concrete can be caused by many factors. Humidity, material quality, freeze-thaw cycles, temperature differences, chemical attacks, reinforcement corrosion, overloading, construction deficiency, design deficiency, and other environmental factors are included (Alazhari, 2017). Besides this, concrete structures are subject to bending stress during their useful life. In this sense, cracks occur when the tensile stress exceeds the tensile strength of concrete. Therefore, concrete is usually reinforced with steel bars in the form of steel beams and laid throughout the structure. Reinforced concrete withstands not only pressure but also bending and other tensile stresses (Shen et al., 2020). Therefore, the smart design allows concrete to withstand both compressive and tensile stresses. Reinforcing bars have a positive effect on crack width limitation by controlling plastic shrinkage (Nama et al., 2015). However, it can't prevent cracking. Other reasons leading to the formation of cracks are form-work movement; shrinkage when drying fresh concrete; thermal stresses during cement hydration; external loads; internal loads; expansion and contraction during wetting and drying cycles; and poor structural design and detailing. Also, in cold regions, the fluid pressure rises due to the frozen water trapped in the matrix, causing cracks when the induced stress exceeds the tensile strength of the concrete (Seifan, 2018). Therefore, monitoring, maintenance, and repair of concrete structures are very essential.

It is difficult to continuously inspect and repair cracks, especially those in infrastructures such as bridges, highways, and tunnels. Infrastructure cracks are not easily accessible and require a great deal of effort and budget, but many of these infrastructures are in continuous operation, making repairs even more difficult. In Europe, it is also reported that 50% of the annual building budget is spent on repairs to extend the life of the structure (Cailleux et al., 2009). In addition to the high cost of repairs, most traditional repairs only take up to 15 years (Mahmoodi et al., 2019; Vegt et al., 2007). Furthermore, the average cost of bridge maintenance and repair in the United States is more than 5 billion dollars (Sangadji et al., 2012). Another study by Silva et al. (2015), states that the direct cost of crack repair and maintenance has been estimated at more than $145/m^3 of concrete. Therefore, those concrete problems must be treated to minimize the maintenance cost as well as to keep the concrete structure for a longer period without deterioration.

2.1.8 Treatment of Concrete Cracks

Engineers have devised several strategies to prevent the cracking of concrete. The first method is traditional manual repair. Cracks are filled, repaired, or damaged concrete is destroyed, and new materials are placed. The most common way to improve and/or extend the life of concrete structures is to fill cracks with epoxy resin. However, the processes require human intervention and incur additional labor costs. The cost of injecting cracks into tunnel elements can be estimated at more than $145 per m^3 of concrete (Silva et al., 2015). Repair is not a permanent solution, as the rebar has already begun to oxidize as soon as the water penetrates the concrete. In these situations, the most effective way to repair a crack is with an automatic repair mechanism that is triggered as needed and restores the function of the concrete structure without human intervention.

2.2 Self-Healing Smart Concrete

2.2.1 Meaning of Self-Healing Concrete

The idea of self-healing concrete was first developed in the early 1990s. This concept deviates from the idea that concrete can heal itself without additives or biological treatments. This process is very slow and not enough to restore water-tightness. Researchers have begun testing ways to speed up the process. Jonkers and Schlangen began investigating encapsulated bacteria as a biological treatment in the mid-2000s. "The key to making self-healing concrete is to repair small cracks before they grow into large cracks." Following their success in the lab, Jonkers and Schlangen built the world's first self-healing concrete building using bacteria (Patel, 2016).

A self-healing mechanism is described as any technique within the material itself related to the healing and, consequently, the development of an overall performance after an advanced action that has decreased the overall performance of the material (Tittelboom et al., 2013). Different mechanisms of self-healing have been added over the years. However, records of self-healing phenomena can be traced back to historic structures and buildings, where cracks were observed to be packed with white crystalline (Mahmoodi et al., 2019).

2.3 Classification of Self-Healing Concrete

2.3.1 Autogenous Self-Healing

Autogenous self-healing is the process that occurs when the restoration of the material after damage involves only the original components (Roig-Flores et al., 2021). In other words, the self-healing ability of concrete and other cement-based materials is possible only under favorable environmental conditions due to their particular chemical composition. Since then, many researchers have not only observed the presence of native healing products in concrete cracks but also sought to check their physio-chemical background (Rajczakowska, 2019; Tang et al., 2015).

2.3.1.2 Mechanisms of Autogenous Self-Healing

The basic mechanisms of autogenous self-healing are given in Figure 2.1. (a) $CaCO_3$ formation from $Ca(OH)_2$; (b) impurity blocking; (c) hydration of unhydrated cement; (d) C-S-H matrix expansion (Tang et al., 2015). The autogenous self-restoration of concrete is most powerful for small cracks between 0.1 and 0.2 mm in width (Reinhardt et al., 2003; Yang et al., 2009). Since larger cracks are not healable by natural means, a new technique that is more efficient was discovered.

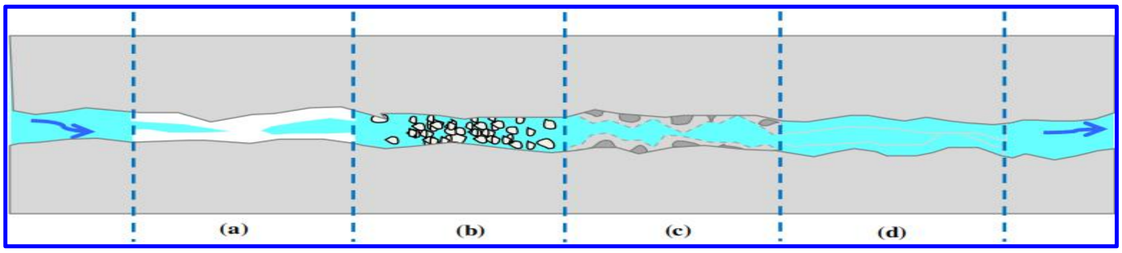

Figure 2.1 Mechanisms of Autogenous Healing

2.3.2 Autonomous Self-Healing Concrete

Autonomous crack healing of concrete refers to the self-healing mechanism that is artificially triggered within the cement-based matrix, primarily by the introduction of chemical or biological factors into the cement-based matrix (Van et al., 2013). The basic idea of autonomous healing is that when an injury (crack) occurs, the remedy is released from the container and responds to several stimuli, thereby triggering the self-healing mechanism. The healing agents are in contact with air, moisture, or heat (Joseph et al., 2010; Nishiwaki et al., 2011), and contact with a cementitious matrix (Wang et al., 2012; Wiktor et al., 2011). It has been shown that the width of a crack that can be healed by autonomous healing can be much larger than the width of autogenous healing. For example, autonomous healing with bio-hydrogel achieved a maximum repair of 0.5 mm (Wang et al., 2014a). In addition, autonomous self-healing of micro-encapsulated bacterial-based concrete has been reported to be able to repair cracks up to 0.5 mm (Wang et al., 2014b). The efficiency of autonomic healing depends on several important factors, including the efficiency of treatment, the efficiency of encapsulation techniques, and the efficiency of the mechanisms by which the self-healing process is triggered (Van et al., 2013).

2.3.2.1 Mechanisms of Autonomous Self-Healing Techniques

Autonomous self-healing is identified by specific terms such as vascular procedures, capsule procedures, bacterial procedures, electro-deposition procedures, shape memory alloy procedures, microencapsulation procedures, and/or induced energies. Different types of healing techiques were investigated by different authors, such as bacteria (Khaliq et al., 2016), admixture (Reddy et al., 2019), encapsulation method (Lv et al., 2016), direct mix (Tang et al., 2021), nano-materials (Lee et al., 2018), vascular methods (Wang et al., 2014a), and the shape memory alloy method (Wang et al., 2012).

Table 2.5 Pros and Cons of different Autonomous Self-Healing Mechanisms

Healing technique	Pros	Cons	Reference
Bacteria	Naturally and environmentally friendly and biologically effective	Bacteria protection is a must, we need requirements.	(Khaliq et al., 2016)
Nano-materials	High mechanical and healing capacity, cheap and energy-saving	High safety requirements	(Lee et al., 2016)
Admixture	Excellent healing efficiency	Undesirable expansion	(Reddy et al., 2019)
Vascular method	healing agent discharge when required, an adjustable high quantity of healing material.	Casting difficulties, less strength due to many tubes in the cement	(Wang et al., 2014b)
SMA	Provided self-restoration, used as coatings for corrosion.	Temperature dependent effect	(Zhang et al., 2018)
Encapsulation method	When necessary, a healing agent is discharged, a medium quantity of healing agent is required, & efficient in healing cracks.	Casting and healing agent release issues, as well as strength issues caused by too many hollow fibres	(Kanellopoulos et al., 2015; Lv et al., 2016)
Direct mix	Self-healing agent is added directly to the mix	The ratio of healing agents differs according to the type of cement used.	(Tang et al., 2021)

2.4 Self-Healing Agents

2.4.1 Self-Healing Based on Bacterial Species

Bacteria are basically unicellular, living microorganisms that can be found everywhere. The types of bacteria already studied for use in bacterial concrete include Bacillus pasturii, Megaterium, sphaericus, Coohni, Subtilis, and Cereus (Amiri et al., 2018; Yang et al., 2020). Bacillus is a type of microorganism that forms spores and can release $CaCO_3$ as a filler and fill cracks as a decisive factor. Depending on the number of bacteria added, compressive strength increases (Vashisht et al., 2020). Among above self-healing bacteria, Bacillus subtilis is a gram-positive bacterium that can be easily cultured in the laboratory at a minimal cost (Saleh, 2019).

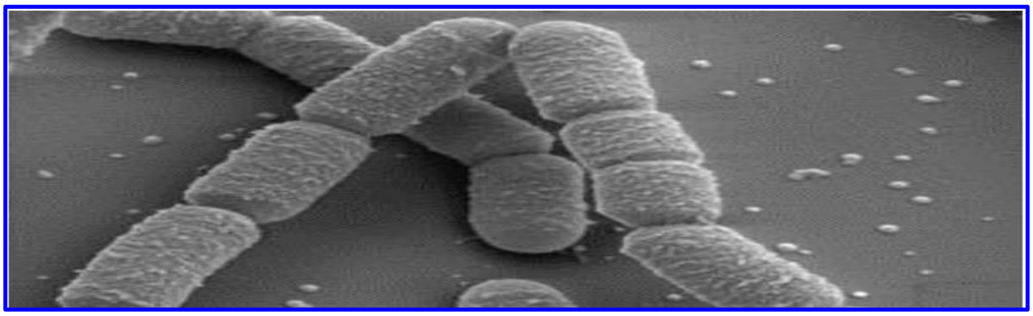

Figure 2.2 Spores of Bacillus Subtilis Bacteria

Bacteria are important reaction factors in self-healing mechanisms in that they increase the production of calcium carbonate, which is required for crack closure (Jonkers et al., 2008). Figure 2.3 shows (a) bacteria are activated on the crack surface by water to precipitate calcite to heal cracks; (b) scanning electron micro-scope image of Bacillus cohnii spores; (c) mineral precipitates on crack surfaces; (d) microscopic images of the crack-healing process before and (e) after 100 days of healing (Yang et al., 2020).

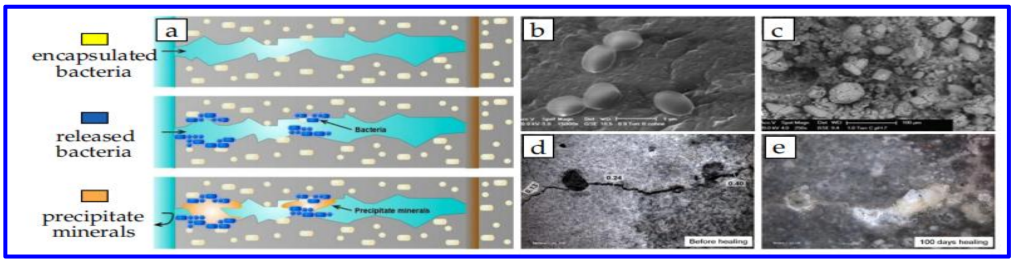

Figure 2.3 Self-Healing Mechanism using Bacterial Spores

2.4.1.1 Formation of Calcium Carbonate Precipitation by Hydrolysis of Urea

In this method, the bacterial cell wall is negatively charged and attracts positive calcium ions (Ca^{2+}) to the surface. These ions then react with the carbonate ions dissolved in water to form a carbonate precipitate from the cell wall. Bacterial cells act as hosts for this carbonation in the following ways (Choudhary, 2020; Saleh, 2019):

$$Ca^{2+} + cell \rightarrow cell - Ca^{2+} \text{……….Equation 2.1}$$

$$Cell - Ca^{2+} \rightarrow CO_3^{2-} \rightarrow cell - CaCO_3 \text{………Equation 2.2}$$

As it can be seen from the following reaction mechanism, $CaCO_3$ precipitated by the hydrolysis of urea produces hydroxyl ions (OH^-), which promotes the spontaneous formation of more carbonate ions than the natural carbonation of urea. Therefore, it is more likely to fill cracks than carbonic acid in the atmosphere. However, the ammonium ions produced as a by-product have a negative effect on the concrete matrix. In addition, the bacteria die after the first sedimentation layer of the cell wall, stopping self-healing. The reaction mechanisms are given below (Hazarika, 2021).

The system of reaction mechanisms are given as:-

$$CO(NH_2)_2 + H_2O \rightarrow NH_2COOH + NH_3 \ldots\ldots\ldots\ldots\ldots\ldots \text{Equation 2.3}$$

$$NH_2COOH + H_2O \rightarrow NH_3 + H_2CO_3 \ldots\ldots\ldots\ldots\ldots\ldots \text{Equation 2.4}$$

$$2NH_3 + 2H_2O \rightarrow 2NH_4^+ + 2OH^- \ldots\ldots\ldots\ldots\ldots\ldots \text{Equation 2.5}$$

$$H_2CO_3 + H_2O \rightarrow HCO_3^- + H_3O^- \ldots\ldots\ldots\ldots\ldots\ldots \text{Equation 2.6}$$

$$HCO_3^- + H_2O \rightarrow CO_3^{2-} + H_3O^- \ldots\ldots\ldots\ldots\ldots\ldots \text{Equation 2.7}$$

$$2H_3O^- + 2OH^- \rightarrow 4H_2O \ldots\ldots\ldots\ldots\ldots\ldots \text{Equation 2.8}$$

The net ionic equation becomes:-

$$CO(NH_2)_2 + 2H_2O \rightarrow CO_3^{2-} + 2NH_4^+ \ldots\ldots\ldots\ldots\ldots\ldots \text{Equation 2.9}$$

The final equation is given in equation (2.4) below as follow:

$$Ca^{2+} + CO_3^{2-} \rightarrow CaCO_3 \ldots\ldots\ldots\ldots\ldots\ldots \text{Equation 2.10}$$

Figure 2.4 indicates the attachment of calcium ions to bacterial cell wall to precipitate calcite as a healing product (Vijay et al., 2017).

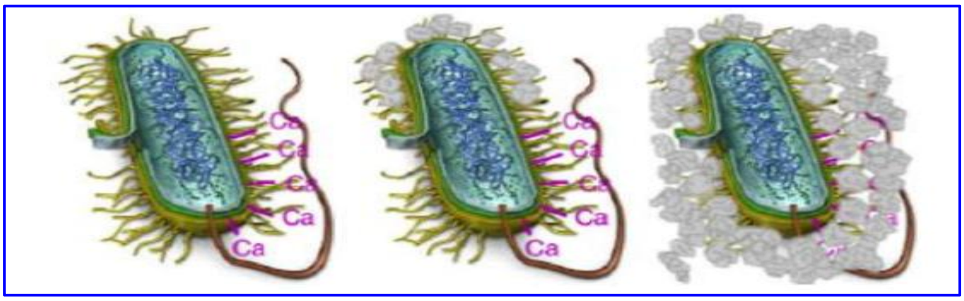

Figure 2.4 Formation of $CaCO_3$ on Bacterial Cell Wall

2.4.1.2 Formation of $CaCO_3$ by Bacterial Respiration

This mechanism avoids the formation of ammonium as a by-product by using CO_2 from bacterial respiration. However, a Ca-rich environment and a high pH value are required to take into account the deficiency of OH^- ions due to the hydrolysis of urea. This high pH requirement is to maintain the spontaneous conversion of carbonate ions to carbonate. The Ca-rich environment of bacterial spores in both mechanisms is usually provided as calcium lactate. In the reaction given by Choudhary (2020), calcium lactate functions as a nutrientrich food source for bacteria. However, the source of the $CaCO_3$ precipitation production process is not economical.

$$C_6H_{10}CaO_6 + 6O_2 \rightarrow CaCO_3 + 5CO_2 + 5H_2O \text{ …….Equation 2.11}$$

The carbon dioxide produced by the breathing of bacteria helps self-healing by reacting with Portland, the product of hydration. Generally, $CaCO_3$ is precipitated with the aid of micro-organisms. The bacteria selected need to face the trouble of excessive pH, temperature, and absence of water in concrete after its hardening (Jakhrani et al., 2019).

2.4.1.3 Formation $CaCO_3$ from Waste Eggshells

An eggshell is the outer shell of a hard-shelled egg, and some egg shapes have a soft outer coat. On the other hand, eggshells are solid waste generated by people with serious environmental problems and are generated by homes, hotels, restaurants, and the food industry (Amibo et al., 2020).

Chemical analysis shows that eggshell contains more than 90% carbonate with a 57% organic membrane (Golakiya, 2020). Eggshells make up approximately 12% of the total egg weight. It is mainly composed of calcium carbonate (95%), magnesium carbonate, and calcium phosphate deposited on the organic matrix (Ray et al., 2017). From a chemical perspective, it is composed of dry matter (98%) and water (2%). Eggshell seems to be a good source of calcium carbonate. It is generally low in heavy metals, reasonably absorbent, and inexpensive (Amibo et al., 2020).

There is currently great interest in finding new sources of pure calcium carbonate to meet the demand for $CaCO_3$. In many countries around the world, egg product companies and some food manufacturers that use eggs produce large quantities of waste eggshells that have lost calcium carbonate, the best natural source of calcium carbonate (Cree et al., 2015). Challenges related to the disposal of eggshells are cost, landfill availability, odor, flies, and grindability. One of the challenges of calcium carbonate supplementation in Ethiopia is the improper use of calcium carbonate sources. Eggshell is one of the main sources of calcium carbonate (Yusuf, 2016). Therefore, given the high calcium carbonate content, disposal costs, and growing environmental concerns, there is an alternative that transforms waste eggshells into valuable items and brings economic benefits to the highly competitive egg processing industry.

2.5 Factors affecting the Efficiency of Bacterial Self-Healing Concrete

2.5.1 Type of Bacteria used as Self-Healing Agent

The main purpose of incorporating bacteria into self-healing concrete is to heal cracks by precipitating $CaCO_3$. Bacillus is a sort of bacteria species that can produce calcite as a healing product. This includes Bacillus Megaterium (Huang et al., 2016), Bacillus Aerius (Hazarika, 2021), Bacillus Subtilis (Joy et al., 2018), Bacillus Consortia (Nain et al., 2019), and Bacillus Pasteurii (Negash, 2018). Bacillus sphaericus bacteria was used as a self-healing agent in the study (Wang, 2013), whereas Bacillus pseudofirmus and Bacillus cohnii were used in the study (Jonkers et al., 2010). Another Bacillus strain used is Bacillus megaterium, which has also been proven as a remedy for concrete (Andalib et al., 2016), and also Bacillus subtilis, used as a healing bacterium (Amiri et al., 2018; Feng et al., 2021). Based on these studies, Bacillus bacteria are widely used and demonstrate their ability to withstand the high alkalinity of concrete media.

2.5.2 Cracking Ages

The concrete structures may crack at any age, and the number of bacteria decreases as the concrete ages. This is due to the absence of a self-healing agent liable for the precipitation of minerals. Other properties, such as the internal structure of the concrete and the degree of hydration, influence the self-healing effectiveness of the concrete at different cracking ages (Huang et al., 2016). Another study by Ren et al. (2014) investigated the potential for self-healing of cracks at an early age in cement-based materials containing bacteria that may produce carbonic anhydrase at 7, 14, 28, and 60 days of age and found that the repair effect diminished over-time. The result shows that self-healing efficiency has an indirect relationship with crack age.

2.5.3 Crack Width

Autogenous self-healing is effective for healing smaller cracks of 0.1–0.2 mm (Talaiekhozani et al., 2014). Autonomous self-healing by incorporating bacteria can heal cracks with a width of 0.46 mm at 100 days of curing (Tziviloglou et al., 2017; Wiktor et al., 2011). The encapsulation method used to apply the bacteria resulted in maximum fissure width healing, which is four times the width of autogenous healing (Wang et al., 2014b). After 20 days of curing, the 0.3 mm wide crack was completely healed, but the 0.8 mm wide crack was partially healed (Luo et al., 2015; Ren et al., 2014). Therefore, self-healing efficiency decreases as crack width increases.

2.5.4 Presence of Water

The availability of free water is very vital in the process of healing cracks. As Bhaskar (2016) previously discovered, the presence of water is critical for accelerating the efficiency of crack healing capabilities. According to Sahmaran et al. (2015) and Zhang et al. (2017) findings, the gradual hydration of unhydrated cement in water is rapid, and the dissolution of $Ca(OH)_2$ to form calcium carbonate as a healing product is encouraged.

2.5.5 Micro-Structure

SEM and XRD have shown that mineral precipitates can improve the ultrafine structure of concrete by adding bacteria (Chahal et al., 2012). Accumulation of $CaCO_3$ deposits improves the airtightness of concrete and acts as a protective layer against infiltrating pollutants. The micro-structure can increase the durability of concrete (Huang et al., 2016).

2.5.6 Size and Dosage of Capsules

The correct dosage of capsules and their correct distribution in the concrete mixture are very important. One of the difficult tasks in designing a concrete mixture is finding the correct dose of self-healing capsules. Adding more doses than necessary will adversely affect the initial strength of concrete. On the other hand, adding a lower dose than necessary causes the capsule not to pass through the crack opening (Fang et al., 2021; Reinke, 2012). In doing so, adding the right dosage of the capsule and its proper distribution inside the concrete mix is very important.

2.5.7 Concentration of Ca^{2+} ions

Freely dissolved calcium ions with sufficient concentrations of carbonate or bicarbonate play a vital role in demonstrating the self-healing mechanism (Stanaszek, 2020). In another study, Choi et al. (2016) confirmed that using saturated $Ca(OH)_2$ solution and CO_2 micro-bubbles promotes Ca^{2+} and CO_3^- which are required for self-healing. Therefore, it can be concluded that the higher the concentration of Ca^{2+} ions, the better the self-healing efficiency.

2.5.8 Methods of Curing

The method of self-healing concrete curing also affects its healing efficiency. Concrete curing underwater is one of the preferred methods for increasing the rate of surface repair in bacterial-based self-healing concrete (Alexander et al., 2008; Luo et al., 2015).

2.5.9 Temperature, Pressure & Healing Time

Concrete structure healing performance improved with higher pressure, higher temperature, and longer healing time (Barría et al., 2021; Meharie et al., 2017).

2.6 Properties of Self-Healing Concrete

2.6.1 Macro-Structural Properties of Concrete

2.6.1.1 Chloride and Sulfate ion Penetration

Chloride intrusion is one of the most dangerous environmental attacks, corroding rebar and leading to the destruction of concrete structures. The addition of Bacillus subtilis improves sulfate and chloride resistance by 4.13% and 5.41%, respectively (Meera et al., 2016). In the case of quartz dust, the use of bacteria leads to a reduction in chloride movement. The addition of Bacillus Pasteuri and Subtilis reduces the penetration of chloride ions into concrete (Huang et al., 2016; Luhar et al., 2015).

2.6.1.2 Water Absorption

Water absorption of bacterial concrete was enhanced due to the calcite production by the action of bacteria inside the concrete matrix and the filling of voids/pores by calcium carbonate. According to the study by Parashar et al. (2021), the water absorption of bacterial concrete was decreased by 18.3% compared to conventional concrete. In another study by Hussein et al. (2019), water absorption of concrete decreased with an increased concentration of bacteria for all ages of concrete specimens by 15–38%.

2.6.1.3 Compressive Strength of Bio-based Self-Healing Concrete

Compressive strength was used to evaluate whether the material could resist some of the applied load. The addition of bacteria to the concrete improves the compressive strength as compared to conventional concrete, as shown in Table 2.6 below, due to the action of bacteria to precipitate calcite to fill microcracks and voids inside the concrete matrix.

Table 2.6 Compressive Strength at different Bacterial Concentration

Types of bacteria	Concentration	Concrete grade	Strength improvement at 28 day	Reference
B.Aerius	10^5 cells/ ml	10%RHA	14.4%	(Hazarika, 2021)
B.Subtilis	$6x10^6$ cells/ml	M-25(FA)	17.1%	(Joy et al., 2018)
S. Pasteurii	10^5 cells/ ml	--	35%	(Rajczakowska, 2019)
B.Subtilis	$2.8x10^8$cell/ml	LWA	12%	(Huang et al., 2016)
B.Subtilis	10^5 cells/ ml	M-40	17.54%	(Amiri et al., 2018)
B.Megaterium	$3x10^6$ cells/ ml	M-50	24%	(Huang et al., 2016)
B.Megaterium	10^8 cells/ ml	M-40	22.54%	(Nain et al., 2019)
B.Consortia			15.86%	
B.Subtilis			14.36%	
B.Subtilis	10^5 cells/ ml	M-20	42.54%	(Meera et al., 2016)
S.Pasteurii	$1.26x10^7$cell/ml	C-25	46.71%	(Negash, 2018)
B.Subtilis			8.01%	

2.6.2 Micro Structural Properties

2.6.2.1 Scanning Electron Micro-Scope (SEM)

Under SEM, the calcite deposition inside the micro-cracks of concrete by bacteria is analyzed. SEM observations revealed that the main crystal shapes that were found in the cracks of mortar samples were $CaCO_3$ (Tziviloglou et al., 2016). Figure 2.5 indicates the SEM image of calcite precipitated along the crack surface (Lucas et al., 2018).

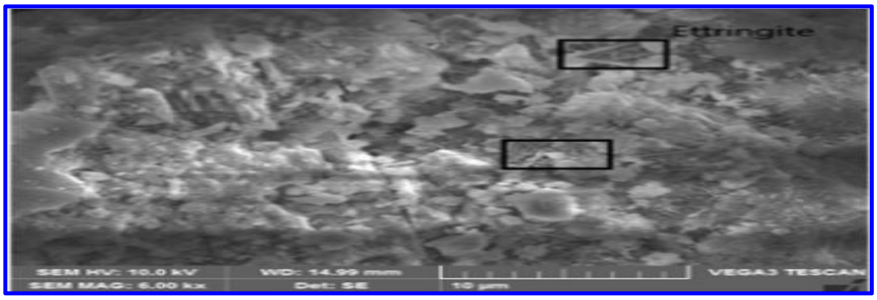

Figure 2.5 SEM image of Calcite in Concrete

2.6.2.2 X-ray Diffraction (XRD)

XRD is a technique that uses the crystal structure of the compounds to identify the chemicals they contain. It also gives information about the crystal structure and chemical composition of a material (Thiyagarajan et al., 2016). Besides, the XRD analysis examines the presence of carbonated crystals in powdered samples (Hazarika, 2021). Figure 2.6 shows the XRD patterns of the self-healing products without significant differences in the diffraction peaks of all samples forming calcite as the major crystal healing product (Luo et al., 2021).

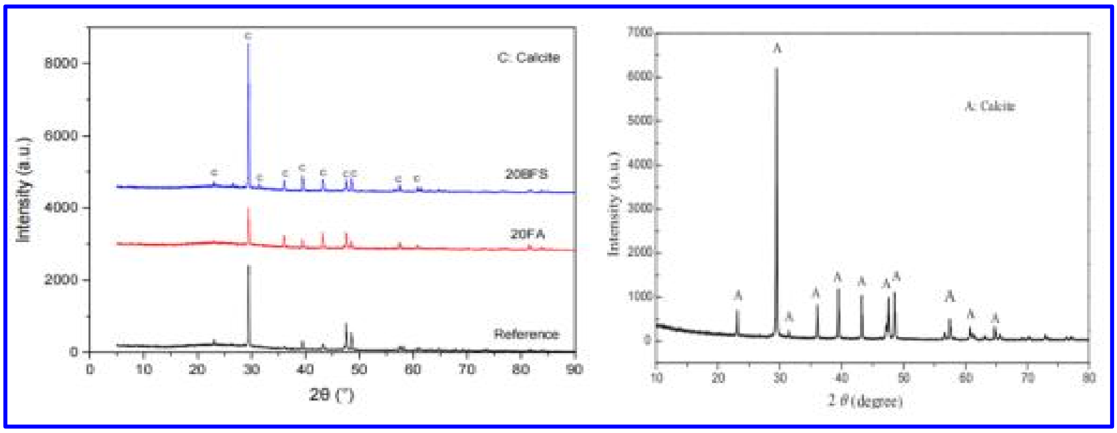

Figure 2.6 XRD Pattern of Precipitations at Cracks Surface with Cementious Material

2.7 Economic and Environmental Evaluation of Self-Healing Concrete

2.7.1 Economic Feasibility of Bacterial Concrete

It's critical to figure out whether the cost of self-healing concrete is affordable in practice. The entire cost of bacterial concrete includes media, labor, waste treatment, biomass production facilities, and downstream and upstream processing (Lee et al., 2018). The higher cost of bacterial concrete is due to the cost of bacteria and nutrients, which account for 80% of the cost of concrete ingredients. Self-healing concrete is obviously more expensive than normal concrete.

Traditional concrete costs approximately \$100 per cubic meter. In contrast, the price of self-healing concrete is 2.3 to 3.9 times that of regular concrete (Srinivasa et al., 2015; Stanaszek, 2020). To be economically viable, a microbial-induced calcite precipitation (MICP) restoration approach must contribute less cost to construction than replacing fractured concrete with new concrete (Lee et al., 2018). The difficulty of preparing the bacteria and the capsule that contains them is the fundamental reason for the greater initial cost of bacterial concrete. Extensive work, aseptic conditions, and growth media are required for the bacteria. Depending on the overall cost of the material, encapsulation costs range from $34 to $57 per kilogram of bacteria generated (Silva et al., 2015). When compared to standard repair procedures, a newly discovered bacterial encapsulation approach cuts the cost of self-healing concrete manufacture by half, saving between $105 and $120 per cubic meter (Jonkers, 2017). As seen in Figure 2.7, the self-healing concrete can eliminate the operation and maintenance costs, which accounts for 50-80% of the total life-cycle costs (Alves et al., 2019). Because of the somewhat higher initial cost, bacterial concrete could be used as a construction material because it eliminates repair and maintenance costs over the structure's lifetime.

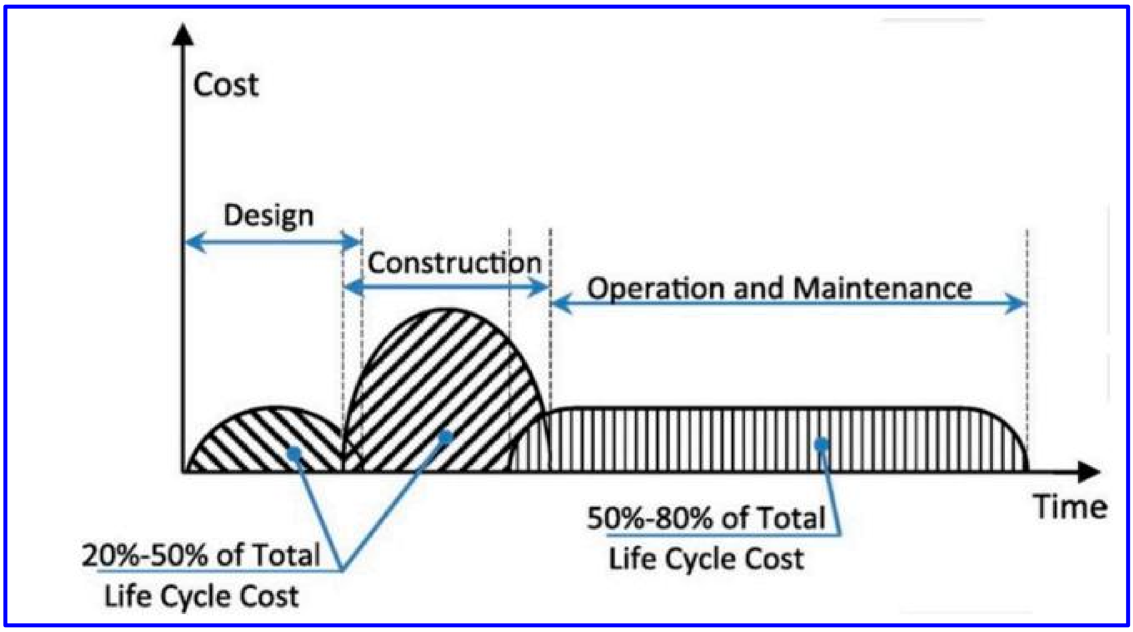

Figure 2.7 Construction Life-Cycle Cost

The bacterial growth medium accounts for up to 60% of the total operating costs (Stanaszek, 2020). Nutrient broth and yeast extract, which are more expensive than standard cement, are used in the media for bacterial growth and calcite precipitation. As a result, developing a lower-cost alternative nutrient supply is critical to enabling the method's widespread implementation. In comparison to the typical nutrient broth and yeast extract media, the use of lactose mother liquor from the dairy industry as a medium successfully induced calcium carbonate and enhanced compressive strength (Achal et al., 2009). It's vital to remember that bacterial concrete is still in its early stages of development, and the initial cost will most certainly drop with time. Furthermore, the cost of repairing a crack in traditional concrete is roughly \$150 per m^3. As a result, bacterial concrete reduces the original cost by eliminating maintenance costs (Silva et al., 2015).

2.7.2 Environmental Feasibility of Self-Healing Concrete

The building industry consumes the rawest resources of any industry. Raw material production consumes energy and releases carbon dioxide (CO_2) into the atmosphere. As reported by Taffese et al. (2019), construction consumes more than 35% of global energy and emits more than 40% of CO_2. Energy and CO_2 emissions are "embodied" within the concrete materials. Concrete has an average life duration of 50 years, and its embodied energy and carbon dioxide emissions are estimated to be 4,273.90 MJ/m^2 and 343.55 kg/m^2, respectively (Syngros et al., 2017).

Traditional concrete is less durable due to environmental stress. Over-dimensioning and reconstructing the structure were the answers to this problem, both of which required more concrete. This over-usage of concrete results in waste and pollution of the environment. As a result, the bacterial concrete fills cracks as they occur. As a result, it tends to reduce pollution by reducing the amount of concrete required. The creation of waste can be reduced since it prevents the need to repair and demolish structures owing to cracks. Waste generation is one of the negative consequences of concrete production, which accounts for a significant portion of global carbon emissions. One of the causes of global warming is CO_2 emissions into the atmosphere. As a result, using self-healing concrete reduces carbon emissions by reducing the amount of concrete utilized (Lee et al., 2018).

Bacteria that create calcite have been shown to improve the strength of concrete. According to Wang et al. (2016), microbial calcite generation has considerable advantages over traditional concrete in terms of environmental friendliness and high compatibility with the concrete matrix. Calcite is a naturally occurring mineral that is made up of bacteria and concrete. Bacteria precipitate the substance, which has little effect on the surrounding ecosystem.

The generation of ammonium ions during the hydrolysis of urea, which are released into the air and hydroxide ions into the water, is the most significant impact of bacterial concrete. The hydroxide ion has a significant impact on the pH of water in concrete, and ammonia causes cancer and respiratory sickness. As a weak acid, ammonia alters the pH of the environment, disrupting the nitrogen cycle. The release of ammonia is a major environmental hazard, and urea hydrolysis may not be adequate (Ivanov et al., 2019).

2.8 Research Gaps

According to literature findings, bacterial self-healing concrete has the ability to cure fractures without the need for human intervention, making it a viable alternative to traditional crack repair. However, structural cracks in concrete remain the leading cause of strength and durability problems due to environmental stress. Concrete cracks also result in expensive repair and maintenance costs, as well as excessive CO_2 emissions and induced energy consumption by the concrete-making materials. Many writers throughout the world have studied the methods for regulating cracks in concrete structures and reducing their impact. The use of self-healing concrete can help to solve these challenges. However, the initial cost of self-healing concrete is higher compared to the cost of conventional concrete due to the higher cost of calcium lactate nutrient and bacterial culture medium. The calcium lactate nutrient was synthesized from waste eggshells and lactic acid in the current study to lower the initial cost of bacterial self-healing concrete. Moreover, yeast extract and molasses were used as a bacterial culture medium to lower the cost of self-healing concrete. The effects of adding calcium lactate and bacterial solution into the concrete mix were also investigated in terms of workability, strength, water absorption, microstructure, self-healing efficiency, and environmental and economic aspects.

3. MATERIALS AND METHODS

3.1 Materials and Chemicals

The materials and chemicals used in this experiment were examined to ensure that their physical and microstructural qualities met the requirements set out by the standard. Materials and chemicals used in the experimental examination of bio-based self-healing concrete were discussed in this part, along with their properties.

3.1.1 Cement

Cement is a finely powdered powder made up of argillaceous, siliceous, and calcareous components that have been chemically mixed with iron oxide, gypsum, and a few other chemicals. Table 2.1 shows the chemical composition of cement. The experiment was conducted using locally available ordinary Portland cement (OPC), which holds the aggregate together when it reacts with water. Because of its superior mechanical qualities, early stripping, and high-grade cement, OPC is widely employed. The chosen OPC was obtained from local shops in Adama, Ethiopia, and it was carefully preserved in an airtight container to protect it from moisture, atmospheric agents, and humidity during the experimental period, which confirms (ASTM C150) standard.

3.1.2 Fine Aggregate

Sand is a byproduct of both artificial and natural disintegration of rock and minerals, and it can be found in rivers, lakes, residual deposits, and windblown deposits. River sand that had been sieved through a 4.75 mm sieve and retained at 150 microns according to ASTM C33 was utilized in this experiment. Silt, clay, and other organic contaminants should be absent from the sand.

3.1.3 Coarse Aggregate

The aggregates retained on the 4.75 mm sieve are basically classified as coarse aggregates. It is an irregular and granular material made of crushed stone, obtained from quarries by crushing by hand or using a crusher. The coarse aggregate must be free from impurities like clay, silt, dirt, and organic matter. Soft, porous rock can limit the strength and wear resistance; it may also disintegrate during concrete mixing, which affects the workability of fresh concrete by increasing the number of fines adversely. The coarse aggregate used to make up the concrete samples in this work consists of crushed gravel, which was collected from a local quarry that confirms the requirements of ASTM C33. Generally, the coarse aggregate used for the experiment should be strong, durable, free from vegetable matter, with less than 5% water absorption, and not sharp and angular as per ASTM C33.

3.1.4 Water

Water is also one of the key ingredients of concrete. Water for mixing should be devoid of oil, alkali, and acid. Water that is fit to drink is generally suitable for use. Impurities in water can impact the strength and longevity of concrete by preventing it from setting properly. Too much water causes the water to segregate, resulting in uneven strength in the concrete. Excess water will cause fine light cement particles to float on top of freshly laid concrete. This is referred to as bleeding, and it must generally comply with (ASTM C1602). The pH value for concrete mixing and curing should be between 6.5 and 8.5 based on the (ASTM C1602) standard. Corrosion occurs when the pH falls below 6, and when the pH rises too high, it loses its binding characteristics and causes cracking.

3.1.5 Hen's Eggshells

Eggshell is the outer covering of hard eggs that can be obtained from hotels, restaurants, homes, food manufacturing industries, and others, which poses a serious environmental problem. According to a previous study by Ray et al. (2017), eggshells contain 95% calcium carbonate and the remaining 5% includes magnesium, phosphorus, sodium, potassium, and silica. The eggshells is a good source of calcium carbonate powder. In this study, calcium carbonate powder was extracted from waste eggshell for the purpose of producing calcium lactate.

3.1.6 Calcium Carbonate

Calcium carbonate is a natural material with a microparticle size as compared to cement particles. This property of $CaCO_3$ improves the particle packing of concrete and is used as a crack healer. $CaCO_3$ was extracted from waste eggshells in the laboratory. The formation of $CaCO_3$ was checked through X-ray powder diffraction at Adama Science and Technology University, Materials Science and Engineering laboratory.

3.1.7 Lactic Acid

Lactic acid is a chemical byproduct of the anaerobic respiration of bacteria during energy production. For the production of calcium lactate, the author acquired commercial lactic acid ($C_3H_6O_3$) from the Addis Abeba chemical laboratory.

3.1.8 Calcium Lactate

Calcium lactate is a white crystalline salt with the formula $C_6H_{10}CaO_6$. It can be prepared commercially by the neutralization reaction of lactic acid with calcium oxide. Calcium lactate ($C_6H_{10}CaO_6$) improves compressive strength and precipitates $CaCO_3$ as water and oxygen enter the cracked concrete. The experimenter prepared $C_6H_{10}CaO_6$ from lactic acid and $CaCO_3$, and its production was checked through XRD at Adama Science and Technology University, Materials Science and Engineering laboratory.

3.1.9 Bacillus Subtilis Bacteria

Bacteria are used as a self-healing agent, and they should be able to survive in a high alkaline environment for a long period of time and be able to form spores that resist mechanical forces during concrete mixing. A bacteria strain was collected from Adama Science and Technology University, Molecular Biology Laboratory. A bacterial solution was prepared at two different concentrations in a medium for use, which could potentially produce calcite-based bio-minerals. In this work, Bacillus subtilis bacteria was used. The reason for using Bacillus subtilis is due to its resistance to alkaline environments and its ability to precipitate calcite to seal cracks.

3.2 Research Methods

Methods in material research refer to a logical and coherent scheme in which experimental investigations are carried out. The current study uses both qualitative and quantitative research methods to interpret and discuss the research output. The research design being employed was an experimental research design. This section clearly outlines the research procedures employed and the type of test conducted to accomplish research objectives. The experimental test results were analyzed by Origin software, X'pert high-score plus software, and Excel. The results of the analysis were presented in the form of tables, graphs, and charts.

The experimental program followed is described in the flowchart given in Figure 3.1 below.

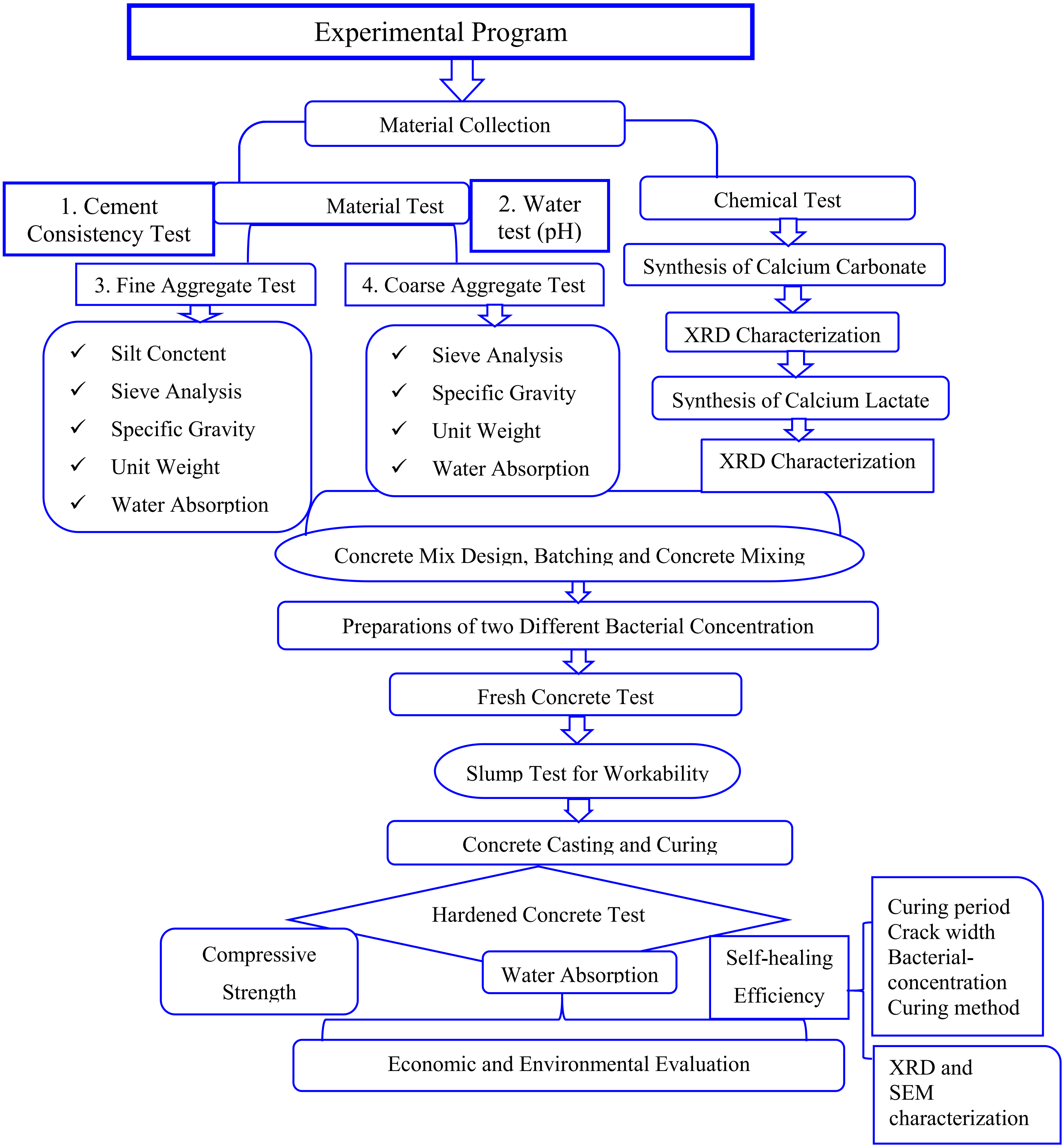

Figure 3.1 Research Method Flowchart

3.2.1 Tests on Cement

3.2.1.1 Normal Consistency Test for Cement

The consistency of cement test is used to evaluate how much water should be added to cement in order to achieve standard consistency or normal consistency. The normal consistency test of cement is recommended to be measssssssured using the (ASTM C 187) method. As a result, a vicat apparatus was used to determine the typical consistency. This test was performed according to the instructions in (ASTM C 187).

1. 400 grams of cement were measured.
2. Water amounting to a percentage of cement (22-30%) was added to cement and mixed.
3. Within 3-5 minutes, properly combine the paste. Gauging time is the time it takes to get cement paste after adding water.
4. filled the paste in the Vicat mold appropriately, and removed any surplus paste with a trowel.
5. Then, set the Vicat mold on the glass plate, making sure the plunger lightly touches the surface of the Vicat mold.
6. Allow the plunger to sink into the test mold after it has been released.
7. Take note of the plunger's penetration from the bottom of the mold as indicated on the scale.
8. Repeat the experiment with varied percentages of water until the Vicat apparatus scale reading is between 5-7 mm.
9. The water added is right and the penetration is between 5 mm and 7 mm.

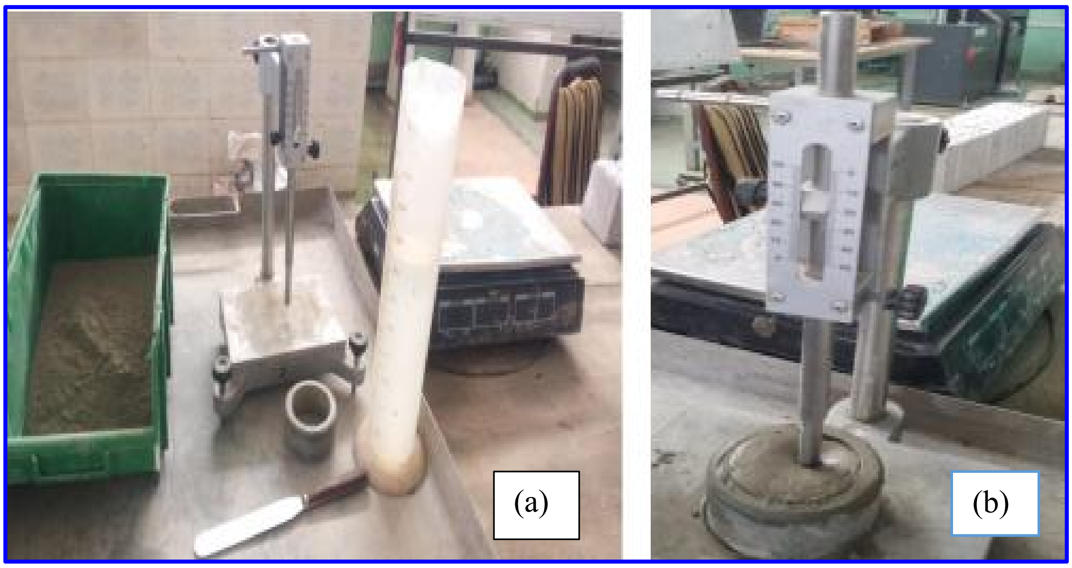

Figure 3.2 Vicat Appratus (a), Normal Consistency Test (b)

3.2.2 Tests for Fine Aggregate

3.2.2.1 Silt Content of Fine Aggregate

Clay, silt, loam, and dust are commonly found in sand. The presence of such particles in sand reduces concrete's compressive strength and long-term durability. As a result, testing the silt content of sand and comparing it to acceptable limits is critical. The major goal of this test was to figure out how much silt was in the sand. For this experiment, sample sand, clean water, a graduated jar, a spoon, a dish for taking a sand sample, and a funnel were used. The following are detailed procedures that were followed based on ASTM C 117.

Test Procedure for Silt Content

1) The researcher took a graduated cylinder having a capacity of 1000 ml.
2) 300 ml of sand was poured into the cylinder.
3) Approximately 3/4 of the jar was filled with water.
4) The jar was shaken vigorously for about a minute.
5) The jar was left for an hour to allow the silt to settle on the layer of sand.
6) The amount of fine forming a separate layer on the top was measured.
7) The silt content was calculated based on Equation 3.1.

Figure 3.3 Silt Content Test

$$\text{Silt content} = \frac{\text{Silt deposited above the sand (A)}}{\text{Amount of clean sand (B)}} \text{ x } 100\% \text{ ………. Equation 3.1}$$

3.2.2.2 Sieve Analysis of Fine Aggregate

Sieve analysis is a procedure used to assess the particle size distribution of granular material by allowing the material to pass through a series of sieves of progressively smaller mesh sizes and weighting the amount of material that is retained in each sieve as a fraction of the whole mass. Hence, the aim of this test was to determine the fineness modulus of fine aggregate with the help of a series of IS sieves having (4.75 mm, 2.36 mm, 1.18 mm, 0.6 mm, 0.3 mm, 0.15, and pan) sizes from top to bottom, respectively, 500 g of fine aggregate, a balance, sieve shaker, shovel, and sieve brush. The test procedure was in accordance with (ASTM C136). The range of fineness modulus is between 2.3-3.1 (ASTM C33).

Procedure for Grading Fine Aggregate

1. The researcher weighted a sample of 2 kg of fine aggregates.
2. The sample was quartered.
3. From the quartered sample, weighing 500 g,
4. The empty sieves were weighted, and the data was recorded properly.
5. The pan was placed on the bottom and the other sieves were put on the pan with increasing opening sizes of the sieves.
6. Placed the 500 g of sample on the top of the sieves (having a larger opening size).
7. Smashed the sample for about 10 minutes in a sieve shaker.
8. Each sieve, together with the aggregate retained on it, was measured and the weight retained on each sieve was calculated.
9. The gradation chart was filled in and the fineness modulus was computed.

$$\text{Fineness modulus} = \sum_{n=1}^{7} (\text{Cummulative retained by mass} / 100) \text{.....Equation 3.2}$$

Figure 3.4 Sieve Analysis of Fine Aggregate Test

3.2.2.3 Unit Weight, Specific Gravity, and Water Absorption of Fine Aggregate

The mass of a particular volume of a material divided by the mass of an equal volume of water is called specific gravity, and it indicates how much heavier the material is than water. The difference between the weight of the aggregate in the surface-dried saturated state and the weight of the oven-dried aggregate is used to calculate the water absorption of an aggregate. The density of fine aggregate varies depending on whether it is wet, dry, or loose. The specific gravity and water absorption capacity of fine aggregate were calculated using the ASTM C128 standard in this experiment. The range of specific gravity is 2.5–3 (ASTM C128).

A) Unit Weight of Fine Aggregate (UWFA) Test Procedure

1. Fill the measure one-third full and level the surface with your fingers. Rod the layer of aggregate with 25 strokes with the tamping rod evenly distributed over the surface. Then fill the measure to two-thirds capacity, level and rod as before. Finally, fill the measuring cup to overflowing and rod as above.
2. Level the surface of the aggregate with your fingers in such a way that any slight projections of the large pieces of the coarse aggregate approximately balance the larger voids in the surface below the top of the measure.
3. When roding the first layer, do not allow the rod to strike the bottom of the measure forcibly. In roding, the second and third layers use only enough force to cause the taping rod to penetrate the previous layers of aggregate.
4. The fine aggregate was weighed and the data were recorded as follow:

X: Fine aggregate plus cylinder weight = 6,674 g.

Y: Weight of empty cylinder = 4,734 g

V: Cylinder volume = 0.001375 m3

$$UWFA = \frac{X - Y}{V} \quad \text{...Equation 3.3}$$

A) Specific Gravity and Water Absorption of Fine Aggregate

Preparation of The Test Specimen:

1) Approximately 1 kg of the fine aggregate was prepared.
2) At 110°C, the sample was dried to a constant weight in a suitable pan. Allow it to cool for 24 hours and then make it saturated.

3) The excess water was decanted with care to avoid loss of fines, spreading the sample on a flat, non-absorbent surface exposed to a gently moving current of warm air.

4) The sample was stirred frequently to get homogeneous drying until achieving the saturated surface dry condition by using the cone test for surface moisture.

5) Hold the mold firmly on a smooth, non-absorbent surface with a large diameter. Placed a portion of partially dried fine aggregate loosely in the mold by filling it to the brim and heaping additional materials above the top of the mold.

6) Lightly tamp the sand into the mold with 25 light drops of the tamper about 5 mm above the top surface of the sand.

7) The surface was adjusted by removing loose sand from the base and lifting the mold vertically. If surface moisture was still present, the sand would retain the molded shape. When the sand slumped slightly, it indicated that it had reached S.S.D. condition.

Procedure:

1. The S.S.D sample was weighted at 500 g.
2. Partially fill the Pycnometer with water and put 500 g of saturated surface dry aggregates into the Pycnometer.
3. Then they filled the pycnometer with additional water to fill it to 90% of its capacity.
4. The pycnometer was rolled and inverted to eliminate all air bubbles.
5. Place the Pycnometer in a water bath at 23 °C for an hour.
6. Brought the water level in the pycnometer to its calibrated capacity.
7. Then, the total weight of the pycnometer, specimen, and water was measured.
8. The researcher removed the fine aggregate from the pycnometer, dried it to a constant weight at 105 °C, cooled it in room temperature air for one hour, and measured it.
9. The weight of the pycnometer filled to capacity with water was determined at 23°C, and the following data were recorded:

X: Weight of oven-dry specimen in air = 482 g

Y: Weight of water-filled pycnometer = 1460 g

Z: Weight of the saturated surface-dry specimen = 500 g

W: Pycnometer weight with specimen and water to calibration mark = 1,767 g

$$\text{Bsg} = \frac{Z}{Y + Z - W} \quad \text{.......... Equation 3.4}$$

$$\text{Asg} = \frac{X}{Y + X - W} \quad \text{.......... Equation 3.5}$$

$$\text{Water absorption} = \frac{Z - X}{X} \times 100\% \quad \text{.......... Equation 3.6}$$

3.2.3 Tests on Coarse Aggregate

3.2.3.1 Sieve Analysis of Coarse Aggregate

The coarse aggregate obtained from the local quarry should be tested against gradation to determine its particle size distribution. Hence, the aim of this test is to determine the fineness modulus of coarse aggregate with the help of apparatus like a series of IS sieves of sizes (20 mm, 19 mm, 12.5 mm, 9.5 mm, 4.75 mm, and pan) from top to bottom, respectively, 2,000 g of coarse aggregate, a balance, sieve shaker, shovel, and sieve brush. The test procedure followed was in accordance with (ASTM C136).

Sieve Analysis for Coarse Aggregate

1. 20 kg of coarse aggregates were weighed.
2. A representative sample was selected by quartering.
3. From the quartered sample, 2 kg was taken.
4. The empty sieves were weighted and the data was recorded properly.
5. Placed the 2 kg of sample on the top sieves (which have a large opening size).
6. smashed the sample for about 10 minutes in a sieve shaker.
7. Each sieve, together with the aggregate retained on it, was measured and the weight retained on each sieve was calculated.
8. The gradation chart was filled in and the fineness modulus was computed. The range of fineness modulus of coarse aggregate according to ASTM C33 is 5.5-8.

$$\text{Fineness modulus} = \sum_{n=1}^{11} (\text{Cummulative retained by mass} / 100) \quad \text{.....Equation 3.7}$$

Figure 3.5 Sieve Analysis of Coarse Aggregate

3.2.3.2 Unit Weight, Specific Gravity, and Water Absorption of Coarse Aggregate

Specific gravity is the ratio of the weight of a certain amount of coarse aggregate to the weight of the same amount of water. This is a measure of the strength or quality of a particular material. Low-density aggregates are generally weaker than high-density aggregates. Water absorption capacity represents the maximum amount of water that the aggregate can absorb. It gives an idea of the internal structure of the aggregate and the strength of the aggregate. The density of coarse aggregate varies depending on the source, nature, and condition, like wet or dry. The researcher determined specific gravity and water absorption capacity based on the (ASTM C127) standard. The unit weight of aggregate ranges from 1200 to 1750 kg/m^3 (ASTM C29).

A) Unit Weight of Coarse Aggregate (UWCA)

1. Fill the measure one-third full and level the surface with your fingers. Rod the layer of aggregate with 25 strokes with the tamping rod evenly distributed over the surface. Then fill the measure to two-thirds capacity, level and rod as before. Finally, fill the measuring cup to overflowing and rod as above.
2. Level the surface of the aggregate with your fingers in such a way that any slight projections of the large pieces of the coarse aggregate approximately balance the larger voids in the surface below the top of the measure.
3. When roding the first layer, do not allow the rod to strike the bottom of the measure forcibly. In roding, the second and third layers use only enough force to cause the taping rod to penetrate the previous layers of aggregate.
4. The coarse aggregate was weighted, and the data was recorded as follows.

X = aggregate plus cylinder weight = 6.977 kg

Y = Weight of the empty cylinder = 4.734 kg.

V = Volume of the cylinder (m^3) = 0.001375 m^3

The unit weight of coarse aggregate can be computed by using Equation 3.8

$$UWCA = \frac{X - Y}{V} \qquad \text{..Equation 3.8}$$

B) Specific Gravity and Water Absorption Capacity of Coarse Aggregate

Test Procedures

1) The researcher took the sample of coarse aggregate by using the sample splitter.
2) The sample was sieved with a 4.75 mm sieve, and the sample passing through the 4.75 mm sieve was ignored.
3) The sample was washed to remove dust.
4) Put the sample in the oven at 105°C for 24 hours.
5) The sample was taken out of the oven, left to cool, and then the weight was measured.
6) The sample was submerged in water for 24 hours.
7) The researcher removed the sample from the water and rolled it in a large absorbent cloth until all visible films of water were removed.
8) The required weight of the sample in its (S.S.D) condition was taken.
9) The researcher immediately placed the S.S.D sample in the sample container, determined the weight in water at 23 °C, and recorded the data.

H: Weight of air-dried oven-dried specimen = 2,950 g

G: Weight of the saturated surface-dry specimen = 3000 g

F: Pycnometer weight with specimen and water to calibration mark = 1,848 g

The Bsg, Asg, and water absorption of coarse aggregate can be computed based on the following Equation:

$$\text{Bsg} = \frac{G}{G-F} \quad \text{......Equation 3.9}$$

$$\text{Asg} = \frac{H}{H-F} \quad \text{......Equation 3.10}$$

$$\text{Water absorption} = \frac{G-H}{H} \times 100\% \quad \text{......Equation 3.11}$$

3.2.4 Water Test

Concrete is affected by the pH of the water. As a result, a pH meter was used to test the pH of the mixing and curing water. The procedure involved preparing the water sample, placing the electrode in the buffer, inserting the electrode into the prepared sample, and reading the pH was the procedure used.

3.2.5 Synthesis of Calcium Carbonate from Waste Eggshells

Calcium carbonate is abundant in the hen's eggshell. As a result, the well-known crack-filling chemical $CaCO_3$ was derived from waste eggshell to keep self-healing costs low and the environment safe, as eggshell is a waste product. As a result, the researcher used a solid-state reaction technique to extract calcium carbonate from discarded eggshells in the following steps below (Figure 3.6).

1. Collection of Waste Eggshells

An eggshell was collected from Adama Science and Technology University cafeteria and stored in a basket after it had been dried. An eggshell was dried to remove the moisture, avoid a bad smell, and stick together during the storage period. After all, it was stored in a basket at room temperature until further treatment.

2. Washing and Drying of an Eggshells

After collecting, drying, and storing an eggshell, it was washed in a washing tank to eliminate any dirt before being allowed to dry at room temperature for two days. This was done because some filthy materials could not be eliminated during the boiling process unless they were washed first.

3. Boiling of an Eggshells

In a water heater, the washed and cleaned eggshell was boiled for 1 hour at 205 °C. The water to eggshell ratio was 40:1 (mL/g), and the eggshell was boiled to eliminate any waste while leaving the extra nutrients intact. The eggshell was boiled to destroy any bacteria or other harmful pathogens.

4. Drying of an Eggshells

After boiling an eggshell in a water heater, it was spread on a stainless-steel sheet and oven-dried for 2 hours at 100 °C to eliminate moisture and make the crushing process easier.

5. Grinding

The eggshell size was reduced to the size required for sieving by grinding it in a grinder. One of the most important processes in the synthesis of calcium carbonate from waste eggshells was this procedure.

6. Sieving

The larger particles were separated from the smaller particles by sieving. To separate the finer particles from the coarser ones, the crushed eggshell was sieved through a 100 µm sieve. The synthesis of calcium carbonate from discharged eggshell was confirmed by XRD

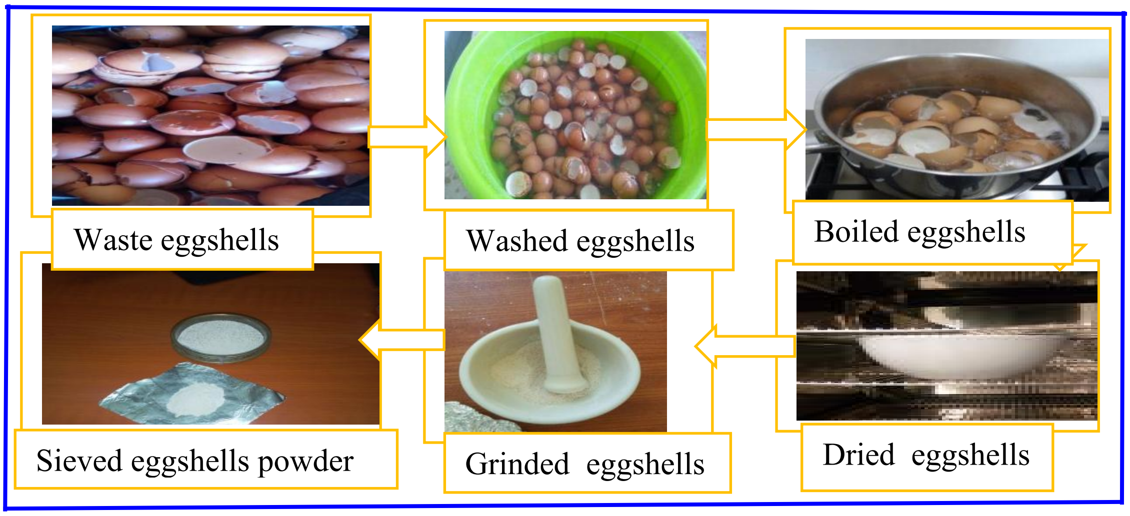

Figure 3.6 Flow Diagram for Extracting Calcium Carbonate from Waste Eggshell

3.2.6 Synthesis of Calcium Lactate

At a temperature of 45 °C, 100 ml of distilled water was mixed with 20 mL of lactic acid and stirred by a magnetic stirrer for 16 minutes to dissolve effectively, then 10 g of calcium carbonate powder was added and stirred by a magnetic stirrer for an additional 2 hours at a temperature of 45 °C with a rotation speed of 550 rpm. After 25 minutes, it was filtered with filtrate paper, dried, pulverized, and sieved to get calcium lactate powder (Figure 3.7).

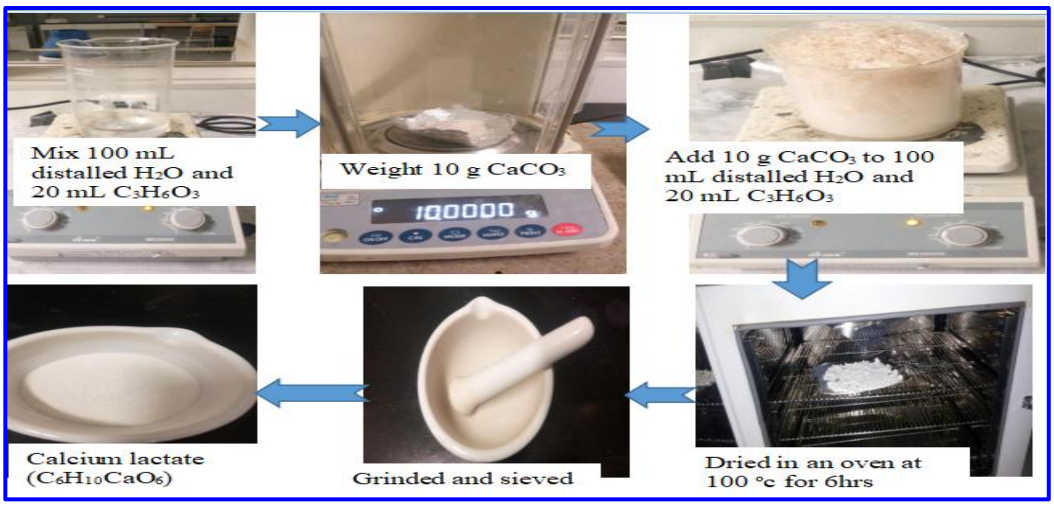

Figure 3.7 Calcium Lactate Synthesis Flow-Diagram

3.2.6.1 Characterization of Calcium Lactate

XRD and SEM images were used to confirm the production of calcium lactate. SEM and XRD analysis were used to confirm the production of calcium lactate from discarded eggshells and lactic acid in this study. The procedure employed here was to take a small amount of powder and do XRD (to determine crystal peaks) and SEM (to determine internal morphology).

3.2.7 Preparation of Bacterial Concentrations

Bacillus subtilus was chosen for this particular study because of its excellent survival in an alkaline, harsh environment and the effectiveness of precipitating $CaCO_3$ to fill cracks. The bacteria strain was taken from Adama Science and Technology University, Department of Biology, Molecular Biology Laboratory, and the bacteria were grown in a liquid medium.

Figure 3.8 Bacillus Subtils Bacteria Strain

3.2.7.1 Preparation of Culturing Media

Media may be solid (agar) or liquid (broth). To grow bacteria, either agar or broth can be used. For this specific work, yeast extract and molasses were used as a culturing medium for Bacillus subtilis bacteria. Culturing media is a solution consisting of nutrients for the growth and survival of bacteria. In this study, 8 g of yeast extract and 4 g of molasses were added to a conical flask containing 400 mL of distilled water and covered with aluminum foil. It is sterilized in an autoclave at 121°C for 15 minutes.

3.2.7.2 Culturing of Bacteria

After sterilization of the media, the conical flask was opened, and 1 mL of the bacteria was added from the microbial bank. Then, the bacteria were incubated at a temperature of 37 °C in an orbital shaker at an average speed of 125 rpm for (24–48) hours to get a different bacterial concentration.

Figure 3.9 Cultured Bacillus Subtilis Bacteria on Yeast Extract and Molasses

3.2.7.3 Viable Cell Measurement

After (24–48) hours of incubation, the bacteria in a colony were measured for absorbency using an optical density reading (OD600). Then, the concentration (cell/mL) was calculated based on a spectrometer reading at OD600 using the formula given (Nain et al., 2019).

Cells/ml = 8×10^8 cells/mL x absorbency (OD600) …………………..Equation 3.12

3.2.8 Mix Design

Concrete mix design is the process of finding the right proportion of cement, fine aggregate, and coarse aggregate for concrete to achieve the desired strength. The mix ratio depends on the mix design. Therefore, the concrete mix design can be specified as concrete mixture = cement: fine aggregate: coarse aggregate for C-30 concrete grade. The C-30 concrete grade was designed because the major application area of bacterial self-healing concrete is in the construction of bridges and in all asphalt concrete as they often experience cracks due to heavy loads and regularly need maintenance. For bridge and road construction, C-30 concrete grade is used.

The amount of cement, fine aggregate, coarse aggregate, and water was determined by the properties of the concrete ingredients and the test results obtained from the ingredients. Different concentrations of bacterial solution (4.56×10^8 and 9.84×10^6) cells/mL were prepared and added to the concrete mix directly. The amount of calcium lactate added to the mix was 1% of the cement since it affects the compressive strength negatively if more than 1% is added. The proportioning of concrete ingredients was done in accordance with ACI the 211.1 method of mixing by the following procedures:

Step 1: Calculating the required mean compressive strength based on characteristic strength of 30 MPa which gives; fck = f'ck +8.5 = 30 + 8.5 = 38.5 MPa

Table 3.1 Average Compressive strength Conversion

Characteristics strength (f'ck, MPa)	Mean strength (fck, MPa)
< 21	F'ck +7
21-35	F'ck +8.5
>35	1.1 x F'ck +5

Step 2: Determining the minimum cement content

From a durability point of view, the minimum cement content was taken as 300 kg/m^3.

Step 3: Choose a Slump Value

For C-30, a concrete slump of 2–10 cm is recommended.

Step 4: Choose the maximum aggregate size.

For higher compressive strength, a reduced maximum size aggregate was selected. In this case, the maximum size aggregate was 20, and the nominal size aggregate was 19 mm.

Step 5: Mixing water and air content determination

The amount of water per unit volume of concrete required for a required slump value is dependent on aggregate grading, amount of entrained air, and maximum size aggregate.

Table 3.2 Mixing Water for different Slump and Maximum Size Aggregate

Slump (cm)	Water (kg/m^3) of concrete for indicated maximum size aggregate in mm							
	10	12.5	20	25	40	50	70	150
			Non-air entrained concrete					
2-10	205	200	185	180	160	155	145	125
8-10	225	215	200	195	175	170	160	140
15-18	240	230	210	205	205	185	180	170-
Amount of entrapped air (%)	3	25	2	15	1	0.5	0.3	0.2

In Table 3.2 above, with a slump of 2–10 cm and a maximum size aggregate of 20 mm, the water content becomes 185 kg/m^3 and 2%, or 20 liters of entrapped air.

Step 6: Determine the water-cement ratio

In a concrete mix, the water-cement ratio is the ratio of the weight of water to the weight of cement.

Table 3.3 Average Compressive Strength with water Cement Ratio

Compressive strength at 28 days (MPa)	Water cement ratio (by mass)
45	0.38
40	0.42
35	0.47
30	0.54
25	0.61
20	0.69
15	0.79

The ACI table above cannot provide the exact value of the water-cement ratio for a 38.5 MPa mean strength. This can be calculated via interpolating the above and below values as follows: 38.5 MPa is found between 35 and 40 MPa.

40	0.42
38.5	x
35	0.47

By interpolation, $$\frac{40-38.5}{0.42-x}=\frac{38.5-35}{x-0.47}$$

By solving the above equation, x = 0.435

Hence, the minimum water cement ratio is 0.435

Step 7: Determination of mix cement content

$$\text{Cement content} = \frac{\text{water content}}{\text{water cement ratio}}$$

$$= \frac{185}{0.435}$$

$$= 425.29 \text{ kg/m}^3$$

Since the mix cement content is higher than the minimum cement use,

Step 8: Estimating the Bulk Volume Per Unit Volume of Concrete

This depends on the fineness modulus, which is 2.78, and the maximum size aggregate of 20 mm.

Table 3.4 Volume of Coarse Aggregate per unit Volume of Concrete

Maximum size of aggregate	Volume of coarse aggregate per volume of concrete for different fineness modulus			
	2.4	2.6	2.8	3.0
10		0.50	0.46	0.44
12.5		0.59	0.55	0.53
20		0.66	0.62	0.60
25		0.71	0.67	0.65
40		0.76	0.72	0.70
50		0.78	0.74	0.72
70		0.81	0.77	0.75
150		0.87	0.83	0.81

The bulk volume of dry rodded aggregate was not found in the above table directly. It can be calculated by interpolation since the fineness modulus of 2.78 is found between 2.6 and 2.8 for a 20 mm maximum size aggregate.

2.6	0.66
2.78	x
2.8	0.62

By interpolation, $$\frac{2.6 - 2.78}{0.66 - x} = \frac{2.78 - 2.8}{x - 0.62}$$

By solving the equation above, $x = 0.624$

Hence, the dry volume of aggregate per volume of concrete is 0.624.

Step 9: Calculate the weight of coarse aggregate (WCA) per m^3 of concrete.

WCA= bulk volume x bulk density of coarse aggregate

WCA = 0.624 x 1631.64

= 1,018.14 kg/m^3

Step 10: Determining the solid volume of coarse aggregate.

$$\text{solid volume of coarse aggregate} = \frac{\text{WCA}}{\text{specific gravity}}$$

$$= \frac{1{,}018.14\ \text{kg/m3}}{2.68}$$

= 379.9 kg/m^3

Step 11: Calculating the solid volume of cement, water, and air

$$\text{volume of cement (VC)} = \frac{\text{weight of cement}}{\text{specific gravity of cement}}$$

$$= \frac{425.29}{3.15}$$

= 135.01 kg/m^3

Volume of water (VW) = 185 kg/m^3

Volume of air (VA) = 2% or 20 kg/m^3

Step 12: Calculating solid volume of sand

Solid volume of sand = 1000 - (VCA + VC + VW + VA)

= 1000 - (379.9 + 135.01 + 185 + 20)

1000 - 719.91

= 280.09 kg/m^3

Solid weight of sand = dry volume of sand x specific gravity

= 280.09 kg/m^3 x 2.75

= 770.25 kg/m^3

Step 13: Adjustments for moisture in the aggregate

Fine aggregate adsorption = 3.7% and coarse aggregate absorption = 1.67%

Water absorbed by coarse aggregate = 1,018.14 kg/m^3 x 0.0167

= 17 kg/m^3

Water supplied by fine aggregate = 770.25 kg/m^3 x 0.037

= 28.5 kg/m^3

Amount of water needed = 185 kg/m^3 + 17 kg/m^3 - 28.5 kg/m^3

= 173.5 kg/m^3

Cement = 425.29 kg/m^3

Fine aggregate = 770.25 kg/m^3 + 28.5 kg/m^3

= 798.75 kg/m^3

Coarse aggregate = 1,018.14 kg/m^3 - 18.05 kg/m^3

= 1001 kg/m^3

Hence, the estimated batch weight for 1 cube of concrete is given in Table 3.5.

Table 3.5 Calculated Batch for 1 m^3 of Concrete

Water	173.5 kg/m^3
cement	425.29 kg/m^3
Fine aggregate	798.75 kg/m^3
Coarse aggregate	1001 kg/m^3

The above result in the mix design ratio can be expressed in Table 3.6 below.

Table 3.6 Mix Ratio for C-30 Concrete Grade

Ingredients	Cement	Fine aggregate	Coarse aggregate
Amount / m^3	425.29/425.29	798.75 /425.29	1001 /425.29
Ratio	1	1.88	2.35

Based on the mix proportion given above, the quantity of each concrete ingredient can be calculated for one cube standard mold.

Wet volume for 1 mold =length x width x height

= 0.15 x 0.15 x 0.15

= 0.00375 m^3

Dry volume = wet volume x 1.55

= 0.00375 m^3 x 1.55

= 0.0058125 m^3

Sum of ratio = 1 + 1.88 + 2.35 = 5.23

$$\text{weight of cement} = \frac{1}{\text{sum of ratio}} \text{ x dry volume x unit weight of cement}$$

$$= \frac{1}{5.23} \text{ x } 0.0058125 \text{ x } 1440$$

$$= 1.6 \text{ kg}$$

$$\text{weight of FA} = \frac{1.88}{\text{sum of ratio}} \text{ x dry volume x unit weight of FA}$$

$$= \frac{1.88}{5.23} \text{ x } 0.0058125 \text{ x } 1{,}410.14$$

$$= 2.95 \text{ kg}$$

$$\text{weight of CA} = \frac{2.35}{\text{sum of ratio}} \text{ x dry volume x unit weight of CA}$$

$$= \frac{2.35}{5.23} \text{ x } 0.0058125 \text{ x } 1{,}631.64$$

$$= 4.26 \text{ kg}$$

$$\text{weight of water} = \text{ amount of water needed} * \text{ dry volume}$$

$$= 173.5 \text{ x } 0.0058125$$

$$= 1.01 \text{ kg (L)}$$

Table 3.7 Summary of Concrete Mix for one Cube Mould

No	Bacterial concentration (cells/mL)	Mix code	Dosage (mL)	Cement (kg)	Fine aggregate (kg)	Coarse aggregate (kg)	Calcium lactate (g) 1% of cement	Water (mL)
1	Control	SHC0	0	1.6	2.95	4.26	0	1010
2	9.84×10^6	SHC10,6	10	1.58	2.95	4.26	16	1010
		SHC20,6	20	1.58	2.95	4.26	16	1010
		SHC30,6	30	1.58	2.95	4.26	16	1010
3	4.56×10^8	SHC10,8	10	1.58	2.95	4.26	16	1010
		SHC20,8	20	1.58	2.95	4.26	16	1010
		SHC30,8	30	1.58	2.95	4.26	16	1010

N. B, In the above mix code, SHC indicates self-healing concrete, 6 and 8 represent cell concentration per mL, and 10, 20, and 30 represent bacterial dosage in mL.

3.2.9 Batching and Mixing

3.2.9.1 Batching

Batching of concrete is the process of measuring concrete ingredients to get concrete mixtures. For this specific experiment, batching by weight was preferred over volume batching to get a proper mix of concrete ingredients since it is difficult to find the exact volume of granular materials because of their voids.

3.2.9.2 Concrete Mixing

Concrete mixing is the process of combining concrete components like cement, fine aggregate, coarse aggregate, water, and other ingredients to get effective and good-quality concrete. In this study, a mixer was used to mix concrete ingredients together to obtain homogeneous, good-quality concrete.

Figure 3.10 Concrete Mixing: Mixer (a), Dry Mix (b)

3.3 Fresh Concrete Test

3.3.1 Slump Cone Test for Workability of Concrete

A slump test is a type of physical property test done on fresh concrete to determine the concrete's ability to be placed, transported, easy flow, and other properties.

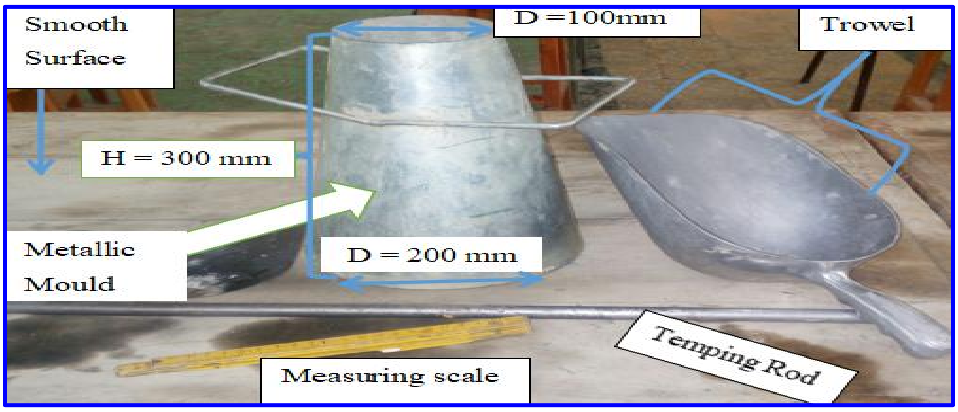

Figure 3.11 Slump Cone Test Apparatus

Therefore, a slump test was conducted to determine the degree of workability and mix quality of the concrete based on the (ASTM C143) standard.

Slump test procedure

1. First, the slump cone was placed on a smooth metal plate.
2. The slump cone was filled with freshly mixed concrete in three different layers.
3. Each layer of the concrete mix was tapped 25 times with a 600 mm long metal rod that was 16 mm in diameter.
4. Extra concrete was removed after filling the last layer from the top of the cone.
5. The slump cone was then quickly lifted upward with two hands. The concrete is then free to fall.
6. After free fall, the remaining height is known as a slump (the difference between the height of the mold and the height of the vertical axis) and was measured.

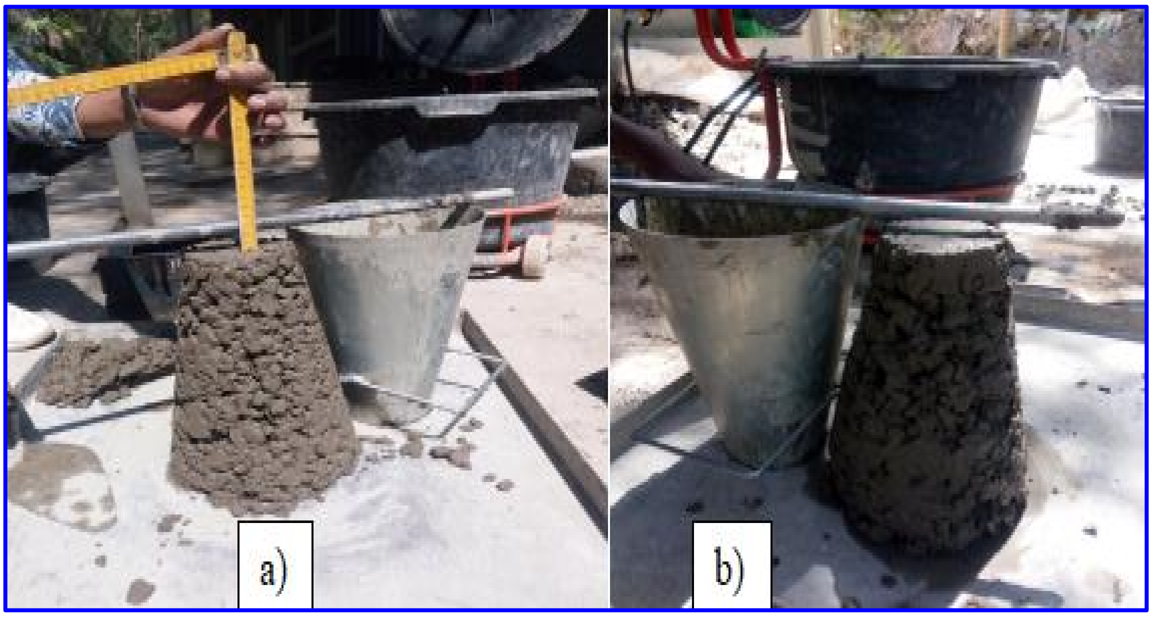

Figure 3.12 Slump Test a) Bacterial Concrete, b) Conventional Concrete

3.4 Casting of Concrete Specimens and Curing

3.4.1 Concrete Casting

The compressive strength of concrete was investigated after casting a concrete cube with a 150 x 150 x 150 mm size. The experimenter prepared concrete specimens by incorporating major concrete ingredients such as cement, fine aggregate, coarse aggregate, and water with two different bacterial concentrations with different dosages (10, 20, and 30) mL from 9.84 x 10^6 and 4.56 x 10^8) cells/mL of bacterial concentrations and calcium lactate (1% of cement). As per the study (Priyom et al. (2018); Sakna et al. (2021)), the amount of calcium lactate does not exceed 1% of cement since it affects compressive strength negatively. The researcher mixed, placed, and compacted the concrete in different layers and demolded the samples after 24 hours.

Figure 3.13 Concrete Casting

3.4.2 Curing of Concrete Specimens

Curing of concrete is a process of providing sufficient moisture, temperature, and time so that the hydration of cement continues till the concrete achieves its desired properties for the intended use based on ASTM C192. After demolding the concrete specimens, the researcher cured the concrete at room temperature for 7, 14, and 28 days in a water curing medium (Figure 3.14). At 7 days of curing, concrete attains 65% of its target mean strength, 90% at 14 days, and it attains 99% of its target mean strength at a curing age of 28 days.

Figure 3.14 Concrete Curing

The properties of hardened concrete were investigated after casting a concrete cube having 150 x 150 x 150 mm size. The experimenter prepared concrete specimens by incorporating major concrete ingredients (cement, sand, coarse aggregate, and water) with different bacterial concentrations and calcium lactate.

3.5 Hardened Concrete Test

Hardened concrete is one of the most durable and robust building materials available, capable of supporting structural and service loads. One of the goals of hardened concrete testing is to guarantee that the concrete used has the strength and durability required.

3.5.1 Compressive Strength Test

Compressive strength is the ability of hardened concrete to withstand axial loads without any cracks or deflection. Therefore, the aim of this test was to determine the compressive strength of concrete with and without bacterial concentration and calcium lactate. The balance, mold, temping road, compressive test machine, trowel, shovel, and brush were used in the test. A concrete cube of sample size 150 x 150 x 150 mm were cast to investigate the compressive strength of bacterial and normal concrete. The researcher determined the compressive strength after 7, 14, and 28 days of curing by using an automatic compressive strength test machine at Adama Science and Technology University, Construction Material Laboratory, in accordance with (ASTM C39). To undergo the compressive strength test, the cast cubes were taken out of the curing water after 7, 14, and 28 curing periods and wiped out excess water from the surface. The test machine was then cleaned, placed the sample in the test machine, and applied the load at a rate of 14 N/mm^2/minute, having a load capacity of 3000 KN. When the specimens failed, the maximum load was recorded, and finally, the compressive strength was calculated.

Compressive strength = Load / cross-sectional area of the sample…………..Equation 3.13

The test results were compared to the target mean and characteristic strengths. The target mean strength is determined by designing the concrete mix according to the code. The characteristic strength is the value of concrete strength at which no more than 5% of the test results fall below the value. The strength range between the highest and lowest individual test results was calculated and found to be below 15% of the mean. An invalid result implies that the test technique has one or more flaws. There were no incorrect results in this study. Aside from that, no more than 5% of individual test results fell below the characteristic compressive strength.

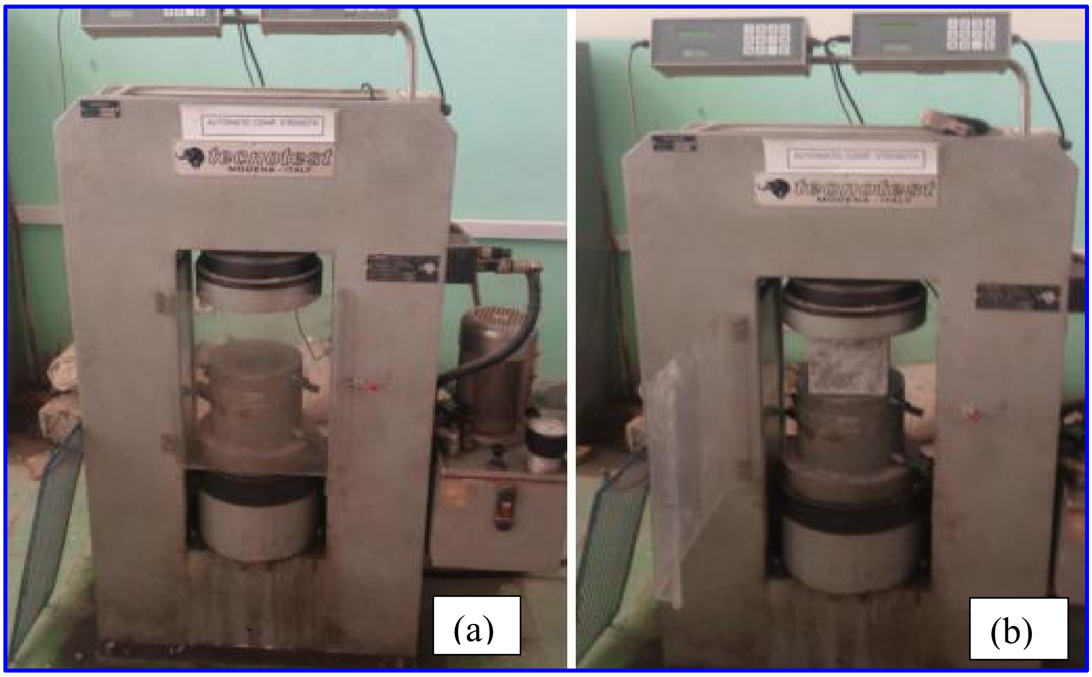

Figure 3.15 Automatic Compressive Test Machine (a), Compressive Strength Test (b)

3.5.2 Durability Test

3.5.2.1 Water Absorption Test

Water absorption is the measure of water penetration resistance of concrete specimens. A concrete cube of sample size 70 x 70 x 70 mm were cast to investigate the water absorption capacity of bacterial and normal concrete. This research examined the water absorption of normal and bacterial concrete at curing periods of 7 and 28 days to determine the water tightness of concrete. The water absorption test procedure followed was: after 7 and 28 days of curing, the samples were taken out of the curing water and dried at a temperature of 105°C for 24 hours, weighed, then immersed in curing water for 72 hours, weighed again, based on (ASTM, C1585), and the highest water absorption limit is 10%. The increase in weight as a percentage of the original weight is expressed as water absorption. The water absorption and percent reduction can be computed based on the formula:

$$\text{Water absorption } \% = \frac{A-B}{B} \times 100\% \quad \text{.............Equation 3.14}$$

Where; A = Weight of saturated surface dry concrete, B = Weight of oven-dry concrete

$$\% \text{ reduction} = \frac{\text{Difference between \% absorption of normal and bacterial concrete}}{\text{\% absorption of normal concrete}} \text{ x } 100\% \text{..Equation 3.15}$$

Figure 3.16 Mould (a), Caste Samples (b), Demold Samples (c), Dried Samples (d)

3.5.3 Characterization of Concrete via XRD and SEM

To test for the existence of carbonated crystal precipitated by bacteria, concrete samples from the top, bottom, and middle are taken after 28 days of curing of a sample containing 9.84 x 10^6 cells/mL of a 20 mL bacterial solution. The samples were then pulverized and sieved to make powder. The powdered samples were subjected to X-ray diffraction at a 2θ angle. The XRD peaks were named from XRD data and by using X'pert Highscore plus software. In addition, the interior morphology of concrete was studied using SEM. After 28 days of curing, a concrete sample from 9.84 x 10^6 cells/mL of a 20 mL bacterial solution and control concrete was obtained from the middle of the concrete and submitted to SEM image analysis at 10 kV by mounting small broken samples on brass stubs.

3.6 Formation of Artificial Crack and Self-Healing Efficiency

The self-healing efficiency of bacterial concrete was checked after casting concrete samples of size 70 x 70 x 70 mm with a mixture of cement (144.5 g), fine aggregate (274 g), coarse aggregate (397 g), and calcium lactate 1% of cement (1.5 g). Liquid bacteria having a concentration of 4.56 x 10^8 cells/mL and 9.84 x 10^6 cells/mL were directly added to the concrete during mixing. After 24 hours, the sample was de-molded from the cube and kept in the curing water for 3 days. After 3 days of curing, the samples were taken out of the curing water and broken into two halves to form artificial cracks by using the compressive machine with the aid of steel as shown in Figure 3.17. Then, the broken samples were tied together with wire, and the crack width was measured using a ruler. Finally, the self-healing efficiency was determined with respect to crack width, bacterial concentration, curing period, and methods of curing. Besides, the healing product was checked through the XRD and SEM analysis methods by scratching the healing product from the crack surface. To determine the effect of the curing method on the self-healing capability of cracked specimens, three environmental exposures were created. Immersion in water: Constant immersion in tap water. Wet-dry cycles: 3.5 days of immersion in tap water followed by 3.5 days of air exposure. Air exposure: The specimens were stored under normal conditions.

Figure 3.17 Process of Artificial Crack Formation

The rate of healing was calculated by using Equation 3.15 (Wiktor et al., 2011).

$$\% \, Healing = \frac{\text{CWi} - \text{CWt}}{\text{CWi}} \, x \, 100\% \ldots\ldots\ldots\ldots\ldots Equation \; 3.15$$

where; CWi = initial crack width, CWt = crack width at a time t

3.7 Environmental and Economic Evaluation of Self-Healing Concrete

The cost and environmental effects of self-healing concrete must be evaluated for the purpose of mass production and field application. According to many articles, the initial cost of self-healing concrete is higher than traditional concrete due to the increased cost of calcium lactate, growing media, and the requirement for substantial work. However, compared to regular concrete, the environmental impact is significantly decreased. As a result, lowering the cost of growing media and calcium lactate is crucial for producing less expensive bio-concrete. The cost and environmental impact of self-healing and regular concrete were compared in this study. To lower the cost of self-healing concrete, calcium lactate was synthesized in the laboratory from waste eggshells and lactic acid. Furthermore, to lower the expense of the bacterial growth medium, the bacteria were cultured in molasses and yeast extract. In the current study, the cost of producing calcium lactate and the cost of preparing bacterial solutions were evaluated. The results of this evaluation were compared with the previously stated cost of self-healing concrete, and a conclusion was drawn in terms of a reduction in cost. The environmental impact was also evaluated in terms of carbon dioxide emissions and embodied energy consumption for 1 m^3 of concrete. Since the bacterial concrete avoids maintenance, it eliminates the over-use of material, which results in a decrease in embodied energy and CO_2 emissions.

4. RESULTS AND DISCUSSION

4.1 Material Test Results and Discussion

The test results of cement, fine aggregate, coarse aggregte, water, calcium carbonate, calcium lactate, and bacteria were covered under this section.

4.1.1 Tests on Cement

4.1.1.2 Normal Consistency of Cement

Normal consistency, or standard consistency, is defined as the consistency that allows the Vicat plunger of 10 mm in diameter to penetrate to a point 5 mm to 7 mm from the bottom of the Vicat mold (ASTM C 187). From the test result, the normal consistency of cement paste was 28% as the Vicat plunger penetrated about 7 mm. This indicates that the amount of water to make a cement paste is 28% of the weight of cement.

4.1.2 Fine Aggregate Test Result Analysis

In this section, the results obtained from the physical tests of fine aggregate were discussed. Silt content, sieve analysis, unit weight, specific gravity, and water absorption of fine aggregate were determined and discussed.

4.1.2 .1 Silt Content of Sand

The amount of silt deposited over the clean sand was measured by silt content analysis. For the quality of the mix and to get a better result, the fine aggregate was washed after the silt content measurement to eliminate silt, clay, dirt, and other impurities (ASTM C 117). The silt content was calculated using Equation Number 3.1. From Table 4.1, the amount of silt that the fine aggregate had was 2.39%, which is in the range to be used for concrete production as per ASTM C 33.

Table 4.1 Silt Content Analysis

Items	Trial 1	Trial 2	Trial 3	Average
A	8	7	6.5	7.17
B	300	300	300	300
Silt content (%) = $\frac{A}{B}$ x 100 %	2.67	2.33	2.17	2.39%

4.1.2.2 Sieve Analysis of Fine Aggregate

Sieve analysis is used to measure the particle size distribution of material. For this work, sieve sizes of (4.75 mm, 2.36 mm, 1.18 mm, 0.6 mm, 0.3 mm, 0.15 mm, and pan) were used. Table 4.2 and Figure 4.1 illustrate the fineness modulus of fine aggregate. The fineness modulus of fine aggregate was computed by using Equation number 3.2. The result indicated that the fineness modulus of the fine aggregate was 2.78 and the percent finer was within the range of (ASTM C33).

Table 4.2 Sieve Analysis of Fine Aggregate

Sieve opening (mm)	Weight of container (g)	Weight of container + FA (gm)	Weight of FA retained (g)	Percent of FA retained (g)	Cumulative percent retained (%)	Percent finer (%)	Range of finer (%)
4.75	444	444	0	0	0	100	98-100
2.36	406	466	60	12	12	88	80-100
1.18	358	443	85	17	29	71	50-85
0.60	331	434	103	20.6	49.6	50.4	25-60
0.30	297	484	187	37.4	87	13	5-30
0.15	279	344	65	13	100	0	0-10
pan	235	253	0	0	0	0	-
	Total cumulative percentage retained by mass				277.6		

The gradation curve of fine aggregate can be given in Figure 4.1 below.

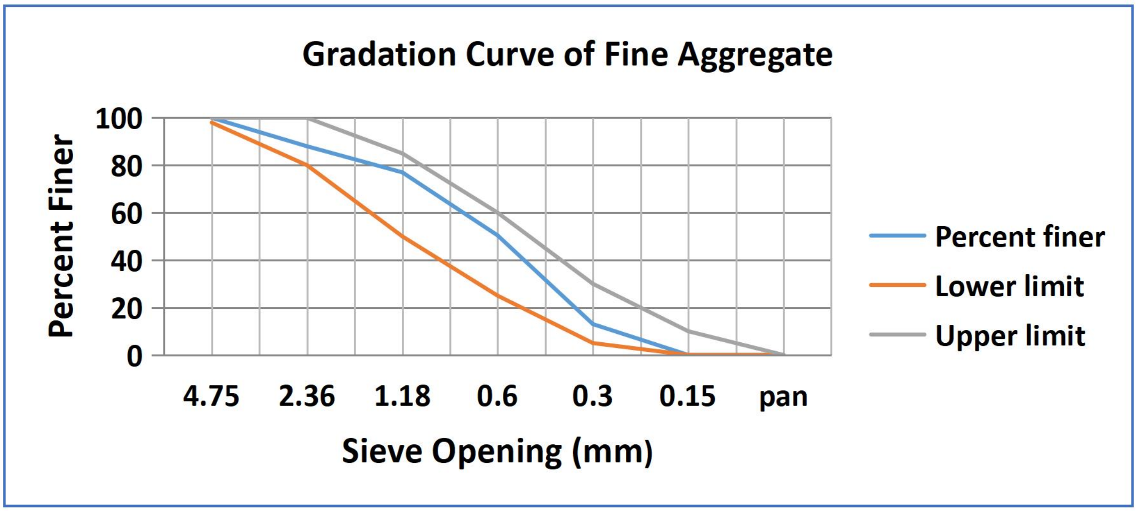

Figure 4.1 Gradation Curve of Fine Aggregate

4.1.2.3 Unit Weight of Fine Aggregate (UWFA)

The unit weight of fine aggregate measures the volume that the aggregate will occupy in the concrete. The UWFA was computed by using Equation 3.3 and the result shows that the unit weight of fine aggregate was 1,410.14 kg/m^3 (Table 4.3) and it confirms the (ASTM C29) standard.

Table 4.3 Unit Weight of Fine Aggregate Calculation

Descriptions	Quantity	Calculation
X= Weight of fine aggregate plus the cylinder	6,674 g	$UWFA = \frac{x - y}{v}$
Y= Weight of the empty cylinder	4,734 g	$= \frac{6,674 - 4,734}{0.001375}$
V= Volume of the cylinder	0.001375 m^3	$= 1,410.14$ kg/m3

4.1.2.4 Specific Gravity and Water Absorption of Fine Aggregate

Specific gravity is the ratio of the mass of a given volume of material to the mass of an equal volume of water. The water absorption of an aggregate is calculated as the ratio of the difference between the weight of the aggregate in the surface-dried saturated state and the weight of the oven-dried aggregate. In this study, the bulk specific gravity (Bsg), apparent specific gravity (Asg), and water absorption of fine aggregate were determined using Equations 3.4, 3.5, and 3.6, respectively. The Bsg, Asg, and water absorption were 2.6, 2.75, and 3.7% (Table 4.4), and all the values were consistent with the (ASTM C33) range.

Table 4.4 Specific Gravity and Water Absorption of Fine Aggregate

Descriptions	Quantity	Calculations
X: Weight of oven dry specimen in air	482 g	$Bsg = \frac{Z}{Y + Z - W}$ $= \frac{500}{1,460 + 500 - 1,767} = 2.60$
Y: Weight of pycnometer filled with water	1,460 g	$Asg = \frac{X}{Y + X - W}$ $= \frac{482}{1,460+500-1,767} = 2.75$
Z: Weight of the saturated surface-dry specimen	500 g	
W: Weight of pycnometer with specimen and water to calibration mark	1,767 g	$Absorption = \frac{Z - X}{X}$ x100% $= \frac{500-482}{482}$ x 100% = 3.7%

4.1.3 Tests on Coarse Aggregate

The aggregates retained on the 4.75 mm sieve are basically classified as coarse aggregates. It is an irregular and granular material made of crushed stone, obtained from quarries by crushing by hand or using a crusher. Under this section, sieve analysis, unit weight, and specific gravity of coarse aggregate were determined and analyzed based on the data obtained during laboratory work.

4.1.3.1 Sieve Analysis for Coarse Aggregate

The coarse aggregate obtained from the local quarry was tested against gradation to determine its particle size distribution. The fineness modulus of coarse aggregate was computed based on Equation 3.7, which gave a value of 7.16. The value of the fineness modulus of coarse aggregate was found within the range of the (ASTM C33) standard.

Table 4.5 Sieve Analysis for Coarse Aggregate

Sieve opening (mm)	Weight of container (g)	Weight of container + CA (g)	Weight of CA retained (g)	Percent of CA retained (g)	Cumulative percent retained (%)	Percent finer (%)	Range of finer (%)
20	1,381	1,381	0	0	0	100	100
19	433	490	57	2.85	2.85	97.15	95 -100
12.5	440	1,150	710	35.5	38.35	61.65	40 - 80
9.5	443	1,163	720	36.0	74.35	25.65	20 -55
4.75	444	957	513	25.65	100	0	0 -10
2.36	406	406	0	0	100	0	-
1.18	331	331	0	0	100	0	-
0.6	297	297	0	0	100	0	-
0.3	279	279	0	0	100	0	-
0.15	235	235	0	0	100	0	-
pan	253	253	0	0	0	0	-
	Total cumulative percent retained by mass				715.45		

$$Fineness\ modulus = \sum_{n=1}^{11} (cummulative\ percent\ retained\ by\ mass\ /\ 100)$$

$$= 715.45 / 100 = 7.16$$

The gradation curve of coarse aggregate can be given in Figure 4.2 below, in which the percent finer is within the range provided by the (ASTM C33) standard.

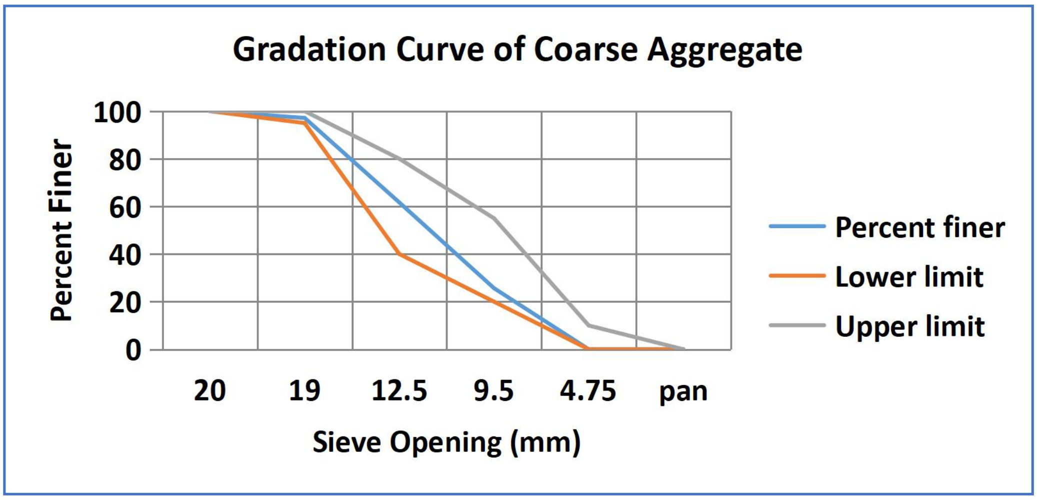

Figure 4.2 Gradation Curve of Coarse Aggregate

4.1.3.2 Unit Weight of Coarse Aggregate (UWCA)

The unit weight of coarse aggregate measures the volume that the aggregate will occupy in the concrete. The UWCA was computed using Equation 3.8 and the result is given in Table 4.6. The result shows that the unit weight of coarse aggregate is 1,631.64 kg/m^3. The test result obtained in this section satisfies the (ASTM C29) standard.

Table 4.6 Unit Weight of Coarse Aggregate Calculation

Descriptions	Quantity	Calculation
X= Weight of coarse aggregate plus the cylinder	6,977 g	$\text{UWCA} = \frac{x - y}{v}$
Y= Weight of the empty cylinder =	4,734 g	$= \frac{6.977 - 4.734}{0.001375}$
V= Volume of the cylinder	0.001375 m^3	$= 1{,}631.64$ kg/m^3

4.1.3.3 Specific Gravity and Water Absorption Capacity of Coarse Aggregate

In this thesis work, bulk specific gravity (Bsg), apparent specific gravity (Asg), and water absorption capacity of coarse aggregate were determined and discussed based on the test results obtained in the laboratory. Table 4.7 illustrates the Bsg, Asg, and water absorption of coarse aggregate, which were computed using Equations 3.9, 3.10, and 3.11, respectively. The test result showed that the Bsg, Asg, and water absorption capacities of coarse aggregate were 2.61, 2.68, and 1.67%, respectively. The test result obtained here satisfies the standard set by (ASTM C127).

Table 4.7 Specific Gravity and Water Absorption Capacity of Coarse Aggregate

Descriptions	Quantity	Calculations
H: Weight of oven dry specimen in air	2,950 g	$Bsg = \frac{G}{G - F}$ $= \frac{3,000}{3,000 - 1,848}$ = 2.61
G: Weight of the saturated surface-dry specimen	3000 g	$Asg = \frac{H}{H - F}$ $= \frac{2,950}{2,950 - 1,848}$ =2.68
F: Weight of pycnometer with specimen and water to calibration mark	1,848 g	$\text{Absorption} = \frac{G-H}{H}$ x 100% $= \frac{3,000 - 2,950}{3,000}$ x 100% =1.67%

4.1.4 Water Test

Water is one of the most important components of concrete. Oil, alkali, and acid should not be present in the water used for mixing. Water impurities can affect the strength and lifespan of concrete by preventing it from properly setting. For concrete mixing and curing, the pH level should be between 6.5 and 8.5 (ASTM C1602). When the pH falls below 6, corrosion occurs, and when the pH rises too high, concrete loses its binding properties and cracks. The pH of mixing and curing water was evaluated using a pH meter, and the result revealed that the pH was 7.56 (Figure 4.3), which is within the permissible range.

Figure 4.3 pH Measurement using pH Meter

The material test results of cement, fine aggregate, coarse aggregate, and water in the current study can be summarized in Table 4.8 below.

Table 4.8 Summary of Material Test Result

Description	Test Result					
	Cement	Fine aggregate		Coarse aggregate		Water
Silt content		2.39%				
Fineness modulus		2.78		7.16		
Unit weight		1,410.14 kg/m^3		1,631.64 kg/m^3		
Specific gravity		Bsg	2.6	Asg	2.68	
		Asg	2.75	Bsb	2.61	
Water absorption		3.7%		1.67%		
Consistency	28%					
pH						7.56

4.1.5 Synthesis of Calcium Carbonate from Waste Eggshell

An eggshell is the outer covering of a hen's egg, and it can be obtained from homes, hotels, and restaurants. It is a good source of calcium carbonate. In the current study, calcium carbonate was synthesized from discarded eggshells via a certain procedure as stated in chapter three section 3.2.5 for the production of calcium lactate. The technique used to extract calcium carbonate from waste eggshells was a solid-waste reaction mechanism. The production of $CaCO_3$ in the current study was confirmed through XRD analysis.

4.1.5.1 X-Ray Diffraction Analysis of Eggshell Powder

X-ray diffraction is a non-destructive technique for determining the structure, phase, crystal arrangement, and crystal defect of $CaCO_3$. The synthesis of calcium carbonate from waste eggshells was confirmed by X-ray diffraction analysis. Figure 4.4 illustrates the XRD spectrum of calcium carbonate synthesized from waste eggshells by the solid waste reaction procedure. An X-ray diffractometer was used to collect the X-ray diffraction pattern in an angle range of $2\theta = 10°$ to $60°$ using CuK radiation with a wavelength of 1.5406A°. The intense diffraction peaks for calcite were found at 23.18°, 29.48°, 36.117°, 39.16°, 43.33°, 47.68°, 48.74°, and 57.66°, which correspond to (012), (104), (110), (113), (202), (024), (116), and (122) diffraction peaks respectively. The highest peaks were obtained at 29.48° at a 2θ angle, having (104) diffraction peaks.

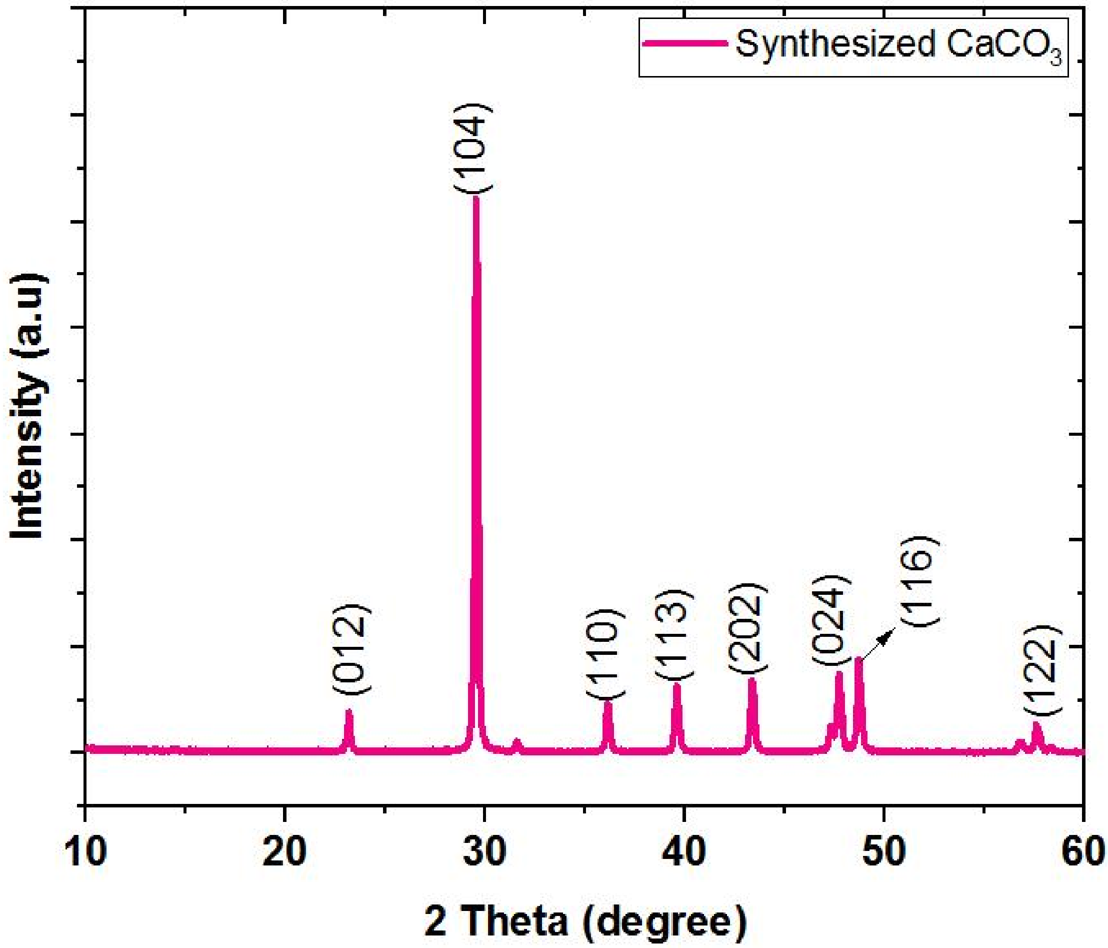

Figure 4.4 XRD Pattern of Synthesized Calcium Carbonate from Waste Eggshell

All the typical peaks were consistent with the work reported earlier (Murakami et al., 2007), and no impurity peaks were observed, indicating that calcium carbonate was synthesized successfully from waste eggshells in the current study.

4.1.6 Synthesis of Calcium Lactate from Calcium Carbonate and Lactic Acid

Calcium lactate added to the concrete is used as an additional source of calcium in the concrete. Calcium lactate is used to improve compressive strength and precipitate $CaCO_3$ as water and oxygen enter the cracked concrete. Commercially, the preparation of calcium lactate involves the chemical reaction of calcium carbonate or calcium hydroxide with lactic acid. The author prepared calcium lactate from lactic acid and calcium carbonate extracted from reduced waste eggshells for this specific experimental study. The synthesis of calcium lactate was confirmed by XRD and SEM analysis.

4.1.6.1 XRD Analysis of Synthesized Calcium Lactate

X-ray diffraction is used to determine the value of the crystal structure, degree of crystallization, orientation, and lattice parameters. The degree of crystallization is an amount that tells the crystal content in a material by contracting the peak area curve with the total area of crystalline and amorphous. XRD analysis used the principles of collision of electrons and atoms of Fe, Cr, Co, Cu, Mo, or W (Prayitno et al., 2022). The XRD result of calcium lactate showed a diffraction angle of 2θ with two major peaks at 7.78° and 9.63°, as shown in Figure 4.5. There was a similarity between the peaks of synthesized $C_6H_{10}CaO_6$ with a diffraction angle of 2θ and the peaks of calcium lactate previously studied (Tansman et al., 2014). This confirms that $C_6H_{10}CaO_6$ was synthesized in the laboratory successfully from waste eggshell powder and commercial lactic acid.

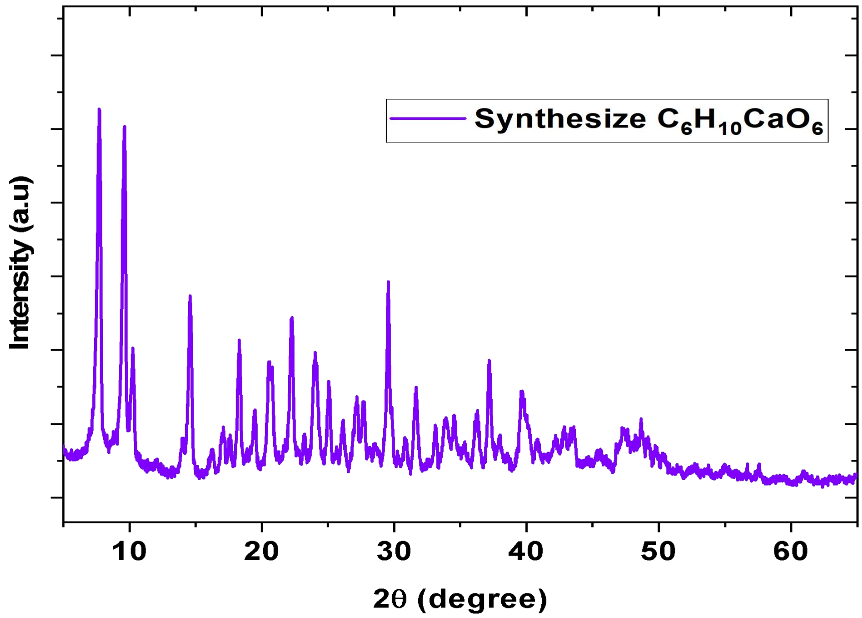

Figure 4.5 XRD Pattern of Synthesized Calcium Lactate

4.1.6.2 SEM Analysis of Synthesized Calcium Lactate

SEM imaging was used to examine the internal structure of calcium lactate, which was made from 10 g of $CaCO_3$ and 20 mL of lactic acid at 45 °C and a rotation of 550 rpm. The presence of a multilayered crystal with a rough surface that creates big aggregate crystals is seen in Figure 4.6. In previous work performed by Park et al. (2008), a similar SEM image was created using commercial $CaCO_3$ and lactic acid.

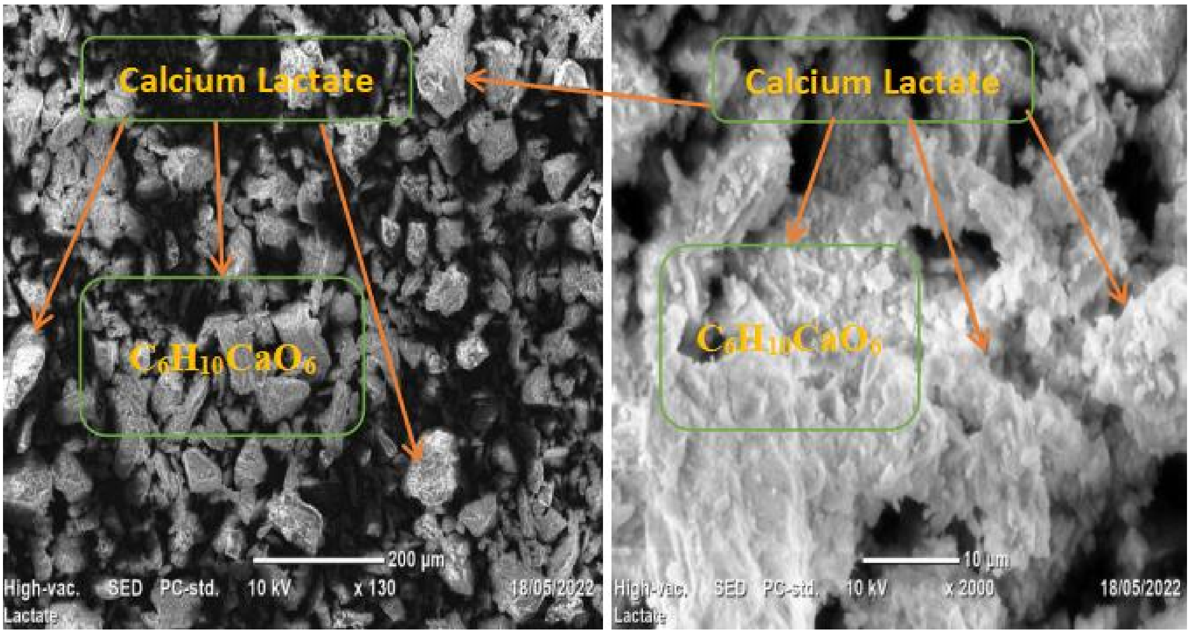

Figure 4.6 SEM Image of Synthesized Calcium Lactate

4.1.7 Viable Bacterial Cell Concentration

Bacillus subtilus bacteria was used to investigate the properties of self-healing concrete. This bacterium is useful for concrete making due to its tendency to resist the alkaline environment of concrete, having a thick cell wall, forming endospores, and precipitating calcite to fill cracks. In the current study, two bacteria concentrations were prepared after culturing the bacteria strain in yeast extract and molasses. After (24–48) hours of culturing, the bacteria's absorbency was measured by optical density measurement and the number of bacterial cells per milliliter was calculated. For the purpose of the current study, two bacterial concentrations (4.56×10^8 and 9.84×10^6) cells/mL were prepared using an OD600 measurement based on Equation 3.12 and the results are indicated in Table 4.9 below.

Table 4.9 Calculation of Bacterial Cell Concentrations

Absorbency level	Equation 3.12	Concentration (cells/mL)
0.57	8×10^8 cells/mL x absorbency (OD600)	4.56×10^8
0.0123	8×10^8 cells/mL x absorbency (OD600)	9.84×10^6

4.2 Slump Test for Workability of Fresh Concrete

The ability of fresh concrete to be mixed, transported, easily flowed, and placed is referred to as workability (ASTM C143). In this experimental investigation, the workability of bacterial and conventional concrete was investigated. In this work, the slump cone test was used to investigate the level of workability of bacterial and conventional concrete. The result of the slump value of bacterial and control concrete can be illustrated in Table 4.10 and Figure 4.7 below.

Table 4.10 Slump value of Bacterial and Conventional Concrete

No.	Mix code	Dosage of bacteria	Trial	Slump value (mm)
1	SHC0	0 m	1	24
			2	23.5
			3	23
			Average	23.5
2	SHC10	10 ml	1	26.7
			2	27.5
			3	27
			Average	27.10
3	SHC20	20 ml	1	30.6
			2	31.5
			3	31.5
			Average	31.20
4	SHC30	30 ml	1	37
			2	36
			3	36.5
			Average	36.5

The slump is a true slump, as shown in Table 4.10 and Figure 4.7, and it increases gradually as the dosage of Bacillus subtilis bacterial solution in the concrete mix increases. This is because as bacterial dosage increase the fluidity mix increaase.

In the current study, adding a bacterial solution to the concrete mixture improved the workability of fresh concrete, and similar results were reported by (Davies et al., 2018; Qian et al., 2021). This increase in slump value indicated that fresh concrete was becoming more workable, allowing it to be easily mixed, poured, and compacted. This may be due to the role of calcium lactate as a retarding agent in the concrete mix which might increases setting time and the fluidity of freshly mixd concrete (Hermawan et al., 2021).

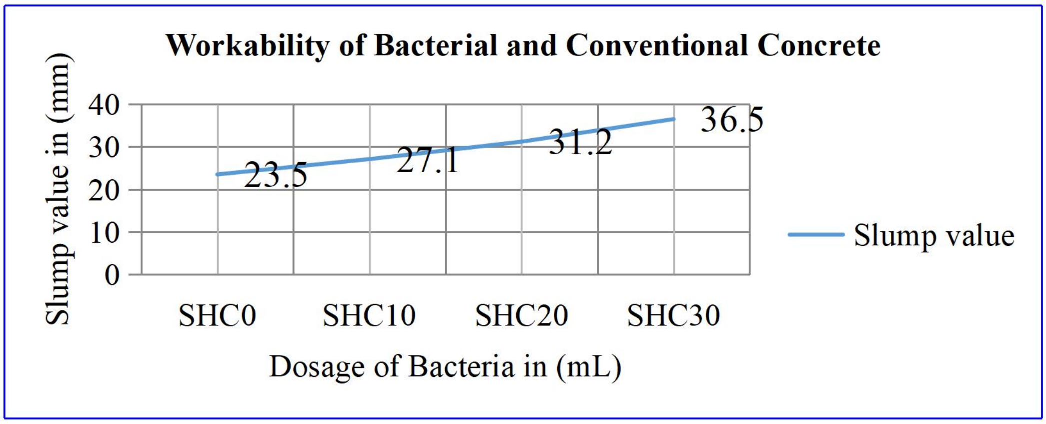

Figure 4.7 Workability of Bacterial and Conventional Concrete

4.3 Hardened Concrete Test Result

Hardened concrete is a type of concrete that is strong and capable of supporting structural and service loads. It is one of the most durable and robust construction materials. Hardened concrete is completely set and can withstand loads. In this section, the compressive strength, water absorption, and microstructure of bacterial and conventional concrete were analyzed based on the test results obtained from the laboratory.

4.3.1 Compressive Strength of Bacterial and Conventional Concrete

The ability of hardened concrete to sustain axial stress without cracking or deflection is known as compressive strength. It is critical for determining the mechanical properties of concrete samples. All concrete specimens with and without bacterial concentration and calcium lactate were examined for compressive strength at 7, 14, and 28 days of curing using an automatic compressive strength test machine (Figure 3.15). By dividing the highest load by the cross-sectional area of the samples (Equation 3.13), the compressive strength was computed. According to the current findings, the compressive strength of all bacterial concrete samples improved as compared to normal concrete. At 28 days of curing, adding 4.56×10^8 and 9.84×10^6 cells/mL of Bacillus subtilis bacterial concentration to the concrete mix increased the compressive strength by 6.42% and 14.37%, respectively, for 20 mL of bacterial dosage (Table 4.11 & Figure 4.10).

Table 4.11 Compressive Strength Test Result for Bacterial and control Concrete

Compressive Strength Test Result of Bacterial and Conventional Concrete									
No	Mix code	Dosage	Test days	Mean Load (KN)	Compressive strength (N/mm²)			strength (N/mm²)	% increase
Compressive Strength Test Result of Conventional Concrete									
					S1	S2	S3	Mean	
			7	509	23.65	21.68	22.53	22.62	
1.	SHC0	0	14	689	29.68	31.51	30.39	30.53	
		mL	28	801	34.78	35.68	36.26	35.57	
Compressive Strength Test Result of 9.84 x 10^6 Cells/mL Bacterial Concrete									
			7	598	26.17	27.88	25.72	26.59	17.55
	SHC10,6	10	14	735	31.57	33.77	32.68	32.67	7.01
		mL	28	849	38.68	36.78	38.77	37.71	6.01
			7	597	27.17	28.95	27.68	27.93	23.47
2.	SHC20,6	20	14	767	35.17	34.63	35.51	35.77	17.16
		mL	28	915	40.68	39.77	41.57	40.68	14.37
			7	562	25.13	24.77	23.78	24.98	10.43
	SHC30,6	30	14	729	32.77	32.68	31.76	32.40	6.13
		mL	28	818	36.33	36.78	35.98	36.36	2.22
Compressive Strength Test Result of 4.56 x 10^8 Cells/mL Bacterial Concrete									
			7	560	24.97	25.68	23.98	24.88	9.99
	SHC10,8	10	14	718	31.64	32.98	31.14	31.92	4.52
		mL	28	823	37.89	35.68	36.17	36.58	2.84
			7	621	26.13	26.88	27.77	26.93	19.05
3.	SHC20,8	20	14	731	32.48	33.33	31.68	32.49	6.42
		mL	28	826	36.8	37.23	36.13	36.73	3.26
			7	546	23.11	24.77	24.97	24.28	7.34
	SHC30,8	30	14	701	31.33	31.28	31.78	31.46	3.05
		mL	28	815	36.6	36.33	35.78	36.23	1.86

N. B. At each curing period, the percent increase in compressive strength was calculated by subtracting control concrete strength from bacterial concrete compressive strength, dividing the result by control concrete compressive strength, and multiplying by 100%.

At 7 days of curing, the highest compressive strength improvement was recorded by 19.05% and 23.47% for 4.56 x 10^8 and 9.84 x 10^6 cells/mL, respectively, for 20 mL of bacterial dosage (Table 4.11 and Figure 4.8). The reason for the highest improvement is that the concrete matrix is porous at an early age, allowing nutrients to reach the bacteria, and $CaCO_3$ deposition enhances the filling of voids or pores. This prevents nutrients and oxygen from reaching the bacterial cells, resulting in endospore formation and calcite precipitation.

At 28 days of curing, the maximum increase in compressive strength (14.37%) was recorded with 9.84 x 10^6 cells/mL of bacterial concentration at a dosage of 20 mL. The increase in compressive strength is mostly due to the formation of C-S-H gel within the concrete matrix, as well as the deposition of microbially induced calcite precipitation on the bacterial cell wall within the concrete pores (Meera et al., 2016; Priyom et al., 2018).

The compressive strength result of conventional concrete and self-healing concrete at 7 days of curing is illustrated in Figure 4.8 below graphically.

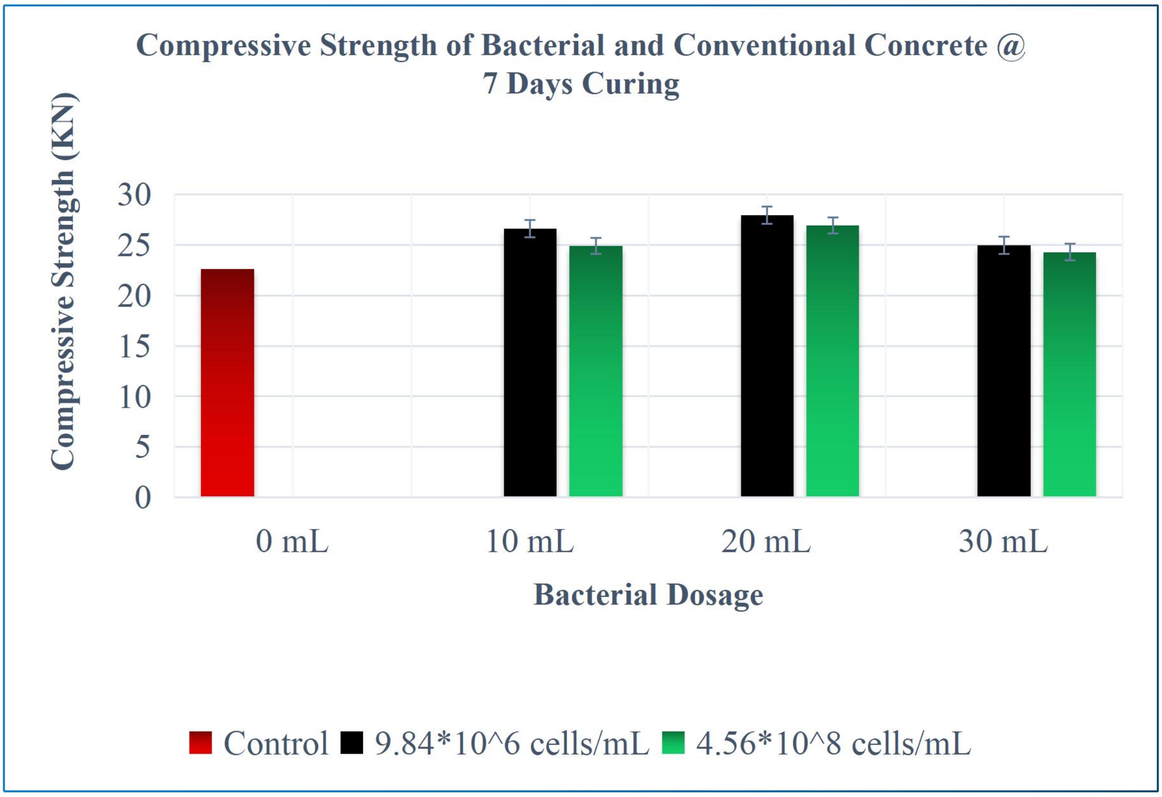

Figure 4.8 Compressive Strength of Bacterial and Conventional Concrete at 7 Days of Curing

The compressive strength result of conventional concrete and self-healing concrete at 14 days of curing is illustrated in Figure 4.9 below graphically.

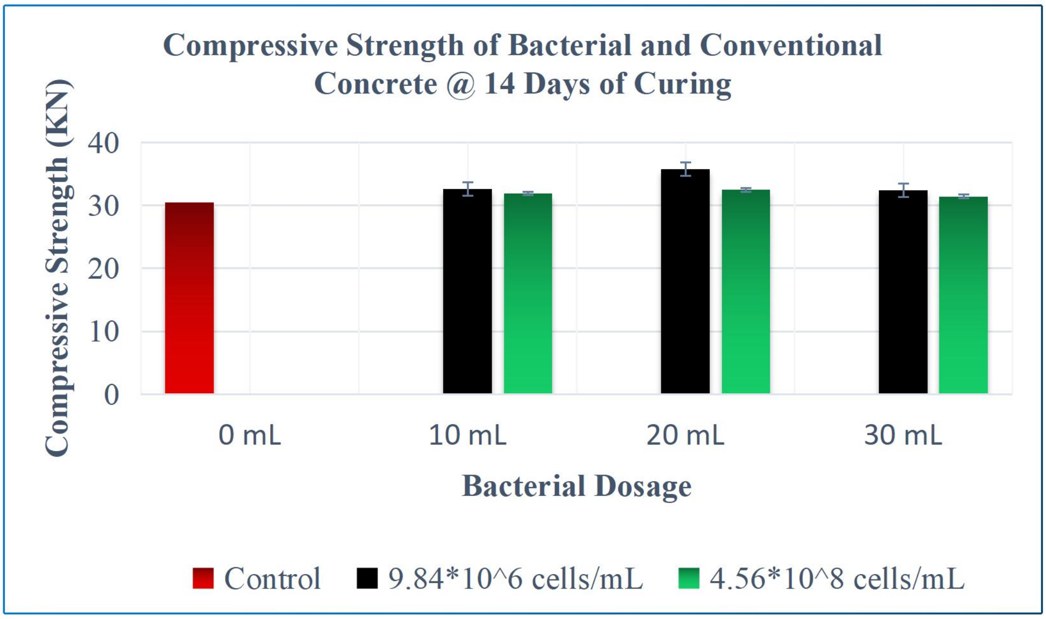

Figure 4.9 Compressive Strength of Bacterial and Conventional Concrete at 14 Days of Curing

The compressive strength result of conventional concrete and self-healing concrete at 28 days of curing is illustrated in Figure 4.10 below graphically.

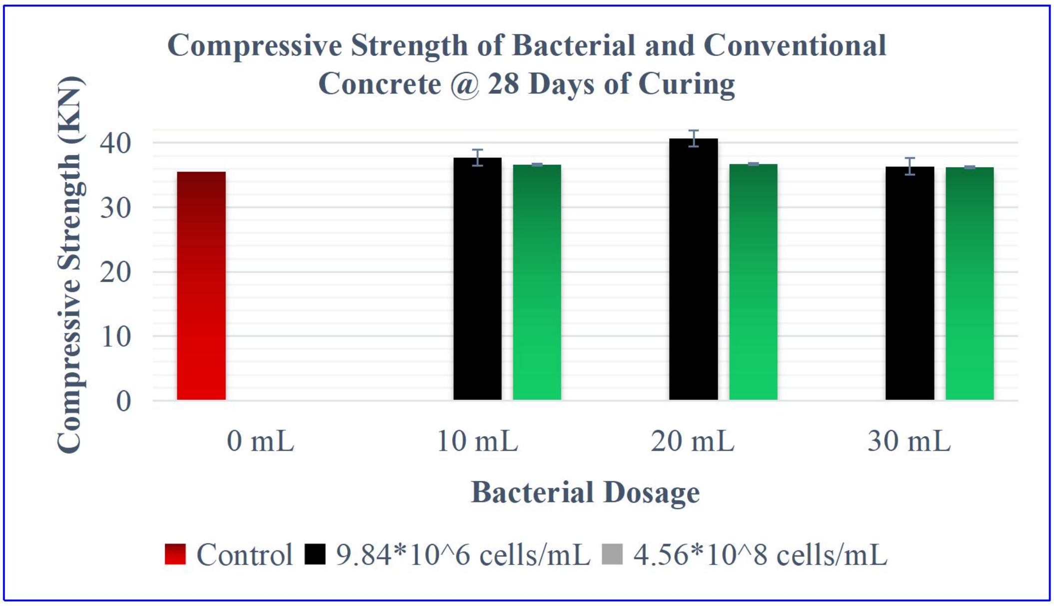

Figure 4.10 Compressive Strength of Bacterial and Conventional Concrete at 28 Days of Curing

The compressive strength of bacterial concrete with a cell concentration of 9.84 x 10^6 cells/mL slightly exceeds the compressive strength of bacterial concrete having a cell concentration of 4.56 x 10^8 cells/mL. This may be due to the bacterial cell absorbs all Ca^{2+} to its surface and creating complex matrix inside the concrete which could distrub the microbilal precipitation of calcite inside the concrete matrix continously.

Bacillus subtilus bacteria chemically precipitated calcite from calcium lactate in between the cement and aggregates, resulting in improved compressive strength. According to the study by Seifan et al. (2016), self-healing concrete specimens had better compressive strength than conventional concrete due to the persistence of nutrition in the bio-curing process. In general, introducing Bacillus subtilis bacteria into concrete mixtures can improve compressive strength significantly.

4.3.2 Water Absorption of Bacterial and Conventional concrete

The resistance of concrete specimens to water penetration is measured by water absorption. Table 4.12, Figure 4.11, and Figure 4.12 show the effects of introducing two bacterial concentrations to concrete samples. The water absorption of bacterial concrete was reduced compared to conventional concrete samples (Parashar et al., 2021; Priyom et al., 2018).

Table 4.12 Effect of Bacterial Concrete on Water Absorption

No	Dosage (mL)	A (g)	B (g)	% of water absorption @ 7 days	% age reduction	A (g)	B (g)	% of water absorption @ 28 days	% age reduction
Water Absorption of conventional Concrete without Bacterial Concentration									
1.	0	757	698	8.5		772	718	7.94	
Water Absorption of Bacterial Concrete with 9.84 x 10^6 cells/mL of Concentration									
	10	763	711	7.3	14.12	763	717	6.42	19.14
2.	20	786	735	6.9	18.82	781	736	6.11	23.05
	30	767	713	7.6	10.59	762	715	6.57	17.25
Water Absorption of Bacterial Concrete with 4.56 x 10^8 cells/mL of Concentration									
	10	771	716	7.7	9.41	765	718	6.55	17.5
3.	20	790	735	7.48	12.0	788	741	6.34	20.15
	30	774	718	7.80	8.24	772	724	6.63	16.5

N.B The water absorption and the percent reduction of water absorption were computed using Equation 3.14 and Equation 3.15, respectively.

The highest reduction in water absorption at a bacterial concentration of (9.84 x 10^6 and 4.56 x 10^8) cells/mL at 7 days of curing was 18.82% and 12.0%, respectively, for 20 mL of bacterial dosage compared to the conventional concrete (Figure 4.11 and Table 4.12).

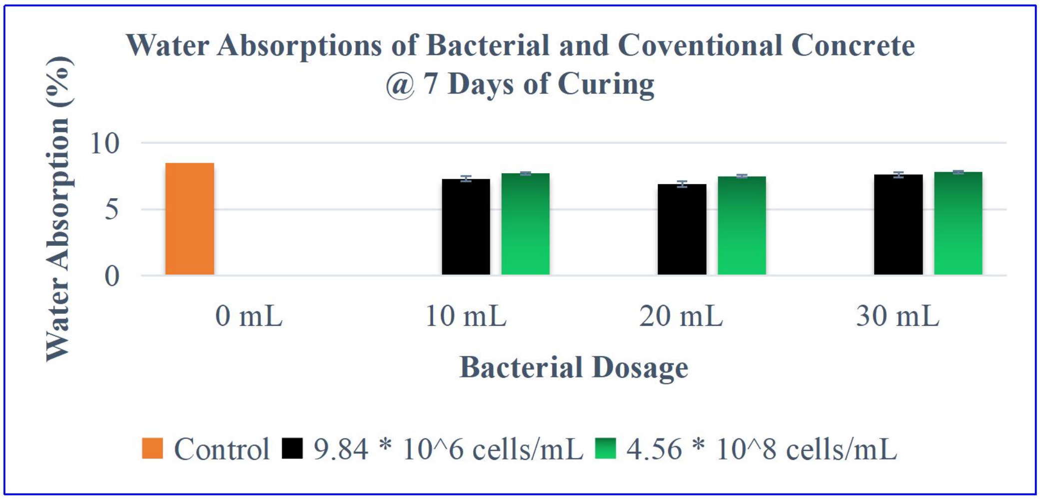

Figure 4.11 Water Absorptions of Bacterial and Control Concrete at 7 Days of Curing

The highest reduction in water absorption at a bacterial concentration of (9.84 x 10^6 and 4.56 x 10^8) cells/mL at 28 days of curing was 23.05% and 20.15%, respectively, for 20 mL of bacterial dosage compared to the conventional concrete samples (Figure 4.12 and Table 4.12). Since a concrete sample containing 9.84 x 10^6 cells/mL showed a greater reduction in water absorption due to the filling of voids and pores by precipitated calcite, it showed a greater improvement in compressive strength than the control concrete by 14.37% at 28 days of curing.

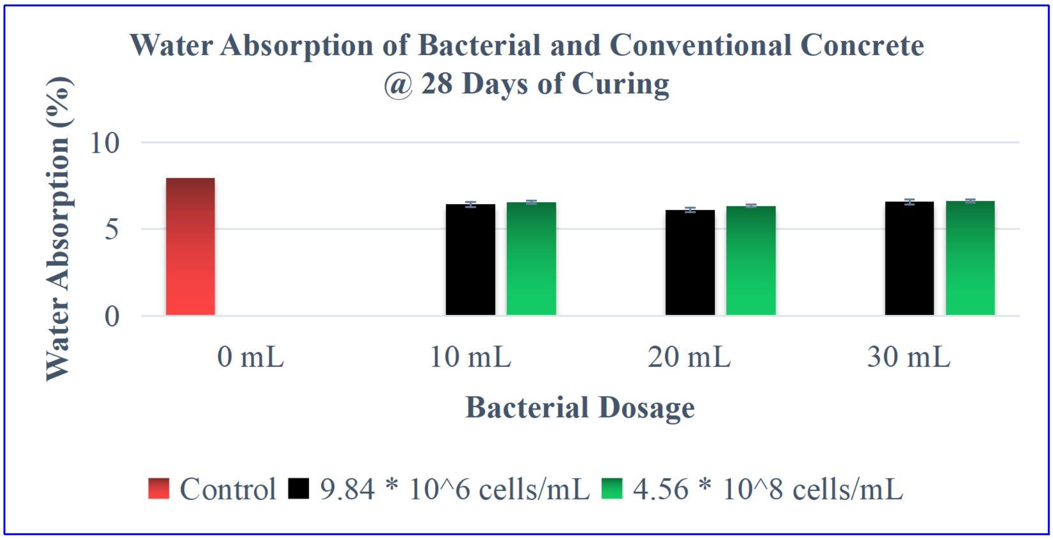

Figure 4.12 Water Absorptions of Bacterial and Control Concrete at 28 Days of Curing

The result indicated that the water absorption capacity of concrete decreased with the addition of different bacterial concentrations (9.84 x 10^6 and 4.56 x 10^8) cells/mL at 7 and 28 days of curing. The reduction in water absorption for both bacterial concentrations was due to the presence of Bacillus subtilis bacteria and calcium lactate. When bacteria consume calcium lactate, they generate calcite, which fills pores and microcracks with calcium carbonate, reducing water absorption and enhancing concrete durability.

4.3.3 Microstructural Analysis of Bacterial and Conventional Concrete

4.3.3.1 XRD Analysis

XRD is a technique that uses the crystal structure of the compounds to identify the chemicals they contain. This approach aids in the identification of chemicals contained in samples. After 28 days of curing, XRD analysis was done on both conventional and bacterial self-healing concrete, with concentrations of 9.84 x 10^6 cells/mL at a dose of 20 mL. XRD was carried out to determine the role of Bacillus subtilis bacteria in the formation of cement hydration products. CuK radiation with a wavelength of 1.5406A° was utilized to gather the X-ray diffraction pattern in an angle range of 2θ = 10° to 80° using an X-ray diffractometer. Cu target radiation at 30 kV and 10 mA is used in the XRD. Both conventional and bacterial concrete samples were crushed and pulverized before being mounted on a glass fiber stub to detect the phase change. The powder crystal X-ray examination of the samples with and without bacteria (Figure 4.13) reveals that standard and bacterial concrete samples have several peaks in their XRD spectra. Major peaks such as portlandite (C-H), C_3S, calcite, and C_2S are prevalent in conventional and bacterial self-healing concrete. At 28 days of cure, the XRD spectra of bacterial self-healing concrete with a 9.84 x 10^6 cells/mL concentration shows higher C-S-H gel formation (Figure 4.13a).

As seen in Figure 4.13, the principal peaks are C-H, C_3S, C_2S, and calcite. The addition of Bacillus subtilis bacteria to the concrete mix does not result in the formation of new chemicals. Furthermore, a higher intensity of portlandite (C-H) is observed in traditional concrete. The appearance of higher intensity C-H peaks in control concrete compared to bacterial concrete shows that C-H is converted into C-S-H more slowly (Thiyagarajan et al., 2016). After 28 days of curing, the XRD pattern observed in Figure 4.13b reveals that the Bacillus subtilis bacteria are efficient in converting C-H into C-S-H.

In 9.84 x 10^6 cells/mL of concentration contained concrete, lower intensity C-H peaks show increased C-S-H gel formation inside the concrete matrix. This phenomenon also manifests itself in compressive strength. Peaks are less intense, there is more C-S-H or calcite, and the strength is higher. As a result, compressive strength is increased either by the production of C-S-H gel or by the bacterial action of filling pores with precipitated calcite. The improved compressive strength of bacterial self-healing concrete found in this study could be attributed to bacterial activity converting C-H into C-S-H or calcite. Calcite is formed primarily by bacterial action, whereas C-S-H is formed by a simple pozzolanic reaction.

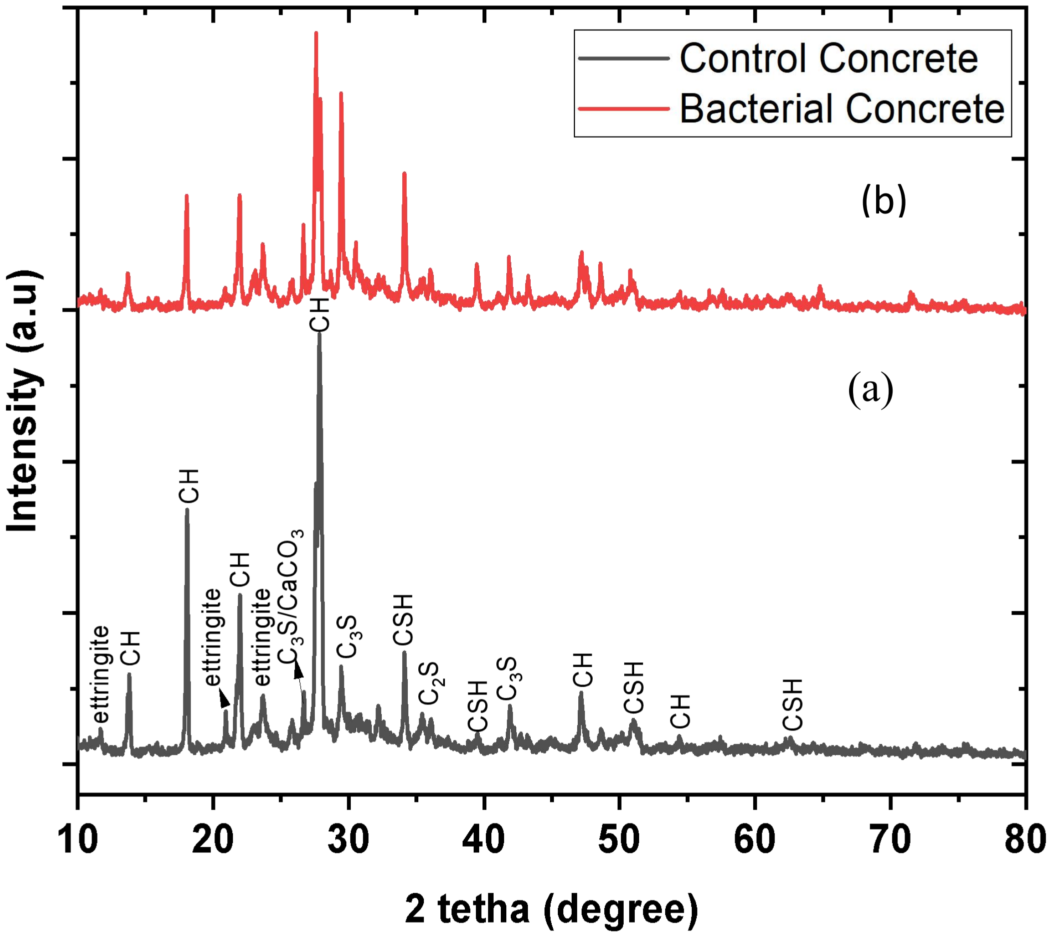

Figure 4.13 XRD Pattern : (a) Conventional Concrete; (b) Bacterial Concrete

Figure 4.13 also revealed the formation of ettringite, which is generally due to the reaction between C_3A and gypsum in the presence of $CaCO_3$ during the early age of setting. Ettringite formation is observed in bacterial and conventional concrete. The formation of ettringite controls the setting of cement and provides a sufficient buffer for hydration (Thiyagarajan et al., 2016).

4.3.3.2 SEM Analysis

After 28 days of curing, scanning electron microscopy analysis was performed on both conventional concrete and bacterial self-healing concrete specimens at a bacterial concentration of 9.84 x 10^6 cells/mL. Figure 4.14a shows a view of standard concrete without the inclusion of Bacillus subtilis bacteria, which clearly shows microcracks and pores or voids. Figure 4.14b shows SEM investigation of concrete samples with bacterial concentrations of 9.84 x 10^6 cells/mL at a dosage of 20 mL that have emerged with distinct calcite crystals generated in concrete.

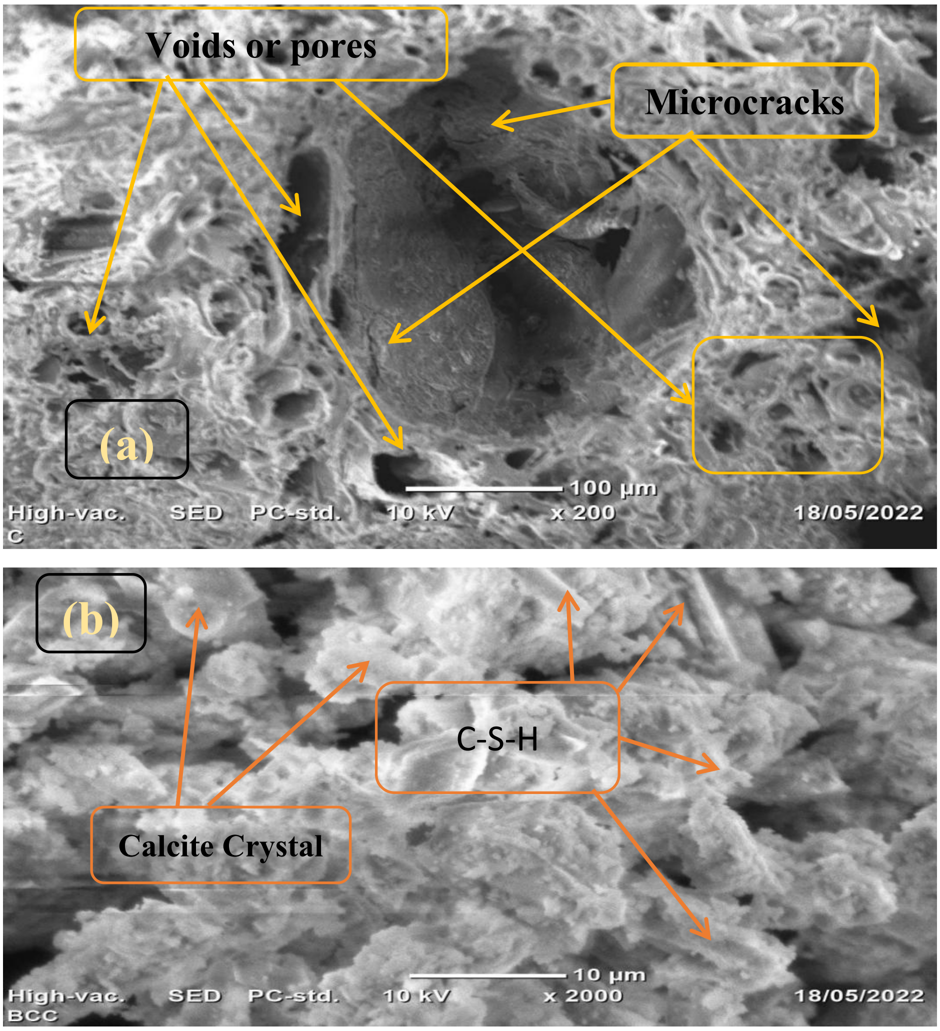

Figure 4.14 SEM image of : (a) Conventional Concrete; (b) Bacterial Concret

Figure 4.14 also reveals the presence of calcite in the form of $CaCO_3$ due to the activity of bacteria. The deposition of calcite inside the concrete matrix, which serves as a barrier to harmful materials, improves the strength and durability of the structure. The findings in this work were in line with the previous studies (Hussein et al., 2019; Khaliq et al., 2016).

4.4 Self-Healing Process of Bacterial Concrete

As the bacterial concrete hardens, the bacteria become inactive and enter a dormant state. When a crack appears on a concrete surface, the bacteria awaken from their dormancy and feed on calcium lactate to produce calcite, the main healing product. Bacillus subtilis bacteria feed on calcium lactate, which produces $CaCO_3$, which heals the crack in the concrete. It was observed that there were whitish crystal formations along the crack surface, indicating small cracks are being healed by the action of bacteria. The formation of calcite along the crack surface was confirmed by XRD and SEM images as indicated in Figure 4.20 and Figure 4.21, respectively. The reason for crack repair is microbial precipitation of calcite caused by the urealytic activity of Bacillus bacteria (Hazarika, 2021). As seen in Figure 4.15, the Ca^{2+} ion from the calcium lactate nutrient was attracted to the bacterial cell wall and formed $CaCO_3$ as a crack healing product.

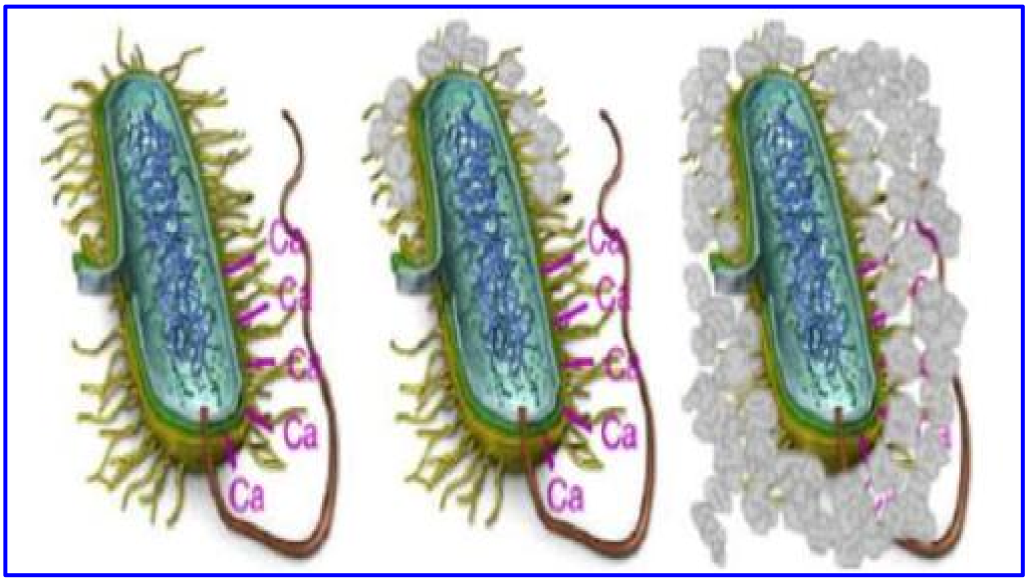

Figure 4.15 Calcite Precipitation on Bacterial Cell wall

Once the crack was healed due to the action of bacteria, the bacteria returned to the stage of hibernation. When any crack happens, the bacteria gets activated and heals the fracture in the presence of moisture.

4.4.1 Self-Healing Efficiency vs Crack Width

Natural or autogenous processes can repair small cracks of (0.1–0.2) mm in width. Bacteria are engaged in sealing bigger cracks up to 0.8 mm by precipitating calcite at the crack surface, which becomes difficult to heal spontaneously as the crack width rises (Luo et al., 2015). In the current study, the self-healing potential of cracks was investigated by incorporating Bacillus subtilis bacteria and calcium lactate as food to repair cracks with respect to crack widths of (0.1–0.72) mm. The result indicated that the bacteria precipitate whitish crystals (calcite) to heal small cracks. Cracks up to 0.5 mm were healed completely in 14 days of curing underwater (Figure 4.16).

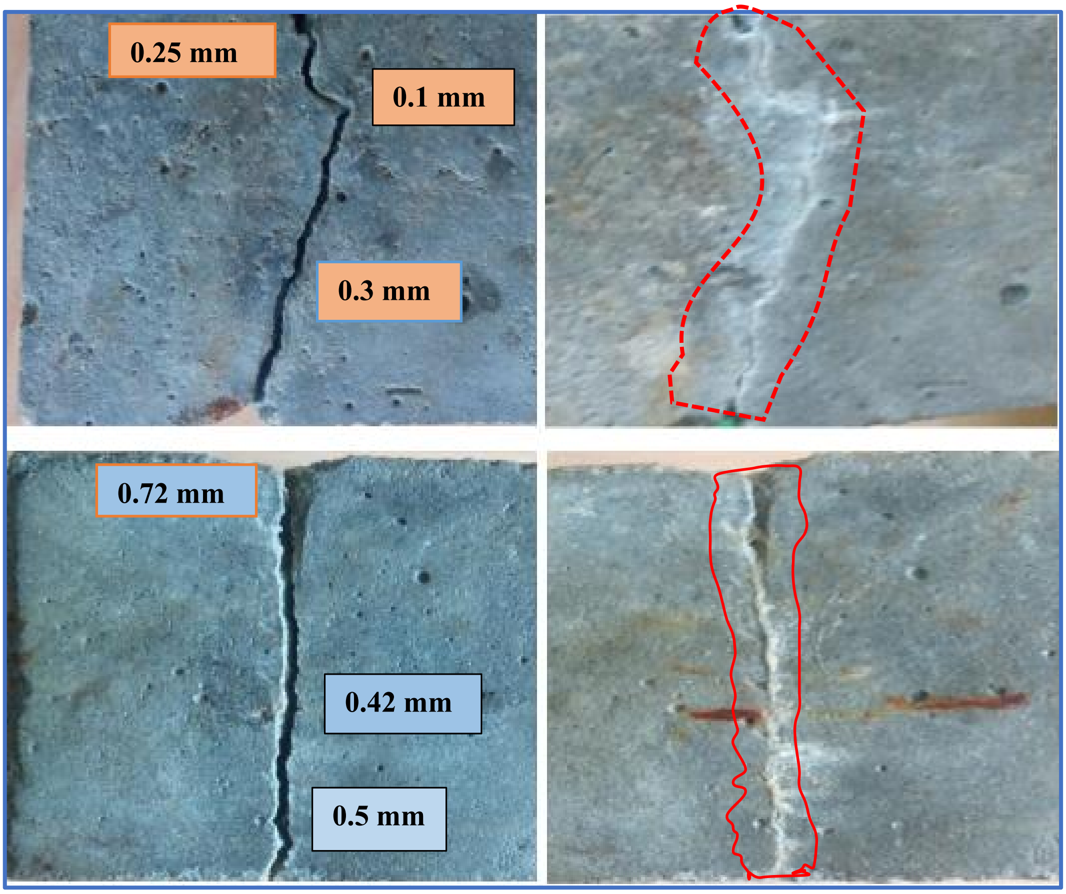

Figure 4.16 Self-Healed Concrete Samples with different Crack Width

A larger crack may take a longer period of time to heal. As a result, it can be concluded that small cracks can be healed more completely than larger cracks in a shorter healing period.

4.4.2 Self-Healing Efficiency vs Bacterial Concentration

The efficiency of crack repair depends on the number of bacterial cells added to the concrete mixture. The number of bacterial cells employed in the concrete can accelerate crack closure by producing calcium carbonate as a healing product. In this study, two bacterial concentrations of 4.56×10^8 and 9.84×10^6 cells/mL were prepared and directly added to the concrete during mixing. A bacteria having a concentration of 4.56 x 10^8 cells/mL showed better healing efficiency than a bacterial concentration of 9.84 x 10^6 cells/mL after 14 days of healing (Figure 4.17). This is because as the bacterial cell concentration increases, the urealytic activity of bacteria also increases, and they precipitate more calcite along the crack surface to repair the crack in a shorter period of time.

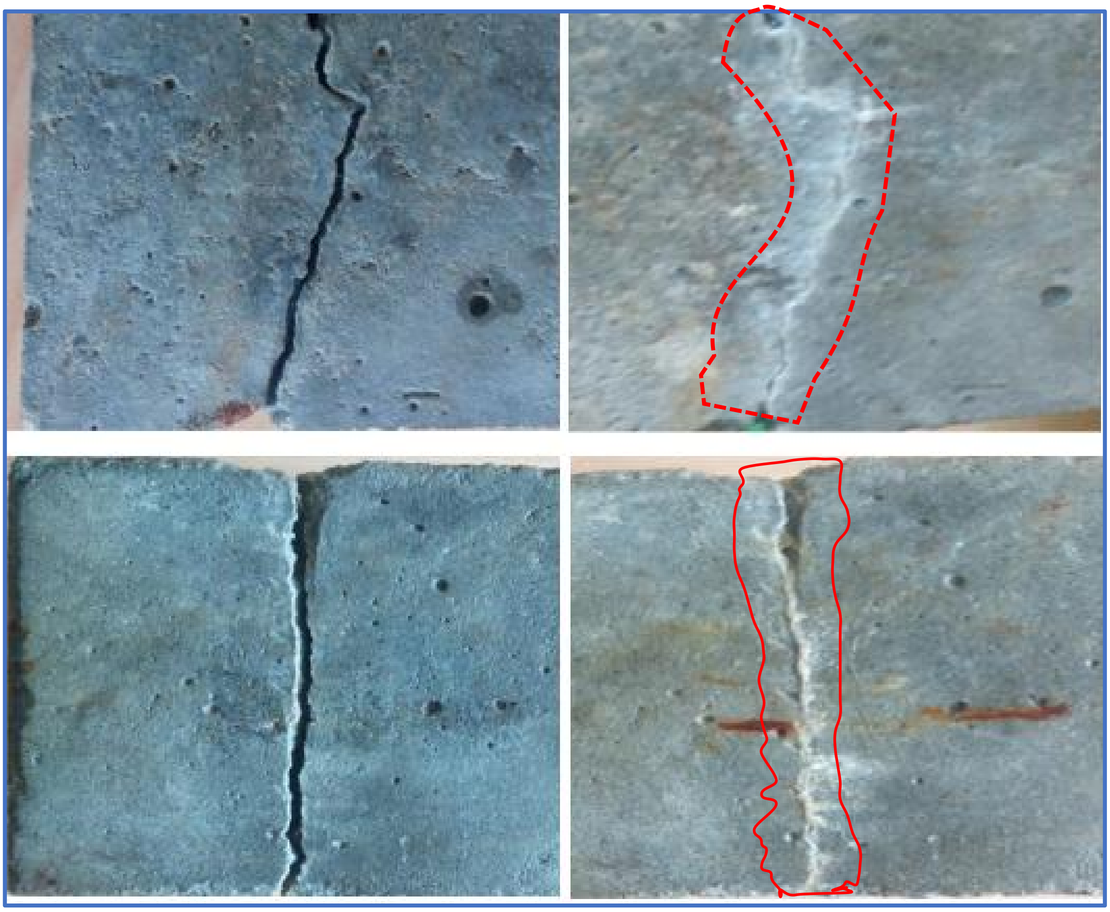

Figure 4.17 Self-Healing Concrete : (a) (9.84 x 10^6 cells/mL); (b) 4.56 x 10^8 cells/mL

The higher bacterial cell concentration led to enhanced precipitation of $CaCO_3$. This was because the bacterial cell wall served as a nucleation site for calcite precipitation. This was in line with previous study conducted by Luo et al. (2015).

4.4.3 Self-Healing Efficiency vs Healing Age

The crack healing efficiency of bacterial concrete is affected by the healing period. The potential healing efficiency of cracks was investigated at a healing age of 7 and 14 days. The result showed that the self-healing efficiency increased as the healing age increased (Figure 4.18). This is because as the healing age increased, the more healing product was precipitated at the crack surface due to bacteria feeding on calcium lactate, and small cracks were repaired successfully (Wiktor et al., 2011).

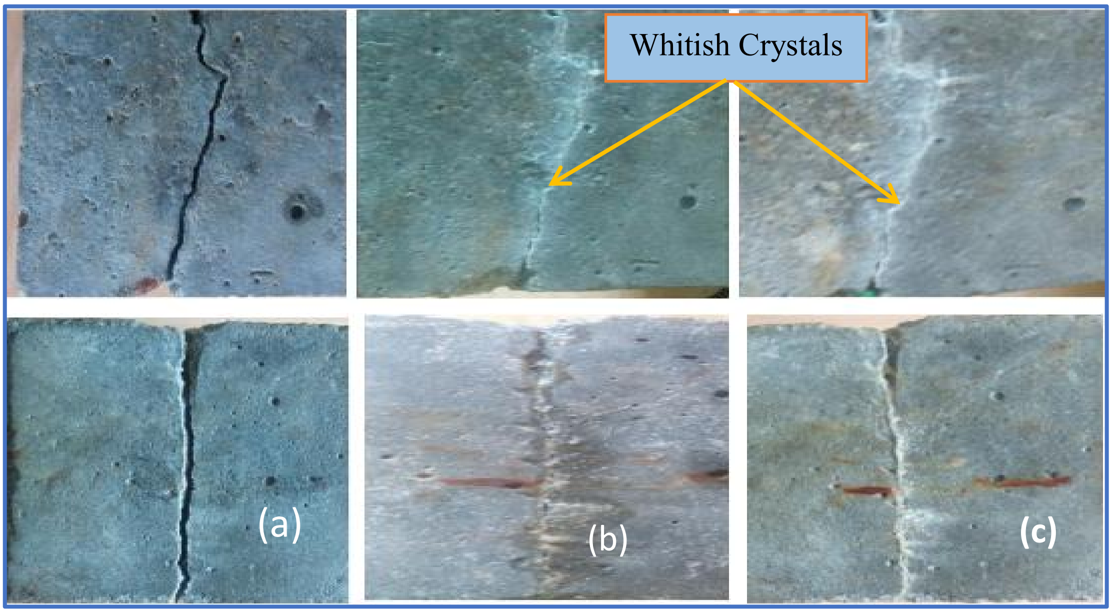

Figure 4.18 Crack Healing : (a) 0 Days; (b) 7 Days; and (c) 14 Days of Curing

4.4.3.1 Quantification of Crack Healing Percentage

From a qualitative point of view, it is clear that crack healing efficiency increases with the increase in healing age. To quantify the crack healing potential, the crack width and length were measured. Then, the crack width was measured at 0, 7, and 14 days of curing at a constant interval of 10 mm. The percentage of healing potential was computed based on Equation 3.15 and presented in Table 4.13.

Table 4.13 Quantification of Crack Healing Percentage

Interval	9.84×10^6 cells/mL contained sample					4.56×10^8 cells/mL contained sample				
	CW_i	CW_t		% healing		CW_i	CW_t		% healing	
0	0	7	14	7	14	0	7	14	7	14
1	0.25	0.01	0.00	96	100	0.72	0.37	0.21	48.6	70.8
2	0.1	0.10	0.00	100	100	0.64	0.22	0.13	65.6	79.7
3	0.18	0.00	0.00	100	100	0.50	0.07	0.00	86	100
4	0.22	0.00	0.00	100	100	0.42	0.04	0.42	90.5	100
5	0.3	0.015	0.00	95	100	0.50	0.07	0.00	86	100

After 14 days of curing, the best crack healing tendency was seen in the bacterial concrete samples. As shown in Table 4.13, an inverse relationship between crack width and healing percentage was found. Moreover, it was found that small cracks were completely healed (100%) after 14 days of the healing period. However, with increasing healing periods, the crack healing percentage of bacterial specimens increased significantly.

4.4.4 Self-Healing Efficiency vs Methods of Curing

The curing method also affects the self-healing efficiency of bacterial concrete. In this study, the efficiency of self-healing was investigated under different curing methods such as water curing, partial curing, and dry curing after 14 days. The result indicated that curing underwater was an effective way to heal cracks effectively (Figure 4.19). The presence of water is critical to encouraging crack healing. This is because water is essential for the dissolution of $Ca(OH)_2$ to form calcium carbonate at the crack surface and for the continual hydration of unhydrated cement (Bhaskar, 2016). The healing of the crack was mainly due to the precipitation of calcite by bacterial metabolic conversion of calcium lactate based on the reaction (Wiktor et al., 2011) as indicated in Equation 1.2.

$$CaC_6H_{10}O_6 + 6O_2 \rightarrow CaCO_3 + 5CO_2 + 5H_2O$$

Therefore, the presence of water is essential for effective way of repairing cracks.

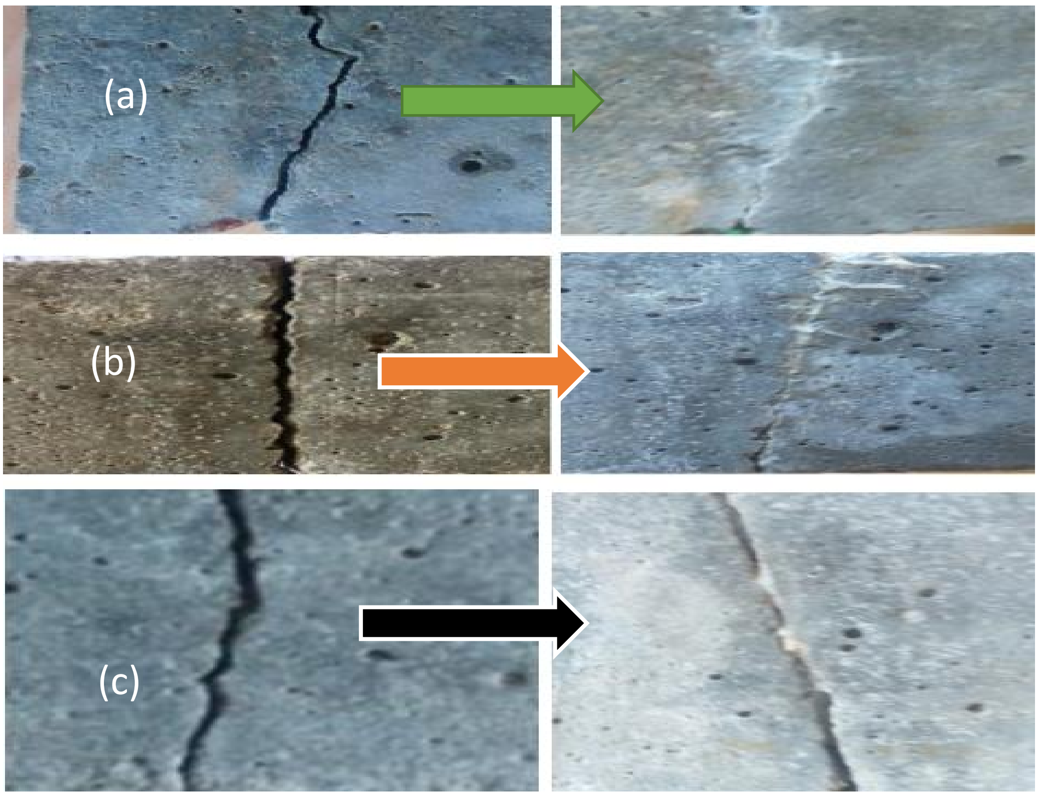

Figure 4.19 Self-Healed Concrete: (a) Water Curing; (b) Wet-Dry Curing; (c) Dry Curing

4.4.5 Analysis of Crack Healing Product in Self-Healing Concrete

To confirm that the precipitate formed around the crack surface by the action of bacteria, producing calcite, the samples were scratched from the healed surface and analyzed by scanning electron microscope (SEM) and X-ray diffraction (XRD) analysis.

4.4.5.1 XRD Analysis of Precipitated $CaCO_3$

The precipitated whitish crystal powder from the crack surface was tested by the XRD analysis method. The result of the XRD pattern showed different diffraction peaks at a 2θ angle for the precipitated calcium carbonate. The result shown in Figure 4.20 confirms the presence of calcite peaks of the product precipitated by Bacillus subtilis bacteria within the concrete specimens. The precipitated calcite peaks are correctly matched with the reference calcium carbonate peaks. The formation of precipitated calcite along the crack surface was checked by XRD, as seen in Figure 4.20, and this confirms that Bacillus subtilis bacteria successfully produce calcite to repair concrete cracks biologically. Therefore, the XRD result in Figure 4.20a confirmed that the produced white crystal along the crack surface of the concrete was $CaCO_3$, and a similar result was obtained in previous research work (Algaifi et al., 2020; Khaliq et al., 2016).

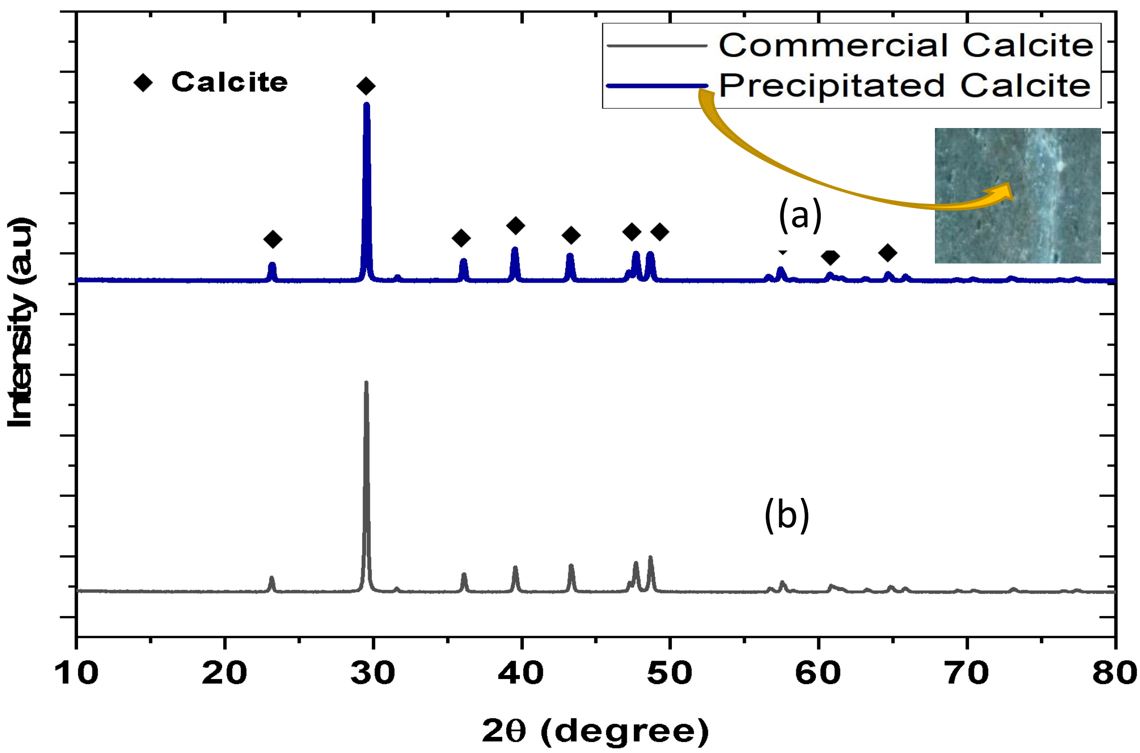

Figure 4.20 XRD image of Precipitated Calcite by Bacillus Subtilis Bacteria

4.4.5.2 SEM Analysis of Precipitated Calcite on Crack Surface

A SEM analysis was conducted to characterize the precipitation of whitish crystals in bio-based self-healing concrete crack surfaces. The SEM image in Figure 4.21 showed the precipitation of $CaCO_3$ along the crack surface after 14 days of the healing process, suggesting that the concrete's healing efficiency was supported by the action of Bacillus subtilis bacteria through the production of calcite. This precipitated calcite filled the cracks on concrete structures and filled pores or voids inside the concrete matrix, which could enhance the compressive strength of bacterial concrete specimens.

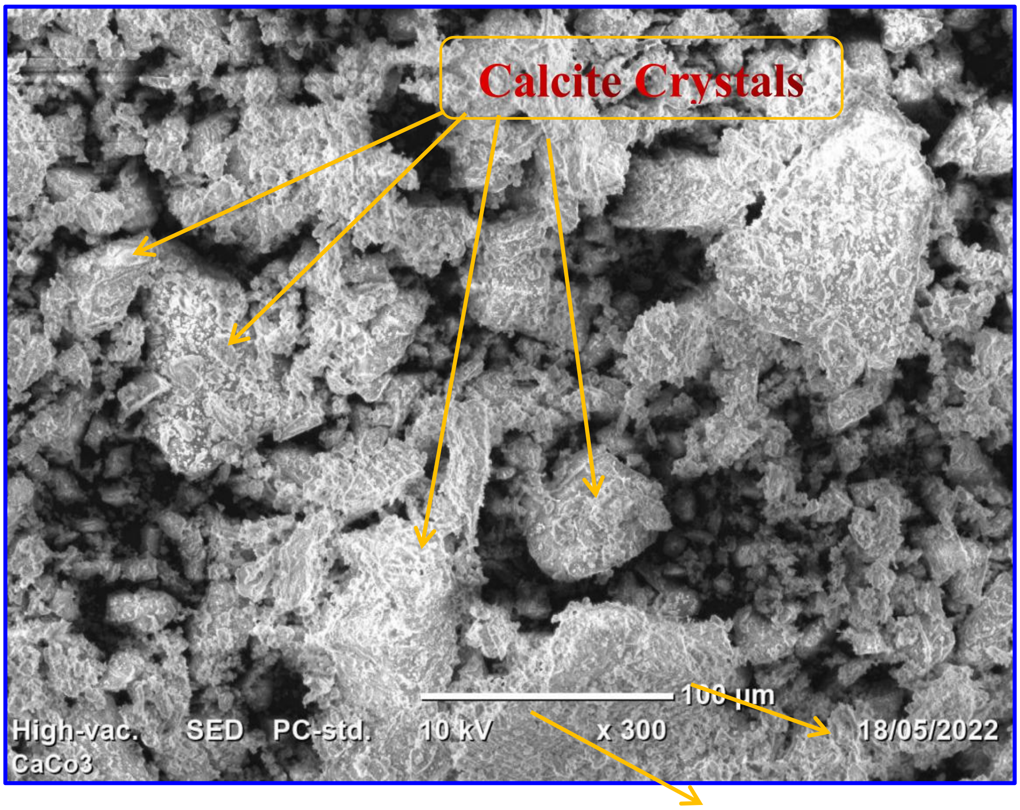

Figure 4.21 SEM image of Precipitated Calcite on Crack Surface after 14 Days of Healing

The precipitated whitish crystal morphology was rhombohedra, as shown in Figure 4.21 above. Hence, rhombohedra crystal morphology was observed in cracks, voids, or pores. It can be summarized as calcite formation along the crack surface was due to the activation of the incorporated Bacillus subtilis bacteria and a similar SEM image was obtained in the previous study by (Khaliq et al., 2016; Luo et al., 2021).

4.5 Economical and Environmental Evaluation of Self-Healing Concrete

4.5.1 Economical Evaluation of Self-Healing Concrete

Cracking is common in traditional concrete structures, reducing their longevity and increasing repair costs. Concrete cracks can now be repaired with bio-based self-healing concrete. The high initial cost of self-healing concrete is one of the key drawbacks of using microbial-induced calcite precipitation to fix cracks in a concrete structure. The cost of conventional concrete is less than $100 per cubic meter. Self-healing concrete costs 2.3 to 3.9 times as much as regular concrete (Stanaszek, 2020), which is considered too expensive. This is due to the expense of growing media, calcium lactate, bacteria, and labor.

According to Table 4.14 below, the cost of conventional concrete is around 5,127 ETB/m^3 ($99.45), while the cost of bacterial concrete is almost 1.742 times the cost of conventional concrete. The cost of self-healing concrete in this work can be reduced by 1.742 times. The laboratory synthesis of calcium lactate from discarded eggshell and lactic acid, as well as the choice of bacterial culture medium (yeast extract and molasses), and non-axenic-based bacterial production from the soil, all contributed to the cost savings. The cost of self-healing concrete can be estimated using literature and current market conditions as follows:

A) The cost for 1 m^3 of conventional concrete was estimated based on the current market price on April 30, 2022.

Table 4.14 Cost Analysis of Conventional Concrete

Material Cost Breakdown				
Types of material	Unit	Quantity	Rate	Cost (ETB/m^3)
Cement (OPC-42.5N)	Quantal	4.5	1,000	4,500
Fine aggregate	M^3	0.29	1,000	290
Coarse aggregate	M^3	0.38	875	332.5
Water	M^3	0.174	20	4.48
	Total Cost of Conventional Concrete			5,127 ($99.45)

B) Cost of producing 6.0 kg of effective ureolytic cultures of bacterial spores

Table 4.15 Cost of Ureolytic Bacterial Spores

Item	Unit	Quantity	Rate	Total Cost (ETB)
1. Bacteria identification from soil				
Labor	2 days	2 hrs/day	25	100
Field assistant	2 days	2 hrs/day	20	80
			Total Cost	180
2. Media preparation (nutrient agar)				
Labor	3 days	3 hrs/day	16.67	150
Nutrient agar	Kg	0.1	6,400	640
			Total Cost	790
3. Serial dillution and innoculation				
Labor	1 day	3 hrs/day	25	75
Assistant	1 day	3 hrs/day	20	60
			Total Cost	135
4. Bacteria isolation and characterization (physical and biological)				
Labor (physio-chemical identification)	3 days	3 hrs/day	16.67	150
Labor (bio-chemical identification)	3 days	3 hrs/day	23.33	210
			Total Cost	360
5. Mass production on yeast extract and molasses				
Labor	3 days	3	23.33	210
Yeast extract	Kg	0.12	4,800	576
Molasses	Kg	0.5	8	4
			Total Cost	790
			Grand Total Cost	2,255 ($43.74)

C) Costs to prepare 5.0 kg of calcium lactate

Table 4.16 Cost of Calcium Lactate Production

Item	Unit	Quantity	Rate	Total cost (ETB)
1. Collection and treatment of waste eggshell				
Labor	3 days	3 hrs/day	16.67	150
2. Chemical used				
Lactic acid	mL	1000	1.00	1000
3. Production cost of calcium lactate				
Labor	Day	2	200	400
			Grand Total Cost	1,550 ($30.16)

D) Total cost of bacterial self-healing concrete

Table 4.17 Total Cost of Bacterial Self-Healing Concrete

No.	Descriptions	Cost (ETB/m^3)
1	Total cost of conventional concrete	5,127 ($99.45)
2	Total cost of ureolytic cultures of bacterial spores	2,255 ($43.74)
3	Total cost of calcium lactate production	1,550 ($30.16)
	Grand total cost of bacterial self-healing concrete	8,932 ($ 173.27)
	Total cost of self-healing concrete based on literature for 1 m^3 of concrete	(2.3-3.9) (cost of normal concrete) then, take the average value (2.3 +3.9)/2 = 3.1 (3.1 x 5,127) = 15,381($ 298.37)
	Amount of cost to be saved	15,381-8,932 = 6,449 ($ 125.1)
	Amount of cost exceed of bacterial concrete	8932/5127 = 1.742 times normal concrete

The use of self-healing concrete can save a reapir and maintenance cost (50-80%) of total life cycle cost of a building. Even though the initial total cost of bacterial self-healing concrete is more than ordinary concrete, it saves money in the long run by avoiding costly repairs. In addition, the structure’s service life, mechanical strength, water absorption, and healing efficiency are superior to that of sandard concrete. The increased initial cost appears less harsh as a result of this benefit. In this regard, there are times when the advantages of bacterial self-healing concrete outweigh the costs. As illustrated by Bravo Silva, there are times when the safety of priceless objects is more important than money. For example, in an underground structure, self-repairing of cracks is critical to the repair of the right conditions to preserve the highly valuable objects (Silva et al., 2015). In circumstances like the one pinpointed by Bravo Silva, bacterial self-healing concrete can prove its value as a long-term solution without the constraint of contractors' warranties. The material also gives benefits in fields outside the economy by being more environmentally friendly than conventional concrete.

4.5.2 Environmental Evaluation of Self-Healing Concrete

The construction industry uses more raw materials by weight than any other industrial sector. As a result, choosing energy-efficient concrete can contribute to environmental protection. The construction industry requires a large amount of cement, sand, and coarse aggregate when using traditional concrete. These materials are depreciable over time, and conventional concrete is less durable due to strain from the environment. The difficulty was solved by either rebuilding the structure or increasing the concrete thickness during construction, which required more concrete. The overuse of concrete materials results in waste and pollution.

Self-healing concrete is currently the best method for reducing waste and CO_2 emissions in the environment. Global warming is caused by CO_2 emissions into the atmosphere. In addition, bacterial concrete fixes cracks on its own, reducing the need for additional concrete to seal them. As a result, it has the potential to minimize pollution. Furthermore, bacterial concrete eliminates the need for repairs and maintenance, perhaps avoiding the need to demolish structures, which are difficult to recycle and reuse, harming the environment. As a result, using self-healing concrete reduces CO_2 emissions.

Analyzing the CO_2 emissions and embodied energy of concrete materials is critical to making the best selection for reducing a structure's overall energy use and environmental impact. Because there is a lack of research in Ethiopia, the study used the Senegalese embodied energy and CO_2 emission coefficients (Taffese et al., 2019).

The embodied energy of concrete can be calculated by summing the embodied energy of its ingredients (cement, sand, and aggregate). The embodied energy (EE) is computed by summing the product of the quantity of each material (Q_M) with its embodied energy coefficient (EE_C) (Nizam et al., 2018). Besides, the carbon dioxide emission (ECO_2) can be calculated based on the formula presented in the study (Kumanayake et al., 2018). It can be computed by summing the product of the quantity of each material (Q_M) by its carbon dioxide emission coefficient (CO_2EC).

Table 4.18 Embodied Energy and Carbon dioxide Emissions

No.	Embodied Energy (EE)				Embodied CO_2 emissions		
1	Materials	Q_M (Kg)	EE_C (MJ/Kg)	EE (MJ)	Q_M (Kg)	CO_2EC (Kg/Kg)	ECO_2 (Kg)
1	Cement	425.25	3.32	1,411.83	425.25	0.73	310.43
2	Sand	798.75	0.06	47.93	798.75	0.04	3.195
3	Aggregate	1001	0.16	160.16	1001	0.010	10.01
Total Embodied Energy of materials				1,619.29	Total CO_2 emission		323.64

The amount of embodied energy consumed by 1 m^3 of concrete materials is 1,619.29 MJ, and the total amount of CO_2 emissions by the material is 323.64 Kg (Table 4.17). Cement is responsible for 87.2% of embodied energy and 95.92% of CO_2 emissions. This study was carried out under the assumption that all of the concrete materials required to manufacture 1 m^3 of concrete were used for infrastructure construction with no waste. Because of ordinary concrete cracks, additional materials are needed to repair and maintain the building in order to keep it in its original condition. This maintenance and repair process uses more resources, and the demolished section becomes waste that is difficult to recycle or reuse. The excessive use of concrete, as well as its waste, resulted in pollution and an increase in embodied energy and CO_2 emissions.

Self-healing concrete eliminates the need for maintenance and repair, which is an energy-efficient material. As a result, it reduces embodied energy and CO_2 emissions while avoiding the overuse of concrete materials. Furthermore, using waste eggshells to make calcium lactate decreases waste deposition in the environment and issues such as disposal costs, odor, insects, and grindability. Additionally, the bacteria used in self-healing concrete are completely safe for human health, non-pathogenic, and environmentally friendly. These advantages may persuade construction companies to begin using self-healing concrete on a large scale in the near future.

5. CONCLUSIONS AND RECOMMENDATIONS

5.1 Conclusions

The production of calcium lactate nutrient from lactic acid and discarded eggshell was effectively synthesized, and the results were examined using XRD and SEM images. Bacillus subtilis bacteria were effectively produced for utilization in yeast extract and molasses. The test results demonstrated that a fresh concrete mix containing Bacillus subtilis bacteria and calcium lactate was more workable than conventional concrete. Furthermore, as compared to conventional concrete samples, the compressive strength of all bacterial concrete samples improved after 7, 14, and 28 days of curing. At a bacterial concentration of 9.84×10^6 cells/mL, the compressive strength increased by 14.47% after 28 days of curing at a dosage of 20 mL compared to conventional concrete. This increase in strength could be attributed to calcite precipitation inside the concrete matrix as a result of bacterial action, which could fill voids and compact the concrete. Due to the filling of pores/voids by microbially precipitated calcite and a quick hydration rate at an early age of curing, the increasing rate of compressive strength for bacterial concrete was higher initially and decreased thereafter. Additionally, after 7 and 28 days of curing, the water absorption of bacterial concrete was reduced for all bacterial concrete samples. After 28 days of curing, the highest reduction in water absorption (23.05%) was reported for 9.84×10^6 cells/mL of bacterial solution at a dosage of 20 mL compared to conventional concrete. This could be due to the filling of voids or pores within the concrete matrix caused by microbially generated $CaCO_3$ produced by bacteria. Furthermore, crack width of up to 0.5 mm was completely healed after 14 days of curing due to calcite precipitation along the crack surface. Moreover, it is found that the cost of self-healing concrete can be reduced to 1.742 times that of regular concrete. Additionally, bacterial self-healing concrete reduces the need for repair and maintenance. It also prevents concrete from being overused. Therefore, CO_2 emissions and embodied energy can be minimized. Despite the greater initial cost of self-healing concrete compared to conventional concrete, it improves workability, compressive strength, water absorption, and crack repair without the need for human involvement, resulting in lower repair costs, embodied energy, and CO_2 emissions.

5.2 Recommendations

Self-healing concrete is environmentally friendly and has improved workability, strength, water absorption, and crack repairability. A bacterial self-healing concrete has proven to be a better alternative than traditional concrete. Moreover, self-healing concrete is safe to use and simplifies the current construction challenges while revolutionizing construction processes. However, there are still certain issues, like increasing the viability of bacteria for a longer period of time inside the concrete matrix, international codes, and standards, that need to be addressed before this cost-effective, ecologically beneficial, and convenient technology can be applied in the field. The current study is limited to tests like (i) workability, compressive strength, water absorption, self-healing efficiency, SEM, and XRD analysis; and (ii) environmental and cost analysis.

The future study will include additional testing such as:

- ➢ Oxygen consumption
- ➢ Flexural strength
- ➢ Chloride attack, and

Microstructural tests such as:

- ✓ Thermo-gravimetric Analysis (TGA).

Furthermore, in future studies:

- ✓ Bacterial encapsulation other than direct mix will be used to prevent microorganisms from dying due to the harsh concrete environment.

REFERENCES

Achal, V., Mukherjee, A., Basu, P., & Reddy, M. S. (2009). Lactose mother liquor as an alternative nutrient source for microbial concrete production by Sporosarcina pasteurii. *Journal of Industrial Microbiology and Biotechnology, 36*(3), 433-438.

Alazhari, M. S. (2017). *The effect of microbiological agents on the efficiency of bio-based repair systems for concrete.* University of Bath.

Alexander, M. G., Beushausen, H.-D., Dehn, F., & Moyo, P. (2008). *Concrete Repair, Rehabilitation and Retrofitting II: 2nd International Conference on Concrete Repair, Rehabilitation and Retrofitting, ICCRRR-2, 24-26 November 2008, Cape Town, South Africa*: CRC Press.

Algaifi, H. A., Bakar, S. A., Sam, A. R. M., Ismail, M., Abidin, A. R. Z., Shahir, S., & Altowayti, W. A. H. (2020). Insight into the role of microbial calcium carbonate and the factors involved in self-healing concrete. *Construction and Building Materials, 254*, 119258.

Alves, L., Alves, L., Mello, M., & Barros, S. d. (2019). *Characterization of Bioconcrete and the Properties for Self-Healing.* Paper presented at the Multidisciplinary Digital Publishing Institute Proceedings.

Amibo, T. A., & Bayu, A. B. (2020). Calcium Carbonate Synthesis, Optimization and Characterization from Egg Shell.

Amiri, M., Majrouhi Sardroud, J., & Pahlaviani, A. G. (2018). Self-healing concrete and environmental health. *International Journal of Epidemiologic Research, 5*(3), 107-112.

Andalib, R., Abd Majid, M. Z., Hussin, M. W., Ponraj, M., Keyvanfar, A., Mirza, J., & Lee, H.-S. (2016). Optimum concentration of Bacillus megaterium for strengthening structural concrete. *Construction and Building Materials, 118*, 180-193.

Arulsivanantham, P., Gokulan, R., Divyalakshmi II, M., Karthikeyan, S., & Achuthan, S. (2015). Bacterial Self-Healing Concrete-An Innovative Repair Technique. *International Journal of Applied Engineering Research, ISSN*, 0973-4562.

ASTM, C. 33-16, Standards Specification for Concrete Aggregates. *Annual Book of ASTM Standard*.

ASTM, C. 39/C39 M-10.(2010). *Standard test method for compressive strength of cylindrical concrete specimens. American Society for Testing and Materials, West Conshohocken, PA*.

ASTM, C. 143/C-143 M, 2000. *Standard Test Method for Slump of Hydraulic-Cement Concrete*.

ASTM, C. (1998). 187-98. Standard Test Method for Normal Consistency of Hydraulic Cement. *United States: ASTM International, 11*(1).

ASTM, C. (2006). 192. 2004. Standard Practice for Making and Curing Concrete Test Specimens in the Laboratory. *Annual book of ASTM Standards, 4*.

Ayodele, F., & Ayeni, I. (2015). Analysis of influence of silt/clay impurities present in fine aggregates on the compressive strength of concrete. *International journal of engineering research and science and technology, 15*(4), 6.

Babu, G. R., Reddy, B. M., & Ramana, N. V. (2018). Quality of mixing water in cement concrete "a review". *Materials Today: Proceedings, 5*(1), 1313-1320.

Barría, J. C., Vázquez, A., Pereira, J.-M., & Manzanal, D. (2021). Effect of bacterial nanocellulose on the fresh and hardened states of oil well cement. *Journal of Petroleum Science and Engineering, 199*, 108259.

Bhaskar, S. (2016). *Self-healing bacterial cementitious concrete composites: Development and performance evaluation.* PhD Dissertation. Department of Civil Engineering, Ryerson University ….

Bikya, R. (2012). *Evaluation of methods for measuring aggregate specific gravity*: West Virginia University.

C150, A. (2016). ASTM C150 standard specification for Portland cement: ASTM International West Conshohocken, Pennsylvania.

Cailleux, E., & Pollet, V. (2009). *Investigations on the development of self-healing properties in protective coatings for concrete and repair mortars.* Paper presented at the Proceedings of the 2nd international conference on self-healing materials, Chicago, IL, USA.

Chabi, E., Lecomte, A., Adjovi, E. C., Dieye, A., & Merlin, A. (2018). Mix design method for plant aggregates concrete: example of the rice husk. *Construction and Building Materials, 174*, 233-243.

Chahal, N., Siddique, R., & Rajor, A. (2012). Influence of bacteria on the compressive strength, water absorption and rapid chloride permeability of concrete incorporating silica fume. *Construction and Building Materials, 37*, 645-651.

Choi, H., Inoue, M., Kwon, S., Choi, H., & Lim, M. (2016). Effective crack control of concrete by self-healing of cementitious composites using synthetic fiber. *Materials, 9*(4), 248.

Choudhary, A. (2020). *Enhancement of autogenous healing in concrete through internal carbonation.* University of British Columbia.

Committee, A. (2008). *Building code requirements for structural concrete (ACI 318-08) and commentary*.

Cree, D., & Rutter, A. (2015). Sustainable bio-inspired limestone eggshell powder for potential industrialized applications. *ACS Sustainable Chemistry & Engineering, 3*(5), 941-949.

Davies, R., Teall, O., Pilegis, M., Kanellopoulos, A., Sharma, T., Jefferson, A., Gardner, D., Al-Tabbaa, A., Paine, K., & Lark, R. (2018). Large scale application of self-healing concrete: Design, construction, and testing. *Frontiers in Materials*, 51.

Dnyanoba, D. P., & MADHUKAR, R. H. (2020). Concrete Curing Method. *Iconic Research and Engineering Journals, 3*(7), 142-144.

Fang, X., Pan, Z., & Chen, A. (2021). Analytical models to estimate efficiency of capsule-based self-healing cementitious materials considering effect of capsule shell thickness. *Construction and Building Materials, 274*, 121999.

Feng, J., Chen, B., Sun, W., & Wang, Y. (2021). Microbial induced calcium carbonate precipitation study using Bacillus subtilis with application to self-healing concrete preparation and characterization. *Construction and Building Materials, 280*, 122460.

Goshu, T. F. (2018). *Optimization of Bagasse Ash to Cement Mix.* ADDIS ABABA SCIENCE AND TECHNOLOGY UNIVERSITY.

Haque, M., Tuhin, I., & Farid, M. (2012). Effect of aggregate size distribution on concrete compressive strength. *SUST journal of science and technology, 19*(5), 35-39.

Hazarika, A. (2021). Study of a New Healing Precursor Derived from Waste Streams For Bacterial Self-Healing Concrete.

Hedidor, D., & Bondinuba, F. (2017). Exploring concrete materials batching behaviour of artisans in Ghana's informal construction sector. *Journal of civil engineering and construction technology, 8*(5), 35-52.

Hermawan, H., Minne, P., Serna, P., & Gruyaert, E. (2021). Understanding the Impacts of Healing Agents on the Properties of Fresh and Hardened Self-Healing Concrete: A Review. *Processes, 9*(12), 2206.

Huang, H., Ye, G., Qian, C., & Schlangen, E. (2016). Self-healing in cementitious materials: Materials, methods and service conditions. *Materials & Design, 92*, 499-511.

Hussein, Z., Abedali, A., & Ahmead, A. (2019). *Improvement properties of self-healing concrete by using bacteria.* Paper presented at the IOP Conference Series: Materials Science and Engineering.

International, A. (2012). ASTM C128: Standard Test Method for Density, Relative Density (Specific Gravity), and Absorption of Fine Aggregate: American Society for Testing and Materials (ASTM).

Ivanov, V., Stabnikov, V., & Kawasaki, S. (2019). Ecofriendly calcium phosphate and calcium bicarbonate biogrouts. *Journal of cleaner production, 218*, 328-334.

Jakhrani, S. H., Qudoos, A., Kim, H. G., Jeon, I. K., & Ryou, J. S. (2019). Review on the self-healing concrete-approach and evaluation techniques. *Journal of Ceramic Processing Research, 20*(Special 1).

James, T., Malachi, A., Gadzama, E., & Anametemok, A. (2011). Effect of curing methods on the compressive strength of concrete. *Nigerian Journal of Technology, 30*(3), 14-20.

Jonkers. (2017). Bio-concrete" set to revolutionise the building industry. MSC NewsWire.

Jonkers, & Schlangen, E. (2008). *Development of a bacteria-based self healing concrete.* Paper presented at the Proc. int. FIB symposium.

Jonkers, Thijssen, A., , G., Copuroglu, O., & Schlangen, E. (2010). Application of bacteria as self-healing agent for the development of sustainable concrete. *Ecological engineering, 36*(2), 230-235.

Joseph, C., Jefferson, A. D., Isaacs, B., Lark, R., & Gardner, D. (2010). Experimental investigation of adhesive-based self-healing of cementitious materials. *Magazine of Concrete Research, 62*(11), 831-843.

Joshua, O., Fagbenle, O. I., Olusola, K. O., Abuka-Joshua, J., Ogunde, A., Amusan, L., & Omuh, I. (2018). A comparative analysis of batching by weight and volume towards improved concrete production.

Joy, M., & Varghese, S. M. (2018). Experimental Study on Strength Characteristics of Self–Healing Concrete with Fly Ash. *International Journal of Engineering Research & Technology (IJERT) ISSN*, 2278-0181.

Kanellopoulos, A., Qureshi, T., & Al-Tabbaa, A. (2015). Glass encapsulated minerals for self-healing in cement based composites. *Construction and Building Materials, 98*, 780-791.

Khaliq, W., & Ehsan, M. B. (2016). Crack healing in concrete using various bio influenced self-healing techniques. *Construction and Building Materials, 102*, 349-357.

Khan, M. (2010). *Bridge and highway structure rehabilitation and repair*: McGraw-Hill Education.

Kumanayake, R., Luo, H., & Paulusz, N. (2018). Assessment of material related embodied carbon of an office building in Sri Lanka. *Energy and Buildings, 166*, 250-257.

Lee, & Park, W. (2018). Current challenges and future directions for bacterial self-healing concrete. *Applied microbiology and biotechnology, 102*(7), 3059-3070.

Lee, Yoon, S. S., & Yarin, A. L. (2016). Solution-blown core–shell self-healing nano-and microfibers. *ACS applied materials & interfaces, 8*(7), 4955-4962.

Lucas, S. S., Moxham, C., Tziviloglou, E., & Jonkers, H. (2018). Study of self-healing properties in concrete with bacteria encapsulated in expanded clay. *Science and Technology of Materials, 30*, 93-98.

Luhar, S., & Gourav, S. (2015). A review paper on self healing concrete. *Journal of Civil Engineering Research, 5*(3), 53-58.

Luo, M., Jing, K., Bai, J., Ding, Z., Yang, D., Huang, H., & Gong, Y. (2021). Effects of Curing Conditions and Supplementary Cementitious Materials on Autogenous Self-Healing of Early Age Cracks in Cement Mortar. *Crystals, 11*(7), 752.

Luo, M., Qian, C.-x., & Li, R.-y. (2015). Factors affecting crack repairing capacity of bacteria-based self-healing concrete. *Construction and Building Materials, 87*, 1-7.

Lv, L., Yang, Z., Chen, G., Zhu, G., Han, N., Schlangen, E., & Xing, F. (2016). Synthesis and characterization of a new polymeric microcapsule and feasibility investigation in self-healing cementitious materials. *Construction and Building Materials, 105*, 487-495.

Magaji, A., Yakubu, M., & Wakawa, Y. M. (2019). A review paper on self healing concrete. *Int. J. Eng. Sci, 8*, 47-54.

Mahmoodi, S., & Sadeghian, P. (2019). *Self-healing concrete: a review of recent research developments and existing research gaps.* Paper presented at the 7th International Conference on Engineering Mechanics and Materials, Laval, QC, Canada.

Meera, C., & Subha, V. (2016). Strength and durability assessment of bacteria based self-healing concrete. *IOSR Journal of Mechanical and Civil Engineering,(IOSR-JMCE)*, 1-7.

Meharie, M. G., Kaluli, J. W., Abiero-Gariy, Z., & Kumar, N. D. (2017). Factors affecting the self-healing efficiency of cracked concrete structures. *American Journal of Applied Scientific Research, 3*(6), 80-86.

Mehndi, S. M., Khan, M., & Ahmad, S. (2014). Causes and Evaluation of Cracks in Concrete Structures. *International Journal of Technical Research and Applications, 2*(5), 29-33.

Murakami, F. S., Rodrigues, P. O., Campos, C. M. T. d., & Silva, M. A. S. (2007). Physicochemical study of CaCO3 from egg shells. *Food Science and Technology, 27*, 658-662.

Nain, N., Surabhi, R., Yathish, N., Krishnamurthy, V., Deepa, T., & Tharannum, S. (2019). Enhancement in strength parameters of concrete by application of Bacillus bacteria. *Construction and Building Materials, 202*, 904-908.

Nama, P., Jain, A., Srivastava, R., & Bhatia, Y. (2015). Study on causes of cracks & its preventive measures in concrete structures. *International Journal of Engineering Research and Applications, 5*(5), 119-123.

Negash, E. (2018). *Dr. Solomon K.* ADDIS ABABA UNIVERSITY ADDIS ABABA.

Ngugi, H. N., Mutuku, R. N., & Gariy, Z. A. (2014). Effects of sand quality on compressive strength of concrete: A case of Nairobi County and its environs, Kenya. *Open Journal of Civil Engineering, 2014*.

Nishiwaki, T., Oohira, A., & Pareek, S. (2011). *An experimental study on the application of self-repairing system to RC structures using selective heating.* Paper presented at the Third international conference self-healing materials, Bath, United Kingdom.

Nizam, R. S., Zhang, C., & Tian, L. (2018). A BIM based tool for assessing embodied energy for buildings. *Energy and Buildings, 170*, 1-14.

Parashar, A. K., Gupta, N., Kishore, K., & Nagar, P. A. (2021). An experimental investigation on mechanical properties of calcined clay concrete embedded with bacillus subtilis. *Materials Today: Proceedings, 44*, 129-134.

Park, J.-W., HAN, C., PARK, J.-K., KIM, H., YOU, K.-S., & AHN, J.-W. (2008). Effects of Precipitated Calcium Carbonate Morphology on the Synthesis of Calcium Lactate. *Resources Processing, 55*(1), 12-15.

Patel, P. (2016). Helping concrete heal itself. *Chemical & Engineering News, 94*(6), 29-30.

Prayitno, A. H., Siswoyo, T., Erwanto, Y., Lindrianti, T., Hartatik, S., Aji, J. M. M., Suryanto, E., & Rusman, R. (2022). Characterisation of Nano-Calcium Lactate from Chicken Eggshells Synthesized by Precipitation Method as Food Supplement. *Jurnal Ilmu Ternak dan Veteriner, 26*(4), 139-144.

Priyom, S. N., Islam, M., & Islam, S. (2018). An experimental investigation on the performance of bacterial concrete.

Qian, C., Zheng, T., Zhang, X., & Su, Y. (2021). Application of microbial self-healing concrete: Case study. *Construction and Building Materials, 290*, 123226.

Rajczakowska, M. (2019). *Self-healing concrete.* Luleå tekniska universitet.

Ray, S., Barman, A. K., Roy, P. K., & Singh, B. K. (2017). Chicken eggshell powder as dietary calcium source in chocolate cakes. *The Pharma Innovation, 6*(9, Part A), 1.

Reddy, T. C. S., & Ravitheja, A. (2019). Macro mechanical properties of self healing concrete with crystalline admixture under different environments. *Ain Shams Engineering Journal, 10*(1), 23-32.

Reinhardt, H.-W., & Jooss, M. (2003). Permeability and self-healing of cracked concrete as a function of temperature and crack width. *Cement and Concrete Research, 33*(7), 981-985.

Reinke, S. K. (2012). Polyurea/polyurethane microcapsules based self healing concrete.

Ren, L., & Qian, C. (2014). Restoration of cracks on surface of cement-based materials by carbonic anhydrase microbiologically precipitation calcium carbonate. *J. Chin. Ceram. Soc, 42*(11), 1389-1395.

Rodrigues, R., Gaboreau, S., Gance, J., Ignatiadis, I., & Betelu, S. (2021). Reinforced concrete structures: A review of corrosion mechanisms and advances in electrical methods for corrosion monitoring. *Construction and Building Materials, 269*, 121240.

Roig-Flores, M., Formagini, S., & Serna, P. (2021). Self-healing concrete-What Is it Good For? *Materiales de Construcción, 71*(341), e237-e237.

Sahmaran, M., Yildirim, G., Noori, R., Ozbay, E., & Lachemi, M. (2015). Repeatability and pervasiveness of self-healing in engineered cementitious composites. *ACI Materials Journal, 112*(4), 513-522.

Sakna, A., Galishnikova, V., Elroba, S., & Nassar, M. (2021). Self-healing bacterial mortar with calcium lactate and improved properties. *Magazine of Civil Engineering, 105*(5), 10503-10503.

Saleh, M. (2019). *Physical and mechanical investigations of self-healing concrete after healed cracks.* Kauno technologijos universitetas.

Sangadji, S., & Schlangen, E. (2012). Self healing of concrete structures-novel approach using porous network concrete. *Journal of Advanced Concrete Technology, 10*(5), 185-194.

Seifan, M. (2018). *Self-healing concrete: a novel nanobiotechnological approach to heal the concrete cracks.* The University of Waikato.

Seifan, M., Samani, A. K., & Berenjian, A. (2016). Bioconcrete: next generation of self-healing concrete. *Applied microbiology and biotechnology, 100*(6), 2591-2602.

Shen, Q., Chen, W., Liu, C., Zou, W., & Pan, L. (2020). The tensile strength and damage characteristic of two types of concrete and their interface. *Materials, 13*(1), 16.

Silva, F. B., Boon, N., Belie, N. D., & Verstraete, W. (2015). Industrial application of biological self-healing concrete: Challenges and economical feasibility. *Journal of Commercial Biotechnology, 21*(1).

Srinivasa, V., SeshagiriRao, M., & Sushma, S. (2015). Feasibility Study on Bacterial Concrete as an innovative self crack healing system. *International Journal of Modern Trends in Engineering and Research, 2*(7), 642-647.

Stanaszek, E. (2020). Bacterial concrete as a sustainable building material? *Sustainability, 12*(2), 696.

Syarif, M., Kırgız, M. S., de Sousa Galdino, A. G., El Naggar, M. H., Mirza, J., Khatib, J., Kenai, S., Nehdi, M., Kinuthia, J., & Khitab, A. (2021). Development and assessment of cement and concrete made of the burning of quinary by-product. *journal of materials research and technology, 15*, 3708-3721.

Syngros, G., Balaras, C. A., & Koubogiannis, D. G. (2017). Embodied CO_2 emissions in building construction materials of hellenic dwellings. *Procedia environmental sciences, 38*, 500-508.

Tabbaa, Litina, C., Giannaros, P., Kanellopoulos, A., & Souza, L. (2019). First UK field application and performance of microcapsule-based self-healing concrete. *Construction and Building Materials, 208*, 669-685.

Taffese, W. Z., & Abegaz, K. A. (2019). Embodied energy and CO_2 emissions of widely used building materials: the Ethiopian context. *Buildings, 9*(6), 136.

Talaiekhozani, A., & Abd Majid, M. Z. (2014). A review of self-healing concrete research development. *Journal of Environmental Treatment Techniques, 2*(1), 1-11.

Tang, Kardani, O., & Cui, H. (2015). Robust evaluation of self-healing efficiency in cementitious materials–A review. *Construction and Building Materials, 81*, 233-247.

Tang, & Xu, J. (2021). Application of microbial precipitation in self-healing concrete: A review on the protection strategies for bacteria. *Construction and Building Materials, 306*, 124950.

Tansman, G., Kindstedt, P., & Hughes, J. (2014). Powder x-ray diffraction can differentiate between enantiomeric variants of calcium lactate pentahydrate crystal in cheese. *Journal of Dairy Science, 97*(12), 7354-7362.

Thiyagarajan, H., Maheswaran, S., Mapa, M., Krishnamoorthy, S., Balasubramanian, B., Murthy, A. R., & Iyer, N. R. (2016). Investigation of Bacterial activity on Compressive Strength of cement mortar in different curing Media. *Journal of Advanced Concrete Technology, 14*(4), 125-133.

Tittelboom, K., & De Belie, N. (2013). Self-healing in cementitious materials—A review. *Materials, 6*(6), 2182-2217.

Tziviloglou, E., Pan, Z., Jonkers, H. M., & Schlangen, E. (2017). Bio-based self-healing mortar: an experimental and numerical study. *Journal of Advanced Concrete Technology, 15*(9), 536-543.

Tziviloglou, E., Wiktor, V., Jonkers, H., & Schlangen, E. (2016). Bacteria-based self-healing concrete to increase liquid tightness of cracks. *Construction and Building Materials, 122*, 118-125.

Ukala, D. (2019). Effects of combined aggregate gradation on the compression strength and workability of concrete using fineness modulus. *Journal of Applied Sciences and Environmental Management, 23*(5), 851-856.

Van, K., & De Belie, N. (2013). Self-healing in cementitious materials—A review. *Materials, 6*(6), 2182-2217.

Vashisht, R., & Shukla, A. (2020). Potential application of bacteria to improve the self-healing and strength of concrete. *Journal of Building Pathology and Rehabilitation, 5*(1), 1-13.

Vegt, I., Breugel, V., & Weerheijm, J. (2007). Failure mechanisms of concrete under impact loading. *Fracture Mechanics of Concrete and Concrete Structures, FraMCoS-6, 1*, 579-587.

Vijay, K., & Murmu, M. (2020). Experimental Study on Bacterial Concrete Using Bacillus Subtilis Micro-Organism *Emerging Trends in Civil Engineering* (pp. 245-252): Springer.

Vijay, K., Murmu, M., & Deo, S. V. (2017). Bacteria based self healing concrete–A review. *Construction and Building Materials, 152*, 1008-1014.

Wang. (2013). *Self-healing concrete by means of immobilized carbonate precipitating bacteria.* Ghent University.

Wang, De Belie, N., & Verstraete, W. (2012). Diatomaceous earth as a protective vehicle for bacteria applied for self-healing concrete. *Journal of Industrial Microbiology and Biotechnology, 39*(4), 567-577.

Wang, Ersan, Y. C., Boon, N., & De Belie, N. (2016). Application of microorganisms in concrete: a promising sustainable strategy to improve concrete durability. *Applied microbiology and biotechnology, 100*(7), 2993-3007.

Wang, Verstraete, W., & De Belie, N. (2014a). Application of hydrogel encapsulated carbonate precipitating bacteria for approaching a realistic self-healing in concrete. *Construction and Building Materials, 68*, 110-119.

Wang, Verstraete, W., & De Belie, N. (2014b). Self-healing concrete by use of microencapsulated bacterial spores. *Cement and Concrete Research, 56*, 139-152.

Wiktor, V., & Jonkers, H. M. (2011). Quantification of crack-healing in novel bacteria-based self-healing concrete. *Cement and concrete composites, 33*(7), 763-770.

Yang, Aldakheel, F., Caggiano, A., Wriggers, P., & Koenders, E. (2020). A review on cementitious self-healing and the potential of phase-field methods for modeling crack-closing and fracture recovery. *Materials, 13*(22), 5265.

Yang, Lepech, M. D., Yang, E.-H., & Li, V. C. (2009). Autogenous healing of engineered cementitious composites under wet–dry cycles. *Cement and Concrete Research, 39*(5), 382-390.

Yusuf, A. A. (2016). Utilization of organic and inorganic calcium and dehydrated food waste in improving egg production and egg quality of village chicken layers. *Master of Science thesis, Universiti Putra Malaysia*.

Zhang, Mai, B., Cai, T., Luo, J., Wu, W., Liu, B., Han, N., Xing, F., & Deng, X. (2017). Optimization of a binary concrete crack self-healing system containing bacteria and oxygen. *Materials, 10*(2), 116.

Zhang, Mengqiu, Zhang, D., Huang, Y., Li, G., & Li, X. (2018). Self-healing mechanisms in smart protective coatings: A review. *Corrosion Science, 144*, 74-88.